

**THE UNIVERSITY OF NEW SOUTH WALES
WATER RESEARCH LABORATORY**

**An Investigation of unconsolidated sedimentary units and their role
in the development of salinity in the Snake Gully Catchment,
Central New South Wales**



**WATER RESEARCH LABORATORY
RESEARCH REPORT**

No. 214

Prepared by

A Smithson and RI Acworth

Water Research Laboratory, School of Civil and Environmental Engineering, King Street, Manly Vale 2093
NSW

January 2005

EXECUTIVE SUMMARY

The Snake Gully catchment, central New South Wales, Australia, has significant erosion and salt affected land, with surface water flows commonly exceeding 6000 mS/cm (6 dS/m), and shallow groundwater salinity up to 14000 mS/cm (14 dS/m). A combination of geoscientific techniques including geological mapping, drilling, radiocarbon dating, particle size analysis, geophysics, groundwater monitoring and hydrogeochemistry have been applied to investigate fine grained unconsolidated sedimentary units and their role in the development of salinity in the catchment.

Gully erosion in the valley floor has exposed a series of sedimentary units with sharp textural contrasts traditionally known as 'duplex' soils thought to have been formed in-situ over 20 to 30,000 years. The units unconformably overlie slightly weathered Palaeozoic bedrock. Three of the sediment units are massive and exhibit strong bimodality, with large angular clasts of local basement supported in a silt-clay matrix, consistent with deposition as debris flows. Radiocarbon dating of the second unit from surface indicates an age of deposition between 180 and 330 years. Particle size analyses of the sub-50 micron component of the units indicate significant sorting consistent with an aeolian origin. The sediment units contain salt and are highly dispersive. Hydrogeochemical and isotopic analyses do not support evaporative concentration of salt, and indicate that sodium chloride dissolution and ion exchange are the main processes affecting the ionic concentration of shallow groundwaters. It is estimated that 1930 tonnes of salt are stored in the unconsolidated sediment units within this 22.6 km² catchment, and erosion of a small section of these sediments of 20 m x 20 m and 2 m thick would release 772 kg of salt into the surface water system.

A number of possible conceptual models have been proposed for salinity in the Snake Gully catchment, and these are assessed against the findings of this study. The results exclude deep groundwater discharge through faults and evaporative concentration of shallow groundwater through in-situ soils as major salinity processes; and support a shallow exotic source of salt in partially confining sedimentary clays mobilised by a shallow pressurised watertable.

An alternative conceptual salinity model is presented in which salt and dust were deposited in the catchment during the dry and windy glacial periods of the Quaternary. These sediments have been reworked and deposited as viscous sheets of unconsolidated sediment across the valley floor. Since deposition, these clay-rich units have controlled catchment salinity processes by impeding groundwater discharge, promoting shallow watertables; and by providing a source of sodium chloride salt, generating dispersive sodic soils. Inappropriate land management practices compounded by severe environmental events have resulted in the problems of shallow watertables, dryland salinity, and erosion that are now apparent in the catchment.

Although the model presented is based upon studies in one catchment, the Quaternary dust transport paths covered a large part of south-eastern Australia, and aeolian deposits are increasingly being recognised across the slopes and tablelands of NSW. The findings of this study clearly demonstrate that clay-rich aeolian derived sediment units have a major role in the development of land and water salinisation in the region.

The management implications of this work are discussed, including a shift in focus to incorporate fine grained salt-rich valley slope and floor sediments in salinity management planning. Protection of the salt-rich sediments from erosion and release of salt should be the priority management strategy; along with on-going actions to minimise local groundwater recharge. In combination, these measures will considerably reduce salt export so that downstream salinity targets can be realised.

This research report is based upon a Masters of Engineering Science Project report by Ann Smithson supplemented by additional material provided by the authors.

ISBN: 0 85 824 054 8

Water Research Laboratory Research Report Number 214 is published on the web. The report can be downloaded from the Water Research Laboratory web site as a pdf document. Further printed copies can be supplied on application to the Librarian, Water Reference Library, School of Civil and Environmental Engineering, King Street, MANLY VALE 2093, Australia.

The Water Research Laboratory web site address is <http://www.wrl.unsw.edu.au/research>

Contents

1	INTRODUCTION	1
1.1	THE SALINITY PROBLEM	1
1.2	SALINITY PROCESSES	2
1.3	PROJECT OBJECTIVE	3
2	REGIONAL SETTING	5
2.1	LOCATION	5
2.2	CLIMATE	6
2.2.1	Rainfall and Relationship with Watertable Levels	6
2.3	LAND USE AND VEGETATION	8
2.4	SOILS	10
2.5	GEOLOGY	10
2.5.1	Regional Geology	10
2.5.2	Local Geology	13
2.6	REGIONAL HYDROGEOLOGY	13
2.7	SALINITY INDICATIONS	14
3	LANDSCAPE SALINISATION AND MANAGEMENT	16
3.1	AUSTRALIAN LANDSCAPE EVOLUTION	16
3.1.1	Quaternary Climate Change	16
3.1.2	Glacial Aridity and Dust Generation	18
3.1.3	Aeolian Entrainment and Landscape Accession	20
3.1.4	Defining and Identifying Aeolian Materials	22
3.1.5	Soil Formation Processes	23
3.1.6	Links of Aeolian Material With Salinity	25

3.1.7	The Role of Groundwater in Salinisation	26
3.1.8	Conclusions	27
3.2	LANDSCAPE CHANGE AND SALINITY IN THE SNAKE GULLY CATCHMENT . . .	27
3.2.1	Landscape Change Since Human Occupation	27
3.2.2	Salinity Investigation and Management	28
3.2.3	Previous Studies	29
3.2.4	Salinity Models for the Snake Gully Catchment	31
4	INVESTIGATION METHODS	32
4.1	GEOLOGY OF SEDIMENTARY UNITS	32
4.2	BOREHOLE DRILLING AND GEOLOGICAL LOGGING	32
4.2.1	Cored Hole CH1	32
4.2.2	Nested Bore Site GW96128	34
4.3	DATING OF UNITS	36
4.3.1	Circumstantial Evidence	36
4.3.2	Trace Fossils	36
4.3.3	Radiocarbon Dating	36
4.4	CORE ANALYSIS	38
4.4.1	Emerson Aggregate Testing	38
4.4.2	Aqueous Extracts	38
4.4.3	Aqueous Extract Major Ions	40
4.4.4	Grain Size Analysis	40
4.5	GEOPHYSICAL TECHNIQUES	42
4.5.1	Introduction	42
4.5.2	EM 31 Survey	42
4.5.3	Electrical Imaging	43
4.5.4	Borehole Geophysical Logging	45
4.6	HYDROGEOCHEMISTRY	47
4.6.1	Introduction	47
4.6.2	Field Measurements and Sample Collection	47
4.6.3	Laboratory Measurements	48

4.7	ENVIRONMENTAL ISOTOPES	49
4.7.1	Introduction	49
4.7.2	Sample Collection	50
4.7.3	Sample Analysis	50
4.8	GROUNDWATER LEVELS	50
5	RESULTS	52
5.1	GEOLOGY OF SEDIMENTARY UNITS	52
5.1.1	Unit One	52
5.1.2	Unit Two	55
5.1.3	Unit Three	58
5.2	BOREHOLE DRILLING AND GEOLOGICAL LOGGING	60
5.2.1	Cored Hole CH1	60
5.2.2	Nested Bore Site GW96128	61
5.3	DATING OF UNITS	61
5.3.1	Circumstantial Evidence	61
5.3.2	Trace Fossils	62
5.3.3	Radiocarbon Dating	62
5.4	CORE ANALYSIS	62
5.4.1	Emerson Aggregate Testing	64
5.4.2	Aqueous Extracts	64
5.4.3	Aqueous Extract Major Ions	66
5.4.4	Grain Size Analysis	66
5.5	GEOPHYSICAL TECHNIQUES	69
5.5.1	Introduction	69
5.5.2	EM31 Survey	70
5.5.3	Electrical Imaging	71
5.5.4	Borehole Geophysical Logging	73
5.6	HYDROGEOCHEMISTRY	77
5.6.1	Unstable Parameters	77
5.6.2	Major Ions	77

5.6.3	Sodium Adsorption Ratio	77
5.7	ENVIRONMENTAL ISOTOPES	82
5.8	GROUNDWATER LEVELS	83
6	INTERPRETATION OF RESULTS	91
6.1	GEOLOGY OF SEDIMENTARY UNITS	91
6.2	UNIT DATING	92
6.3	CORE ANALYSIS	92
6.4	GRAIN SIZE ANALYSIS	93
6.5	GEOPHYSICAL TECHNIQUES	93
6.6	HYDROGEOCHEMISTRY	94
6.7	ENVIRONMENTAL ISOTOPES	95
6.8	GROUNDWATER LEVELS	95
6.9	SALT STORAGE AND EXPORT	95
6.9.1	Average Salt Store in Unconsolidated Sedimentary Units	96
6.9.2	Salt Stored In Catchment	96
6.9.3	Salt Exported During Erosion Of Sedimentary Units	96
7	CONCEPTUAL MODEL FOR SALINITY	97
7.1	ALTERNATIVE SALINITY MODELS	97
7.1.1	Salinity Due To Deep Groundwater Discharge Through Faults	97
7.1.2	Salinity Due To Evaporative Concentration of Shallow Groundwater Through In-situ Soils	98
7.1.3	Salinity Due To A Shallow Exotic Salt Source In Partially Confining Clay, Mobilised By A Shallow Pressurised Water Table	98
7.2	CONCEPTUAL MODEL FOR SALINITY IN SNAKE GULLY	99
8	CONCLUSIONS	103
8.1	MAJOR FINDINGS	103
8.2	IMPLICATIONS FOR SALINITY MANAGEMENT	104
8.3	FURTHER WORK	105
8.3.1	Refinement of Conceptual Model	105
8.3.2	Assessment of the Regional Distribution and Nature of Debris Flow Type Units	105

List of Figures

2.1	Study Site in Snake Gully	6
2.2	Regional Location of Study	7
2.3	Annual Rainfall From "Binginbar" Since 1934	8
2.4	Cumulative Deviation from Mean Annual Rainfall for "Binginbar"	9
2.5	Isolated Kurrajong Trees in Cropping Paddock	9
2.6	Regional Geology	11
2.7	Vegetation Species Zonation With Increase in Soil Salinity	14
2.8	Sheet Erosion At Study Site Prior To Rehabilitation	14
2.9	Salt Efflorescence on Edges of Incised Channel	15
2.10	Salt Efflorescence	15
3.1	Quaternary Dust Paths	18
3.2	Dust storm over eastern Australia - 23 October 2002	19
3.3	Griffith - 12 November 2002	19
3.4	Modern dust activity near Narromine - 12 November 2002	20
3.5	Recent dust activity in Western NSW - March 2003 - accumulations behind vegetation . .	21
3.6	Recent dust activity in Western NSW - March 2003 - accumulations behind stock fences .	21
3.7	Upper Snake Gully Landscape	31
4.1	Airphoto Showing Bores and Sample Locations at the Study Site	33
4.2	Drilling Cored Hole CH1 (January 2001)	34
4.3	First Metre of Core From CH1	34
4.4	Sampling Core From CH1	34
4.5	Drilling Nested Monitoring Bore Site GW96128	34
4.6	Nested Monitoring Bore Site GW96128	35

4.7	Trace Fossils In Unit Three	36
4.8	Radiocarbon Dating Charcoal Clast Sample 10882 Prior to Excavation	37
4.9	Radiocarbon Dating Charcoal Clast Sample 10882 Cavity Following Excavation	37
4.10	Emerson Aggregate Dispersion Testing	39
4.11	Preparation of 1:5 Extracts	39
4.12	Agitation Wheel For 1:5 Extracts	39
4.13	Aqueous 1:5 Extracts Settling Period Prior to Measurement	40
4.14	Measurement of pH and EC From 1:5 Aqueous Extract	40
4.15	Electrical Resistivity Image Line One and Borehole Geophysical Logging at GW96128 . .	44
4.16	Electrical Resistivity Image Line Two	44
4.17	ABEM SAS4000 Terrameter Used For Electrical Resistivity Imaging	44
4.18	Borehole Geophysical Logging At GW96128 Site	46
4.19	Pumping Bore GW96128/3 With Grundfos Pump	47
4.20	Pumping Shallow Bores With Amazon Pump, Measurement of Unstable Parameters, and Sample Collection	47
4.21	Surface Water and Groundwater Sampling Locations	48
4.22	Filtering and Preservation of Water Samples	49
4.23	Field Titration For Unstable Parameters	49
4.24	View South From 'Binginbar" Across Upper Snake Gully Catchment	51
5.1	Eroded Creek Section in Snake Gully Exposing Units One, Two, and Three	53
5.2	Representative Stratigraphic Column For Unconsolidated Sedimentary Units Mapped in Eroded Creek Section in Upper Snake Gully	54
5.3	Beds of Calcrete Clasts in Unit One	55
5.4	Lenses of Charcoal and Calcrete Clasts in Unit One	55
5.5	Clast Imbrication in Unit One	55
5.6	Scour and Fill Structure in Unit One	55
5.7	Salt Concentrating at the Top of the Capillary Zone in Unit One	56
5.8	Unit Two Exposed in North Branching Tributary of Snake Gully Creek (100 m N of CH1), Note: Unit one not present at this location	56
5.9	Clast Detail Unit Two	56
5.10	Large Angular Clast of Basement Siltstone Entirely Supported by Matrix , Showing the Strong Bimodality of Unit Two	56

5.11 Bleaching in Unit Two Adjacent To GW96128 Bore Site	57
5.12 Relict Tree Roots In Unit Two	57
5.13 Palaeosol at Top of Unit Two	57
5.14 Hexagonal Shrinkage Cracks and Surface Frittering In Unit Two	57
5.15 Area of crop germination failure due to entrainment of Unit 2 material	58
5.16 Columnar Shrinkage Cracks and Salt Efflorescence on Surface of Unit Two	58
5.17 Manganese Nodules and Relict Carbonate Stringers in Unit Three	58
5.18 Clasts In Unit Three Exposed In Creek Platform	58
5.19 Matrix Supported Clasts In Unit Three	59
5.20 Incised Channel in Unit Three	59
5.21 Unconformable Angular Contact of Sedimentary Units With Basement	60
5.22 Unconformable Angular Contact With Basement	61
5.23 Plough Disc Entrained During Deposition of Unit One	62
5.24 Variation in EC1:5 With Depth for CH1	65
5.25 Major Ions, TDS, and EC with Depth in CH1	66
5.26 Piper Diagram of 1:5 Extract Fluids for CH1 at Study Site in Snake Gully Catchment . .	68
5.27 Sub-50 Micron Particle Size Frequency for Selected Samples from CH1 and GW96128 . .	69
5.28 EM31 Image For Study Site Paddock at "Murrawega"	70
5.29 EM31 Survey Draped Over Elevation Data	71
5.30 Electrical Resistivity Image Line One	72
5.31 Electrical Resistivity Image Line Two	72
5.32 Electrical Resistivity Image Line passing through GW96122	72
5.33 Electrical Resistivity Image Line over the valley at Mindawanda	73
5.34 Downhole Gamma and EC for GW96128/3	74
5.35 Downhole Gamma and EC for CH1	75
5.36 Downhole Gamma and EC for CH1	76
5.37 Piper Diagram of Groundwaters and Surface Waters From the Snake Gully Catchment . .	80
5.38 Ionic ratios for waters from the study site	81
5.39 Oxygen-18 and Deuterium Isotope Data	86
5.40 Hydrographs for Nested Bore Site GW96128 From October 2001 to July 2002 - Dip readings	87
5.41 Hydrographs for GW96128/2 and GW96128/3 from 4 January to 5 May 2002	87

5.42	Hydrographs for GW96128/2 and GW96128/3 From 2 to 9 February, 2002	88
5.43	Hydrographs for GW96128/2 and GW96128/3 From 21 February to 1 March, 2002	89
5.44	Hydrographs for all 3 GW96128 monitoring bores and barometric pressure from September 2002 to March 2003	89
5.45	Hydrographs for 3 monitoring bores and barometric pressure from 6 October to 5 November 2002	90
7.1	Conceptual Model - Pre-Quaternary	99
7.2	Conceptual Model - Quaternary to 200 BP	100
7.3	Conceptual Model - 1850's to 1940's	100
7.4	Conceptual Model - 1940's to Present	101
7.5	Gullying and Groundwater Seepage at Study Site	101
7.6	New Gully Head Progressing Back Up Creek Line In Snake Gully Catchment	102

List of Tables

2.1	Stratigraphy of the Snake Gully Region	12
3.1	Studies Reporting Significant Aeolian Contribution to Landscape in South-Eastern New South Wales	21
3.2	Generalised Late Quaternary Piedmont Stratigraphy in the Belarbon-Nulchara Lake Region, Showing Major Phases of Aeolian Dust Influx to the Area	23
3.3	Age and Sequence of Cainozoic Deposits in Upper Dicks Creek, Yass	24
4.1	Construction Details For GW96128 Nested Monitoring Bores	35
5.1	Summary Geological Characteristics of Unconsolidated Sedimentary Units at Study Site .	53
5.2	Summary Lithology in Bore GW96238/3	61
5.3	Radiocarbon Dating Results for Unit Two at Snake Gully	63
5.4	Mean 1:5 Extract and Emerson Aggregate Test Data - Cored Hole CH1	63
5.5	Relationship of Emerson Aggregate Class Number With Dispersibility	64
5.6	Relationship Between Emerson Class Number and Sodicity	64
5.7	Salinity Classification of Soils Based on Aqueous Extract Conductivity	65
5.8	Groundwater related studies at the Hudson site.	67
5.9	Mean Geochemical Data For Cored Hole CH1	67
5.10	Hydrogeochemistry - Field Measurements	78
5.11	Groundwater related studies at the site.	79
5.12	Mean Unstable Parameters By Water Source	79
5.13	Geochemical Analyses By Water Source	82
5.14	Mean EC ($\mu\text{S}/\text{cm}$) By Catchment Location and Water Source in Snake Gully	82
5.15	Sodium Hazard Rating Based on SAR	82
5.16	Oxygen-18 and Deuterium Stable Isotope Data for Study Site, Snake Gully. Data for the Ballimore (Schofield 1998) included for comparison	84

5.17 Rainfall Oxygen-18 and Deuterium Stable Isotope Data for Ballimore (Schofield 1998) and Gunnedah (Timms et al. 2002) included for comparison	85
6.1 Proposed Date of Deposition For Sedimentary Units at Snake Gully	92

Chapter 1

INTRODUCTION

1.1 THE SALINITY PROBLEM

Salinity is recognised as a major problem currently threatening Australia (MDBMC 1999; NLWRA 2001; CSIRO 2001). Salinisation is the increase of salts in soil and water causing degradation and loss of land and water resources. As new salinity statistics are released, the enormity of the potential economic, environmental and social impacts of salinity in Australia are being realised (NLWRA 2001; CSIRO 2001).

A key finding of the independent 2001 Australian "State of the Environment" report (CSIRO 2001) was that "degradation of lands and waters remain of critical concern". The report found that the increase in dryland salinity in the Murray-Darling Basin was a major cause of water quality decline and land degradation. Several catchments were predicted to have salinity levels that will exceed drinking water guidelines within the next 20 years. Further, the report stated that land degradation, including erosion, was a major contributor of turbidity and nutrients in waterways, as well as to loss of soil fertility.

According to the 2001 National Land and Water Resources Audit, about 5.7 million hectares, mostly in the agricultural regions, are at risk of or are affected by salinity, potentially increasing to 17 million hectares in 50 years. Further, up to 20,000 km of inland waters could be salt affected by the year 2050, up to two million hectares of native remnant vegetation could disappear over the next 50 years and at least 200 rural towns could experience salt damage over the next 50 years (NLWRA 2001).

The Murray-Darling Basin Ministerial Council's "Salinity Audit" identifies the Central West region of New South Wales as a key salinity risk area (MDBMC 1999). Based on rates of groundwater rise, the Macquarie River (Central New South Wales) faces a sharp increase in salt loads and salinity levels, to a point where thresholds for consumptive use of water will be exceeded on average (MDBMC 1999). By the year 2020, salt loads mobilised to the land surface by rising watertables in the Macquarie catchment are predicted to more than double, from 240,000 tonnes in 1998 to 490,000 tonnes by 2020 (MDBMC 1999). The average salinity for the Macquarie River is predicted to exceed the 800 EC threshold within 20 years, and the 1500 EC level within 100 years (MDBMC 1999). With these projected salinity increases, water quality will deteriorate below safe levels for town water supply, irrigation, and wetland ecosystem health (MDBMC 1999).

In NSW, the premier has responded to these predictions by calling a salinity summit early in 1999, which led to the release of the State Salinity Strategy in 2000. At the Murray-Darling Basin scale, the Murray-Darling Basin Commission released their salinity strategy in 2000, and in 2001 the National Action Plan for Water Quality and Salinity (NAP) was announced by the Federal Government.

Australia's emerging salinity problem is proving a significant challenge to scientists and natural resource managers. The causes and solutions of salinity are the subject of much conjecture and debate. This is partly due to the enormity and widespread nature of the problem, the diversity of climatic regime, topography, geology and land use across which the problem occurs, and the significant time lag periods

observed in groundwater systems. Changing climate regimes (possibly exacerbated by the greenhouse effect), and anthropogenic effects add further complexity.

1.2 SALINITY PROCESSES

Salinisation is the process where the concentration of salts in water and soil is increased due to natural or human-induced processes (Ghassemi et al. 1995).

Three conditions are required for salinisation to occur: a source of salt, a supply of water to mobilise the salt, and a concentration mechanism (Williamson 1998).

A number of sources supply salt to the Murray-Darling Basin. These are: salt carried in rainfall as cyclic salts derived from marine aerosols; salts released by weathering of rocks; marine salts from connate fluids trapped in pores at the time of rock deposition; and salts deflated from inland areas by strong westerly winds in arid glacial phases of the Quaternary (Ghassemi et al. 1995; Taylor 1996; NLWRA 2001; Acworth & Jankowski 2001).

Salt stores develop in the landscape because the amount of salt entering the system is greater than the amount of salt being removed. When changes occur in the landscape water balance, the amount of water entering the watertable can increase, causing watertables to rise (NLWRA 2001). The rising groundwater mobilises salt stored in the ground. If the watertable intersects the land surface, saline seepages occur. Evapotranspiration from a shallow watertable results in salt being concentrated at the soil surface, and during wet periods, this salt is carried into waterways by surface runoff (NLWRA 2001).

High ion concentration in the soil causes changes in plant species, or death of vegetation and loss of soil cover (Taylor 1996). Ion exchange of calcium and magnesium for sodium in clays, generates sodic dispersive soils with a high erosion hazard (Taylor 1996; Charman & Murphy 2000). Consequently, salinised areas are often focal points for soil erosion (Downes 1954). In addition, a high rate of runoff resulting from vegetation loss initiates gulying of lower areas (Logan 1958; Junor 1989).

Primary salinity is that which occurs entirely due to landscape features and natural processes mobilising and accumulating salt. These include evaporation in excess of precipitation, low landscape gradients, long groundwater flow paths, low groundwater system hydraulic conductivities, relatively closed drainage basins, impeded drainage, climatic pattern, and episodic rainfall (Ghassemi et al. 1995; Taylor 1996). Secondary salinisation is the result of salt that is stored in the ground being mobilised by extra water due to human activities such as irrigation, or reduction in vegetative cover (Ghassemi et al. 1995; Taylor 1996; NLWRA 2001).

The Murray-Darling basin has all of these features, and salt accumulation and land and water salinisation are significant processes in its landscape. Salts are recycled in the Murray-Darling Basin from west to east by the wind, and from east to west by flow in groundwater and river systems.

Salinity has often developed in the landscape because of the climatic variations during the Quaternary, occurring in many cases because of significant lag in response time between the climate and the groundwater system. Groundwater systems of the Murray-Darling Basin can have extremely long flow paths. In these systems it takes thousands of years for groundwater heads to decrease after rainfall recharge diminishes in response to climate change. Even where salinity management options are implemented, there may be a significant time lag before groundwater systems show a response to change (NLWRA 2001).

Of particular interest to natural resource managers is the ability to predict where dryland salinisation will occur, what the likely salt loads emanating from particular regions will be over time, and the response mechanisms of the salt and water system to a variety of land management options. Central to solving the question of salt load spatial and temporal variability, is some knowledge of where salt is stored in the landscape and how it is accessed by the water systems (Evans 1998).

An understanding of the sources of salt, and its mechanisms of transport through the hydrosphere is necessary for the long-term management and protection of natural resources (Herczeg et al. 2001).

1.3 PROJECT OBJECTIVE

Initially, the objective of this project was an investigation of land and water salinisation processes in Snake Gully, a salinity affected area of the Macquarie River catchment, central New South Wales; however, during the first field visit to the study area, a reconnaissance of the drainage line revealed unconsolidated sedimentary units with a strong similarity to Quaternary age dispersive debris flow units at Yass.

The units at Yass have an aeolian component that contains a significant store of salt. Soil erosion, gullying, and land and water salinisation are severe at both sites. If the unconsolidated sedimentary units at Snake Gully have a similar origin to those at Yass, a new salinity model is required for the Macquarie catchment. This model would change the focus of salinity management in the region.

The refined objective of this research project was to investigate the unconsolidated sedimentary units and their role in the development of salinity in the Snake Gully catchment.

Salinity is a complex problem involving geology, topography, climate, groundwater, soils, vegetation, and land use. An integrated approach, combining a number of investigative techniques was adopted in order to satisfy the project objective.

Work completed includes:

1. A literature review of Australian palaeoclimate, dust generation, landscape entrainment, and associated salinity and groundwater processes.
2. Literature review and landowner interviews to determine the effects of recent climatic events, natural history, and land management, on distribution of unconsolidated sedimentary units, erosion, and loss of land to salinity in the Snake Gully catchment.
3. Consideration of alternative models for salinity in the catchment.
4. Stratigraphic mapping, drilling, sampling, and downhole geophysical logging to characterise the lithological units at the study site.
5. Radiocarbon dating and use of circumstantial evidence to establish dates of emplacement for the sedimentary units.
6. EM31 and electrical resistivity imaging to determine the distribution of the unconsolidated sedimentary units.
7. Grain size analyses to indicate whether the unconsolidated sedimentary units at the study site have an aeolian component.
8. 1:5 aqueous extracts to establish whether the unconsolidated sedimentary units at the study site contain salt.
9. Emerson Aggregate testing to determine the susceptibility of each unconsolidated sedimentary unit to dispersion and erosion.
10. Continuous groundwater level logging to investigate groundwater dynamics at the study site.
11. Analysis of major ions in 1:5 aqueous extracts, surface waters, and groundwaters, to investigate salinity processes.
12. Oxygen and deuterium isotope analysis to investigate environmental processes affecting surface and groundwaters.

13. Evaluation of results and development of a conceptual model for salinisation in the Snake Gully catchment based on the research findings.
14. Review of project findings and assessment of the implications for land management in the catchment and the region.
15. Recommendation for additional investigation to refine the work conducted by this study.

Chapter 2

REGIONAL SETTING

2.1 LOCATION

The study site is principally focussed on a 1 kilometre section of the upper Snake Gully catchment located on the property "Murrawega", Gollan, in central New South Wales, (Figure 2.1 and Figure 2.2) with further observations from the more general area. The Snake Gully catchment covers 22.6 km² and incorporates the properties "Attunga", "Binginbar", "Mindawanda", "Randwick", "Murrawega", and "Ben Hoden". The catchment is approximately 400 km west of Sydney, 55 km east of the nearest regional centre, Dubbo, and is located on the Dunedoo 1:50 000 Topographical Series Sheet (8733-N). The study area is accessed by the Dubbo-Mudgee Road, or the Wellington-Dunedoo Road, and then Binginbar Road, and farm tracks.

The Snake Gully catchment drains westwards, and crosses the Dubbo-Mudgee Road before joining Spicers Creek, which flows north into the Talbragar River. At Dubbo the Talbragar joins the Macquarie River, a tributary of the Murray-Darling system. The creek in Snake Gully is ephemeral and only flows after heavy rainfall or prolonged wet periods.

The Snake Gully catchment comprises gently undulating hills with slopes generally less than 5°, however some low escarpments with steeper slopes occur along the edge of the Triassic sedimentary sequences. Elevation ranges from 470 m Australian Height Datum (AHD) at the head of the catchment, to 340 m AHD ten kilometres west, at the mouth of the catchment where it enters Spicers Creek. The overall gradient of the catchment is approximately 0.013.

In upper sections of the Snake Gully catchment, the creek has cut several metres into unconsolidated sediments deposited on the valley floor. Further downstream, the creek meanders through broad depositional floodplains consisting of several shallow braided channels.

The study site is located within 3 kilometres of the regional surface water and groundwater divide between the Spicers Creek and Baragonumbal Creek catchments.

The site was chosen because of its proximity to salt affected soils and saline seepage, and the very good exposure of the unconsolidated sedimentary units and bedrock in steep (one to four metres deep) erosion faces and creek platforms. The incised erosion occurs for up to one kilometre along the creek at the study site.



Figure 2.1: Study Site in Snake Gully

2.2 CLIMATE

The Snake Gully catchment experiences a semi-arid climate characterised by hot dry summers and cool wet winters, with slightly summer dominant rainfall.

The meteorological stations at Cooreena Road Dubbo, and Dubbo Airport are operated by the Bureau of Meteorology. Together, these stations provide 131 years of regional meteorological data. For Dubbo, the mean annual rainfall is 584 mm, mean summer temperature ranges from 24 to 39 °C and mean winter temperature ranges from 12 to 19 °C (Commonwealth of Australia, 2002, Bureau of Meteorology).

Pan evaporation data for the last 25 years was available from the Wellington Research Station (approximately 45 kilometres southeast of Snake Gully catchment), operated by NSW Department of Land and Water Conservation (DLWC). The mean summer monthly evaporation at Wellington ranges from 210 to 270 mm and the mean winter monthly evaporation ranges from 51 to 78 mm.

2.2.1 Rainfall and Relationship with Watertable Levels

Rainfall records since 1934 were available from the property "Binginbar" in the Snake Gully catchment. Based on the last 68 years of rainfall data, the mean annual rainfall of the area is 532 mm. Monthly mean rainfall ranges from 42 to 52 mm in summer and 38 to 45 mm in winter. Annual rainfall is shown on Figure 2.3.

Comparison of the "Binginbar" rainfall data with Wellington evaporation data shows that evaporation greatly exceeds precipitation. An excess of evaporation over precipitation is a contributing factor in the salinity process.

The residual annual rainfall mass curve (Figure 2.4) shows the cumulative deviation from average annual rainfall. The slope of the curve indicates whether the area was experiencing a relatively wetter or drier

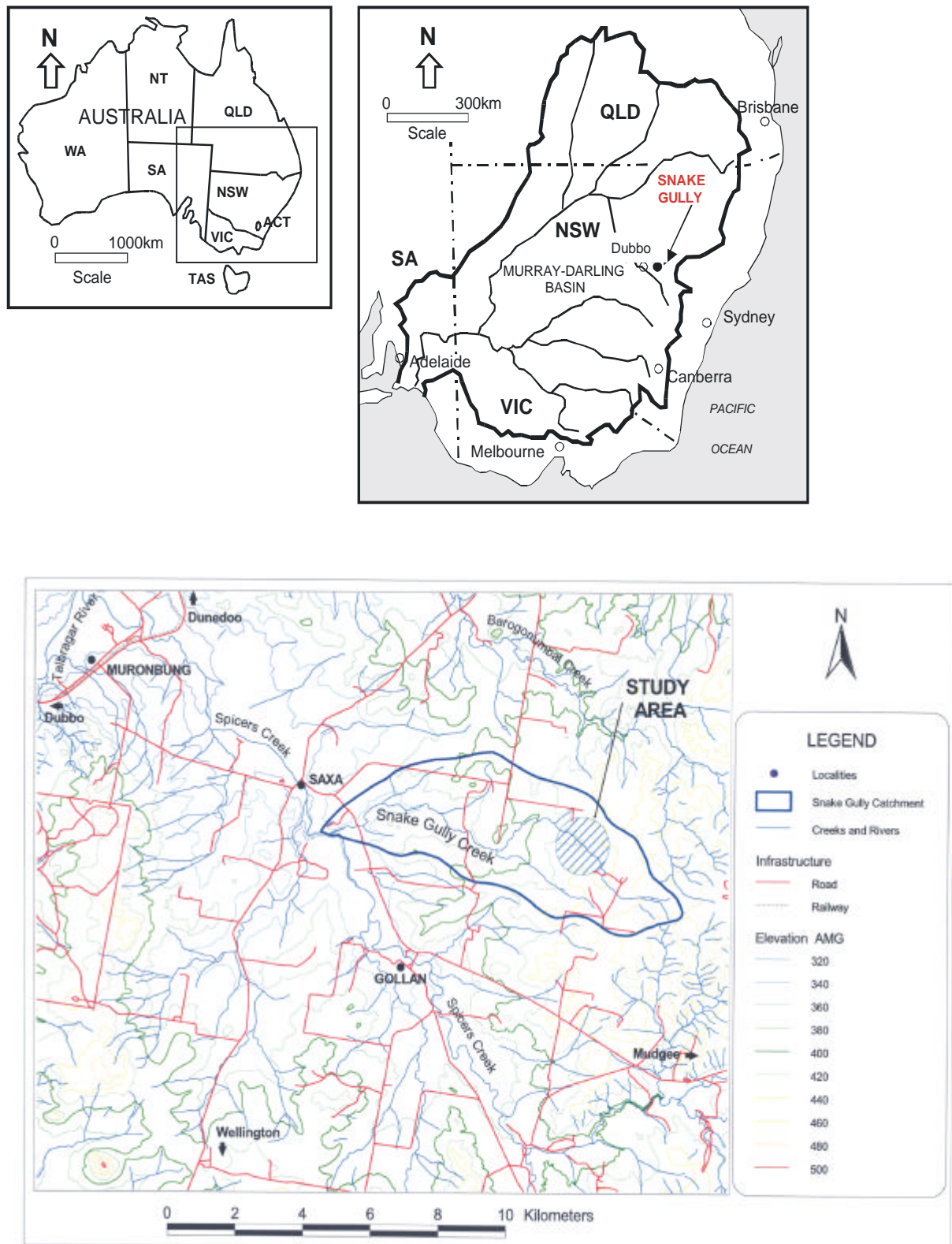


Figure 2.2: Regional Location of Study

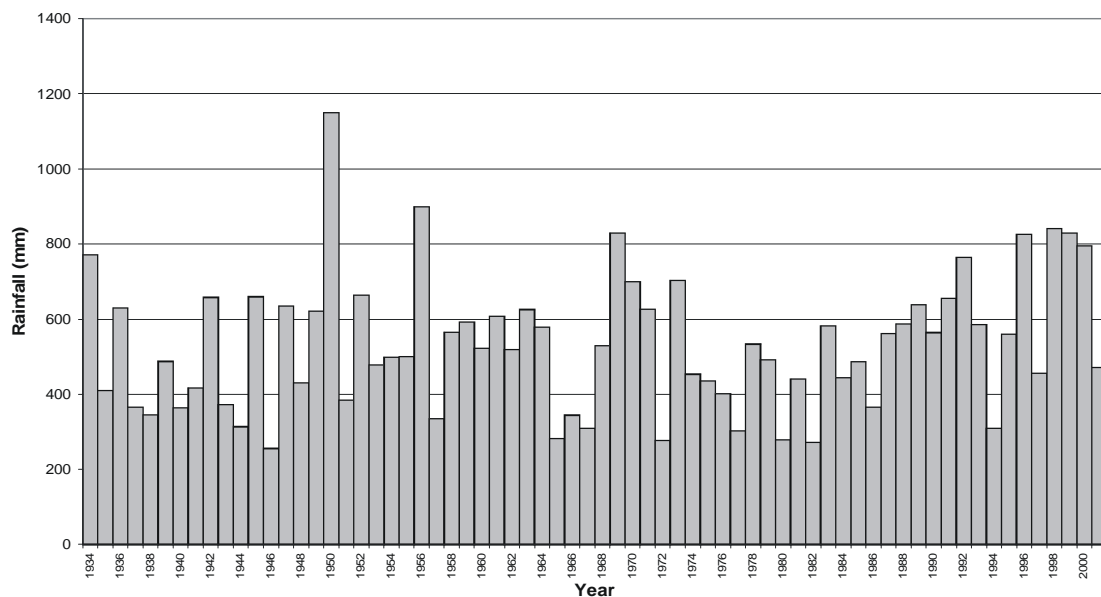


Figure 2.3: Annual Rainfall From "Binginbar" Since 1934

period compared to average. For the periods 1934 until 1948, 1965 to 1967, and 1974 to 1986 annual rainfall tended to be less than the long term average for the catchment. From 1949 until 1964, 1968 to 1973, and 1987 to 2000 annual rainfall tended to be more than the long term average.

The residual mass curve demonstrates one of the larger scale temporal fluctuations that affect rainfall pattern, this one occurring over a period of several decades. These fluctuations are part of global climate change phenomenon such as the El Nino Southern Oscillation (ENSO) and glaciations.

2.3 LAND USE AND VEGETATION

Mixed farming predominates in the Snake Gully catchment, and consists of cereal, lucerne, and canola cropping, and sheep grazing. The majority of cropping in the Snake Gully area is conducted on slopes of 5% (5.55°) or less.

A large proportion of the Snake Gully catchment has been cleared of original stands of native vegetation for farming. Pockets of bush and trees remain on rocky hilltops, in fenced reserves, and in tree strips. Cropping and grazing paddocks contain isolated mature trees (Figure 2.5). Ironbark (*Eucalyptus sideroxylon*) is found on the lighter soils of the sandstone hills and ridges. Kurrajong (*Brachychiton populneus*), white pine (*Calitris glaucophylla*), white box (*Eucalyptus albens*) and grey box (*Eucalyptus microcarpa*) are found on the red soils of the mid-slopes. River red gum (*Eucalyptus camaldulensis*) is found on the alluvial soils closer to Spicers Creek.

Native grasses, particularly red grass (*Bothriochloa macra*) are common in areas which have not been cropped. This genus is common in areas that have been overgrazed (Harden 1993). Cottonbush (*Maireana* sp.) is common in the paddocks around the study site and is an indicator of soil sodicity (S Gibbs 2001, pers. comm., 11 Nov.). A number of other vegetation species are being trialled in small blocks as part of salinity mitigation schemes.

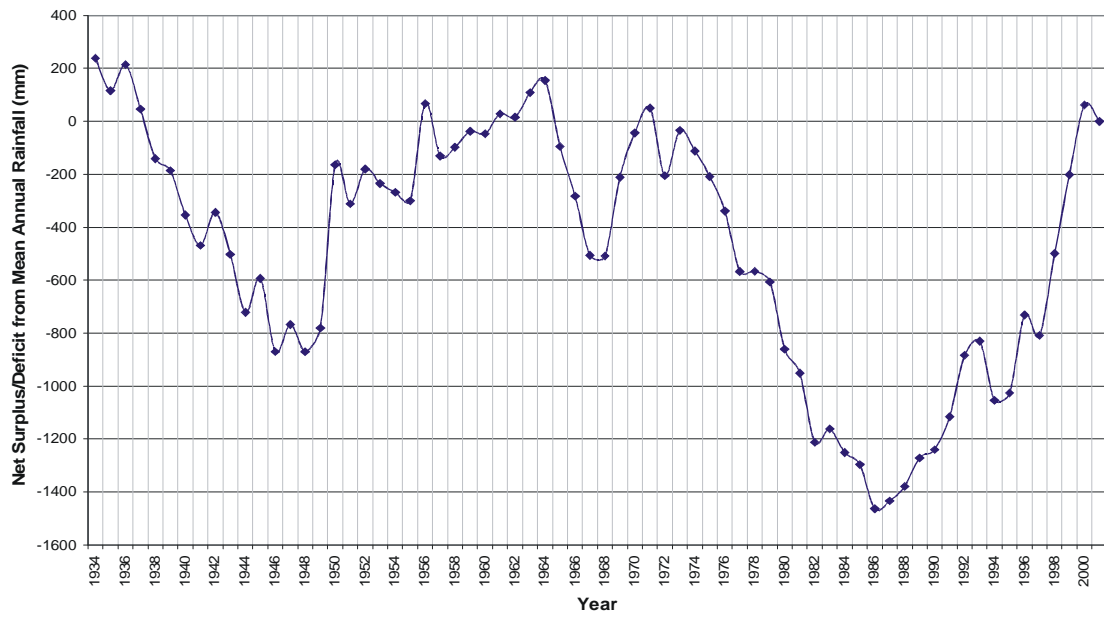


Figure 2.4: Cumulative Deviation from Mean Annual Rainfall for "Binginbar"



Figure 2.5: Isolated Kurrajong Trees in Cropping Paddock

2.4 SOILS

The Snake Gully catchment encompasses three main soils landscapes as shown by the Dubbo 1:250 000 Soil Landscape Series Sheet SI 55-4 (Murphy and Lawrie 1999).

These are:

1. The Red-Brown Earths of the Ballimore Soils Landscape (underlain by Mesozoic sedimentary rocks) on the northern slopes and hills of the catchment;
2. Euchrozems of the Bodangora Soils Landscape (underlain by Palaeozoic rocks) along the creek line and the southern slopes and hills of the catchment and;
3. Alluvial Soils of the Mitchell Creek Soils Landscape close to Spicers Creek at the mouth of the catchment.

The Ballimore Soils Landscape predominates at the study site (J Lawrie 2002, pers. comm., 16 July). This landscape consists of undulating low hills, underlain by "Ballimore Sandstone" (superseded formation name now remapped to include sedimentary rocks of the Gunnedah and Surat Basin). Relief is 20 to 40 m and slopes are 3 to 6%. The soils consist of Red-Brown Earths, non-calcic Brown Soils, and red and yellow Solodic Soils on lower slopes and depressions. Other soils include shallow Siliceous Sands, and Red, Yellow and Grey Earths on flat crests (Murphy & Lawrie 1998a).

The Red-Brown Earths have a reddish-brown weakly structured sandy loam A horizon. This has a clear boundary over a reddish-brown sandy clay or light-medium clay B horizon which displays strong sub-angular blocky structure and sometimes has calcium carbonate nodules present (Murphy & Lawrie 1998a).

The clear textural boundary between the A and B horizons defines this soil type as a "duplex" soil (Charman & Murphy 2000).

Limitations of the Ballimore Soils Landscape include high erosion hazard under cultivation, surface soils structurally degraded and low in organic matter, low fertility, sodic subsoils on lower slopes, and several localised occurrences of salinity (Murphy & Lawrie 1998a).

2.5 GEOLOGY

2.5.1 Regional Geology

Geology for the area is presented in Figure 2.6 and is summarised in Table 2.1. The description of the regional Geology has been extracted from the Cobbora 1:100,000 Geology Sheet 8733 (Meakin et al. 1997).

Basement in the region is formed by Palaeozoic units of the Molong Volcanic Belt. This is a horst structure within a regionally extensive north-south trending zone of intensely deformed rocks known as the Lachlan Fold Belt.

The Palaeozoic units consist of Ordovician to Permian low grade regional and contact metamorphosed igneous, volcanic, and sedimentary rocks. These units have been strongly folded and faulted so that they lie juxtaposed against and often truncated by each other, in north-northwest trending meridional belts. Commonly, lithological boundaries are faulted contacts, which have experienced multiple phases of reactivation.

A number of regional northwest trending faults are shown on the Cobbora 1:100,000 geological sheet. In addition, a series of northeast trending regional structures are interpreted from the regional airborne

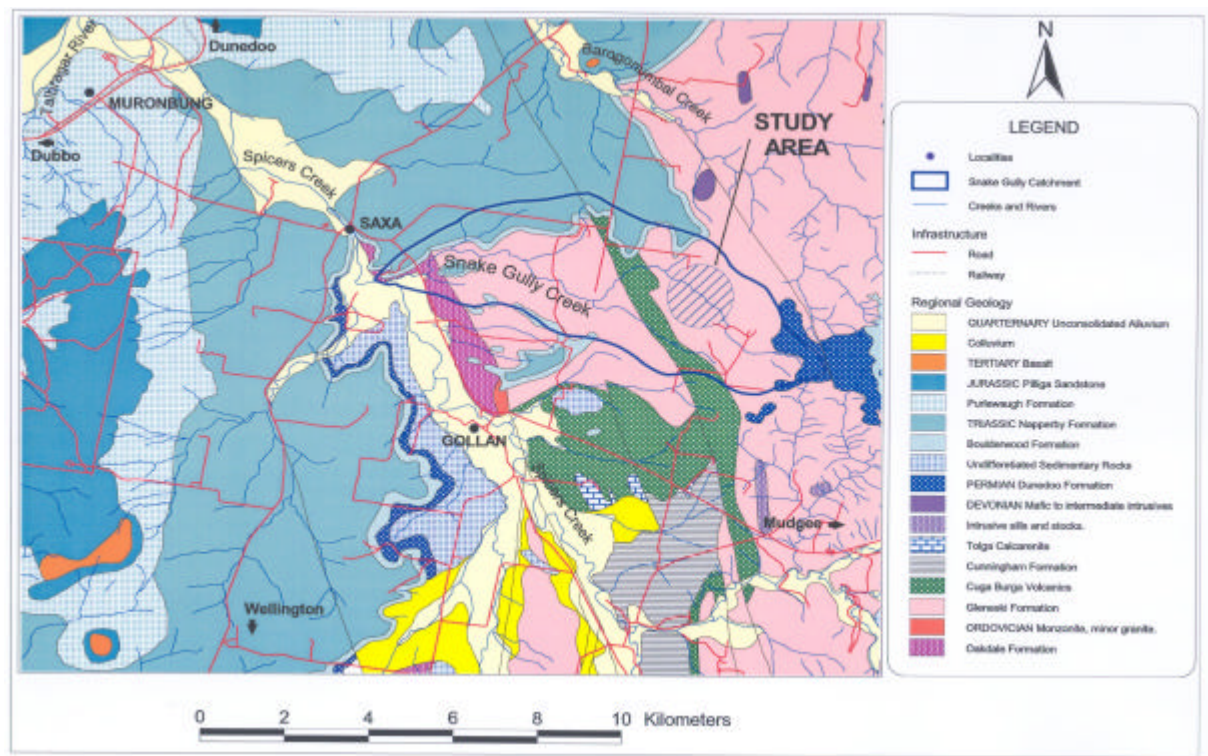


Figure 2.6: Regional Geology

magnetics (NSW Department of Minerals and Energy, Discovery 2000) flown at 200, 250, and 400 metre line spacings across the area.

The Palaeozoic units outcrop in the central and southern areas of the region. Three main Palaeozoic units occur in the Snake Gully catchment.

The Oakdale Formation in the Cabonne Group consists of basalt, andesite, latite, and associated volcanoclastic and sedimentary rocks. The Silurian Gleneski Formation of the Mumbil Group unconformably overlies the Oakdale Formation, frequently with a faulted contact. The Gleneski Formation consists of felsic rhyolitic and latitic volcanics and volcanoclastic sedimentary rocks. The Gleneski Formation is conformably overlain by the Devonian Cuga Burga Volcanics, a sequence of intermediate latitic volcanics and volcanoclastic sedimentary rocks, and minor carbonate rocks.

The Ordovician Oakdale Formation occurs in the west of the Snake Gully catchment and is faulted against a central band of Silurian Gleneski Formation. In the east of the catchment, faulting and folding have repeated the Gleneski Formation and included part of the younger Devonian Cuga Burga Volcanics.

During the Permian and Triassic, a series of sediments were deposited unconformably over the Palaeozoic basement into the Sydney-Gunnedah Basin. Late Permian coal swamps developed in a foreland basin forming the economically important Illawarra Coal Measures further east and the equivalent Dunedoo Formation in this region. After a hiatus, alluvial sediments (Boulderwood Formation) and fluvio-lacustrine to deltaic sediments (Napperby Formation) were deposited during the Early to Middle Triassic.

A period of erosion preceded deposition of fluvio-lacustrine quartzose sediments into the Surat Basin during the Jurassic (Purlawaugh Formation, Pilliga Sandstone). These sedimentary rocks form part of the Great Artesian Basin.

Regionally, the Permian and Mesozoic sequences thicken and dip to the northwest. Locally, bedding in the units is gently dipping with variable orientation. These sedimentary rocks outcrop on hills and slopes, and form broad flat to gently undulating plateaus. Remnant rafts of these units often sit atop hills, forming mesa-like landforms. The units develop low escarpments or cliffs adjacent to rivers and

Table 2.1: Stratigraphy of the Snake Gully Region

Era Ma	Period	Formation	Description
CAINOZOIC 0 - 65	QUATERNARY		Unconsolidated alluvial, colluvial and aeolian sand, silt, clay and gravel.
	TERTIARY		Tholeiite, alkali basalt, alkali ultramafic dykes, plugs, and sills.
MESOZOIC 65 - 250	LATE JURASSIC	Pilliga Sandstone	Massive to cross-bedded coarse pebbly lithic-quartz sandstone, minor lithic sandstone, and siltstone.
	EARLY TO LATE JURASSIC	Purlewaugh Formation	Ferruginised red siltstone, carbonaceous mudstone, fine to medium grained lithic sandstone, ironstone, minor coal.
	EARLY TO MID TRIASSIC	Napperby Formation	Siltstone thinly interbedded with fine to medium grained lithic-quartz sandstone, minor conglomerate; coarsening up sequence.
	EARLY TRIASSIC	Boulderwood Formation	Thick-bedded quartz-lithic conglomerate, coarse pebbly quartz-lithic sandstone, and siltstone.
PALAEOZOIC	LATE PERMIAN	Dunedoo Formation	Pebbly quartz-lithic sandstone to conglomerate, white claystone, and coal.
	DEVONIAN		Mafic to intermediate intrusives, sills and stocks.
	EARLY DEVONIAN	Cuga Burga Volcanics	Mafic to intermediate lava and intrusives, lithic volcanoclastic sandstone, breccia, siltstone, shale, and allochthonous limestone. Minor rhyolitic ignimbrite and quartzose sandstone.
	LATE SILURIAN	Gleneski Formation	Rhyolitic, felsic to latitic lava, intrusive, tuff and volcanoclastic sandstone.
	LATE ORDOVICIAN	Oakdale Formation	Andesitic-latitic volcanoclastic siltstone, sandstone, conglomerate, breccias, minor primary volcanics and hematite/magnetite bodies.

major creeks at the margins of the plateaus.

An episode of intraplate basaltic lava eruption in the Tertiary period produced sills, plugs, and flows. These have been dated at 12.5 million years in the Dubbo region. The magma solidified in plugs forming small hills and flows along topographic lows. In the present landscape, softer sedimentary sequences have frequently been eroded away, leaving more resistant basalt capped hills.

Records from boreholes drilled in the region indicate that basalt occurrences may be more widespread than is shown by published geological mapping. Dubbo and Geurie are thought to have formed eruptive centres in the region. DLWC groundwater bore records note numerous unmapped water bearing basalt sills in the Dubbo locale. Regional airborne magnetics suggest several magnetic bodies at depth below sedimentary strata that may represent sub-volcanic basaltic plugs.

A layer of expandable lattice clays typical of those weathered from mafic units occurs in many of the regional valleys. Murphy & Lawrie (1998a) state that the source of these clays was erosion of the basalt units during the late Tertiary and Quaternary.

A variety of unconsolidated alluvium, colluvium and aeolian sediments were deposited during the Quaternary period on mid-slopes and valley floors by rivers, surface run off, gravity, and wind.

2.5.2 Local Geology

The Snake Gully catchment sits at the margin of the Sydney-Gunnedah Basin and Palaeozoic Lachlan Fold Belt rocks.

Palaeozoic basement geology at the site is mapped as Silurian 'Gleneski Formation' (described above). This is exposed in the creek bed at several locations upstream of the study site, where it outcrops as a slightly weathered to fresh, steeply east dipping, north-south trending, strongly foliated, grey, cream, pink and orange, felsic siltstone. It contains silicified lenses and bedding parallel quartz veins up to 20 cm wide.

Permian sedimentary rocks of the Dunedoo Formation outcrop at the head of the catchment. Triassic sedimentary rocks of the Napperby and Boulderwood Formations form the northwestern catchment boundary and outcrop locally on hilltops approximately one kilometre northwest of the study site. These units dip gently east and are composed of fine to conglomeratic sandstone, and siltstone. In many places, the siltstone and finer sandstones have been strongly ferruginised.

2.6 REGIONAL HYDROGEOLOGY

Schofield (1998) examined groundwaters in the Ballimore region extending from the city of Dubbo in the west, to Dunedoo in the east; and from Bodangora in the south, to Boomley in the north. His study incorporates the whole of the Spicers Creek and Snake Gully catchments. He identified a regional and a local groundwater flow system, with groundwater being controlled by stratigraphy and structure in these systems.

The regional groundwater system is restricted to the metamorphosed Palaeozoic basement rocks and is an isolated Na-Mg-Cl-rich system that does not mix with the local system. The local system is divided into three cells. The deep Na- HCO_3 -rich cell consists of late Permian and early Triassic sedimentary rocks, with groundwaters derived from meteoric recharge mixing with CO_2 of magmatic origin. The intermediate cell consists of Napperby and lower Purlawaugh Formations, and the shallow cell consists of Pilliga Sandstone and Tertiary and Quaternary sediments. The intermediate and shallow cells contain Na-Cl-rich groundwaters (Schofield 1998).

Schofield (1998) regarded the intermediate cell of the local groundwater system as containing a continuum of mixing between the shallow and deep cells in that system, resulting in a variety of water types and



Figure 2.7: Vegetation Species Zonation With Increase in Soil Salinity



Figure 2.8: Sheet Erosion At Study Site Prior To Rehabilitation

salinities throughout the intermediate cell.

2.7 SALINITY INDICATIONS

There are clear indications of land and water salinisation in the Snake Gully catchment. Salts effloresce on soils adjacent to the creek line and on the erosional face within the creek. The creek has an electrical conductivity of approximately 6 dS/m when running. The creek water is clear, indicating flocculation of suspended clays due to high dissolved salt content.

Other characteristic features include many native and exotic salt and waterlogging tolerant species. These occur on hillslopes in or close to the drainage lines. These species often display zonation, one species replacing another as soil salinity changes. Common species include annual beard grass (*Polypogon monspeliensis*), sea barley grass (*Hordeum marinum*), sand spurrey (*Spergularia* sp.), and couch (*Cynodon dactylon*). Cumbungi (*Typha* sp.) is common in the creek line. Secondary indicators of salt affected areas are active sheet, rill, and gully erosion, caused by sodic dispersive soils.



Figure 2.9: Salt E² orescence on Edges of Incised Channel



Figure 2.10: Salt E² orescence

Chapter 3

LANDSCAPE SALINISATION AND MANAGEMENT

Climate change during the late Tertiary and Quaternary has had a major influence on the sedimentary history and salinisation of the Murray-Darling Basin (Ghassemi et al. 1995). Changes brought about by human occupation have further impacted the landscape.

3.1 AUSTRALIAN LANDSCAPE EVOLUTION

3.1.1 Quaternary Climate Change

The late Cainozoic has been a period of significant world climatic fluctuation (Bowler 1990). During the late Tertiary and Quaternary, a global pattern of climatic oscillation was established. This appears to be linked to cyclical changes in the earth's orbital path around the sun and in the tilt of the earth's axis (Williams et al. 1993).

In particular, the Quaternary was a period of frequent and rapid changes in climate (Williams et al. 1993). By comparison with earlier Tertiary climates, those of Quaternary times have been dry, relatively cold and climatically unstable (Bowler 1976). These climatic oscillations have been attributed to the present expression and diversity of arid features recorded in the dunes, lakes and soils over large areas of the arid and semi-arid zone of Australia (Bowler 1976).

According to Bowler (1990) at the start of the Pliocene, six million years ago, the climate was relatively wet, with high summer rainfall. The sea covered large areas of the Murray Basin and rainforest extended across the landscape. During this time, significant groundwater recharge must have occurred (Young et al. 2002). Four million years ago, the climate became drier, the sea began to retreat and vast inland lakes developed (Bowler 1990).

Cores from Lake George indicate that lake levels began to oscillate between full-lake and lake-dry conditions from 2.5 million years ago, suggesting the development of a new pattern of oscillatory wet-dry climates. With the transition into the Quaternary, about 1.2 million years ago, changes in lake sedimentation rate indicate amplification in the magnitude of these oscillatory climate events (Bowler 1982).

Over the past million years, the inland lakes began to dry up and the climate underwent a series of very intense oscillations (Bowler 1990). A characteristic cycle of slow cooling and build-up to full glacial conditions was followed by rapid warming, ice melting and deglaciation. This resulted in cold, dry and windy glacial maxima alternating with warm, wet interglacials (Williams et al. 1993).

The onset of a drier climate, which alternated between arid and semi-arid conditions took place around 500,000 years ago. Dramatic changes in the pattern of sedimentation accompanied the increasing aridity (Evans et al. 1990).

From 50,000 to about 30,000 years ago, the surface depressions of the Murray Basin were full of fresh water. This period has been termed the Mungo lacustral phase (Bowler 1976). Prior to 25,000 years before the present (BP) lake levels and watertables were high and desert dunes were relatively stable (Bowler 1976).

Between 36,000 and 25,000 years ago a substantial change occurred. The availability of surface water diminished, watertables began to fall and lakes became partially dry with increased salinity (Bowler 1990).

From 25,000 years ago, conditions became much colder and drier, leading up to the Last Glacial Maximum at about 18,000 years ago. This marked the commencement of a major period of aridity, which continued until 13,000 BP. The causes of major aridity are greatly intensified atmospheric circulation aided by increased continental extent corresponding to glacial low sea levels and reduced seasonal precipitation (Bowler 1976).

The trend towards aridity in the Quaternary reached its peak about 18,000 - 16,000 BP, during the Last Glacial Maximum. Mean annual temperatures were between 3 and 10 degrees lower than present, and mean annual precipitation was 30 to 50 percent lower (Wasson & Donnelly 1991). Lake levels and precipitation to evaporation ratios were low at this time. On the drying lake floors groundwater discharge continued as a delayed response to the previous period of a much wetter climate (Bowler 1976; Evans et al. 1990).

In the more arid playas, during periods of low water level, seasonal exposure of saline mud flats permitted the efflorescence of salts, especially halite and gypsum, breaking clays into pelletal aggregates (Bowler 1976).

Wind speeds during the Last Glacial Maximum were higher than present. In Tasmania, it is estimated that sand shifting winds were two and a half times more frequent than at present (Bowler 1983). During this period, the substantial intensification of prevailing westerly winds constructed clay and gypsiferous dunes on the shores of playas in Western Australia, Lake Frome, and south-eastern Australia (Bowler 1976).

Conditions remained cold and arid until 12,000 years ago. Rapid post-glacial warming appears to have preceded an increase in precipitation so that maximum aridity is expressed in many pollen diagrams at about 13,000 years ago. By about 9,000 years ago, lake levels were generally rising but not at their peaks, and dune building was minimal. Temperature began to rise after the Last Glacial Maximum and peaked at about 6,000 BP, along with precipitation (Wasson & Donnelly 1991).

The period at 6,000 BP is well marked in almost all natural records of the Holocene environment. Mean annual temperatures were between 0.5 °C and 2 °C higher than present. Pollen records from Tasmania imply higher than present precipitation. Lake levels were at their highest, and the precipitation to evaporation ratio peaked at this time. Increases of mean annual precipitation of between 20 and 50 percent are suggested from lake water balance combined with pollen records (Wasson & Donnelly 1991). Young et al. (2002) suggest that groundwater recharge in the Namoi Alluvial Plain region of NSW was much more rapid 6000 years ago than at present.

About 2,000 years ago, the climate became cooler and drier than the immediately preceding and present day periods. New South Wales had become cooler by as much as 3 °C. Inland, the climate was close to that of today, and was a period of renewed dune construction. Aboriginal burning may have contributed to this dune building (Wasson & Donnelly 1991).

Particularly mild temperatures were dated between 1,200 AD and 1,400 AD, and are referred to as the 'Medieval Warm period'. Sudden chills have been identified as interrupting the glacial interlude, the most recent lasted 400 years, from approximately 1,400 AD to 1,800 AD. This period has been termed the 'Little Ice Age' with global temperature 0.5 °C to 1.0 °C lower than today (Crowley 1996; Melis 1998).

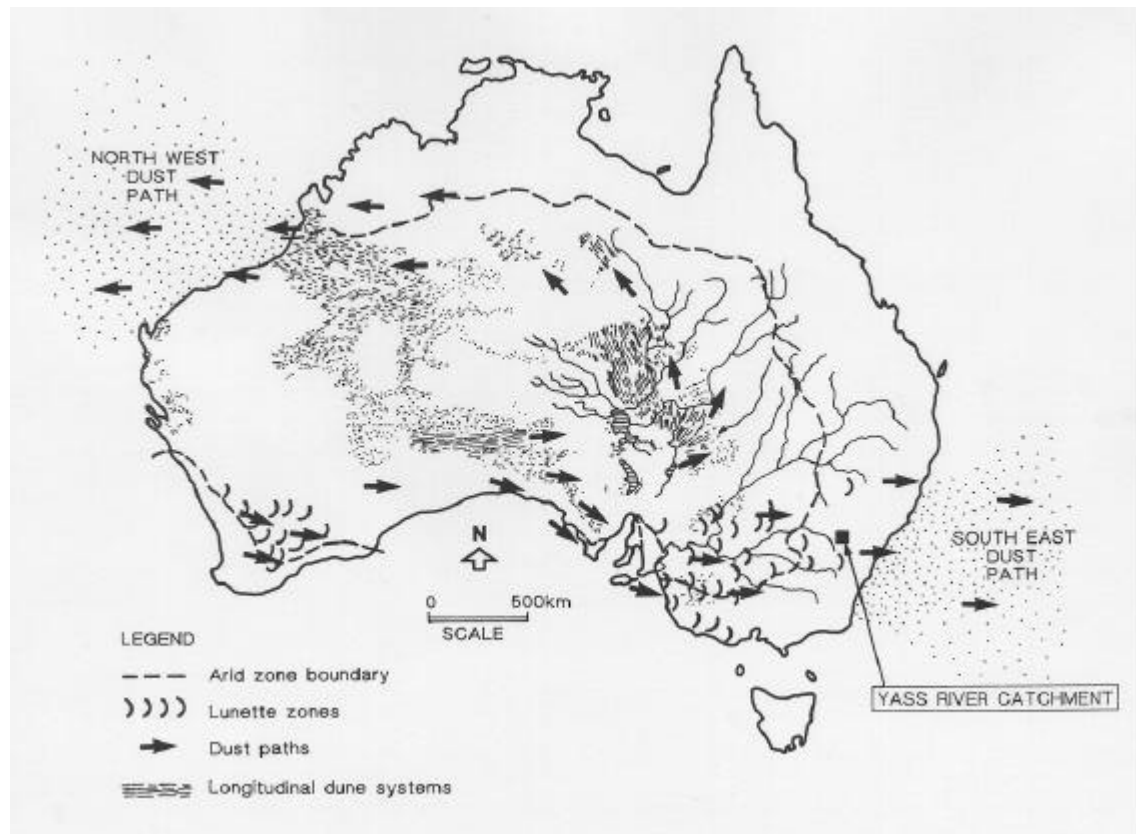


Figure 3.1: Quaternary Dust Paths

3.1.2 Glacial Aridity and Dust Generation

A growing body of evidence from deep-sea cores, lake deposits and ice cores shows that times of lowest world temperature during the Quaternary ('glacial maxima') were times of greatest aridity on land. These periods generated massive export of desert dust offshore, and even to New Zealand and central Antarctica (Williams et al. 1993).

Earlier aeolian episodes in glacial periods are indicated about 120,000 and 300,000 years ago; however, the Last Glacial Maximum was the major period of aridity and dust generation experienced in Australia throughout the past 100,000 years (Bowler 1976). Australia has experienced later trends in aridity and associated dust transport between 6,000 to 3,000 BP, and within the last 2,000 years, but these have been much closer to the range of present climatic regime (Bowler 1976).

Based on dune orientations, Bowler (1976) proposed that two major Australian dust transport pathways were formed during the period 25,000 to 13,000 BP (Figure 3.1 after McTainsh (1989)).

McTainsh & Lynch (1996) suggest dust entrainment and transport rates were up to 52% higher in the Pleistocene in south-eastern Australia, and Wasson (1986) estimated wind speeds at the Last Glacial Maximum between 120% to 150% higher than present mean wind speed.

McTainsh (1989) highlighted the importance of finer grain sized aeolian suspension processes, in addition to saltation type dune building processes. He suggested that sediments were supplied to these dust paths via the internally draining river systems and lakes of Lake Eyre and Murray-Darling Basins. Supplies of alluvial sediment to the south-eastern dust path would have been enhanced by a sediment feedback relationship between aeolian and alluvial systems, in which dust deposition over the eastern headwaters of the Murray-Darling Basin supplied fine sediment to the rivers, which in turn discharge westwards to resupply dust source areas.

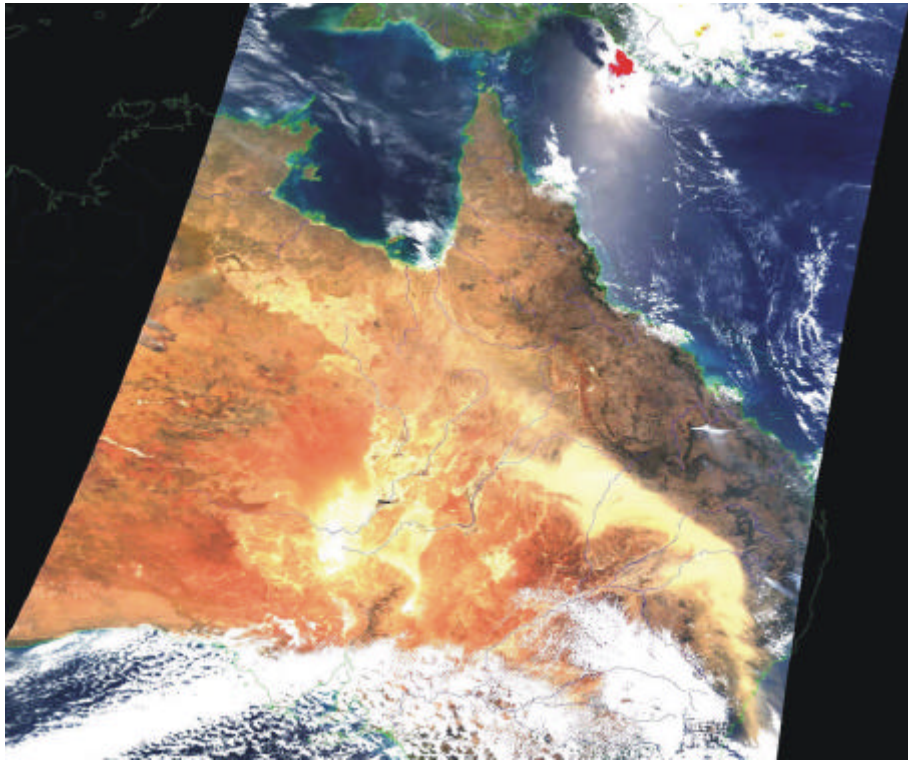


Figure 3.2: Dust storm over eastern Australia - 23 October 2002



Figure 3.3: Gri±th - 12 November 2002



Figure 3.4: Modern dust activity near Narromine - 12 November 2002

Recent studies of these dust pathways and associated processes (Knight et al. 1995; Kiefert 1995) indicate that they persist today, although their position and intensity may be different from the past (Sprigg 1982). Figure 3.4 shows a dust storm that occurred near Narromine in central NSW (Figure 3.4 courtesy of W. Radburn).

3.1.3 Aeolian Entrainment and Landscape Accession

Large tracts of the continent have been traversed by dust-laden winds, and the soils in these areas have received a large input of dust (McTainsh 1989). Hesse (1994) concluded that sedimentation in the Tasman Sea, and Pacific and Indian Oceans, correlated well with the two dust paths.

A study by Hesse (1994) used marine sediment oxygen isotopes in deep sea cores taken from the Tasman Sea to determine chronologic sequence and mass accumulation rate of aeolian dust. This work confirmed that, in glacial periods, the flux of dust to the Tasman Sea, increased by between one-and-a-half and three times in response to increased deflation in the interior of south-eastern Australia.

Further, Hesse (1994) reported low fluxes of dust coming from Australia prior to 350 000 which were followed by an increase around 350 000. High fluxes of dust occurred in peak glacial periods thereafter. Hesse (1994) concluded that the initiation of higher dust fluxes around 350 ka was consistent with previous estimates of the age for onset of aridity in the source area.

Walker & Costin (1971) showed that modern dust from inland Australia is often carried to the humid continental margin during droughts. They sampled reddish dust deposited in snow in the Mount Kosciusko region following a severe drought and extensive dust storms in 1968. They found that the dust had a median diameter of 4 microns, and had annual accession rates of up to 1,515 kg/ha. They noted that dust storms of sufficient magnitude to affect the eastern highlands of Australia in this way have occurred with a frequency of at least once in twenty years during the twentieth century.

Further, Walker & Costin (1971) suggested that if dust was deposited once in twenty years at this rate,

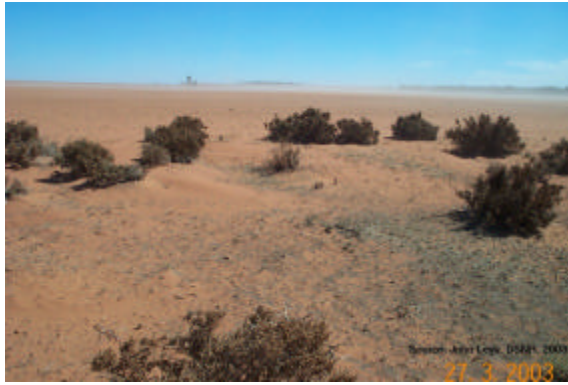


Figure 3.5: Recent dust activity in Western NSW - March 2003 - accumulations behind vegetation



Figure 3.6: Recent dust activity in Western NSW - March 2003 - accumulations behind stock fences

Table 3.1: Studies Reporting Significant Aeolian Contribution to Landscape in South-Eastern New South Wales

Author	Location of Studied Deposit
Butler and Hutton 1956	Riverine plain south-eastern Australia
Butler 1958	Riverine plain south-eastern Australia
van Dijk 1958	Grieth-Yenda, NSW
Beattie 1970	Eastern Riverina, NSW
Beattie 1982	Wagga Wagga, NSW
Butler 1982	SE Australia
Chartres and Walker 1988	SE Australia
Broughton 1992	Dicks Creek and Begalia, Yass, NSW
Summerell et.al. 2000	Young, NSW
Chen 2001	Wagga Wagga, NSW
Williams et.al. 1991	Central western NSW
Melis 1998	Dicks Creek, Yass, NSW
Melis and Acworth 2001	Dicks Creek, Yass, NSW

then 19 to 113 tonnes/ha of dust would have accumulated during the 15,000 years of post glacial time. They concluded that an increment of this order of magnitude would certainly modify the nature of a soil profile.

Butler (1956) was the first to suggest that extensive regions of south-eastern Australia had been affected by deposition of clayey aeolian material generated in arid phases of the Pleistocene due to climate fluctuation. He termed the material 'parna', noting that it consisted of clay aggregates, not primary mineral particles, which was distributed in a direction from west to east as numerous uniform sheets.

Parna-type deposits have subsequently been reported in many areas of south-eastern New South Wales. A summary of references to studies reporting significant aeolian contribution to this part of the landscape is given in Table 3.1.

Recent studies indicate that soils in central and northern New South Wales have also been affected by addition of aeolian materials. Images showing recent accumulations of dust during the March 2003 dust storms in western NSW are shown in Figure 3.5 and Figure 3.6. These images were taken by John Lees of DNSR.

Townsend (1997) sampled soils on hilltops overlying a variety of topographical and lithological types in the Eastern Highlands and Macquarie River plain in central NSW. A number of his study sites were in the Wellington area. He identified discrete mineral grains consisting dominantly of quartz with a

characteristic grain size mode of 30 to 40 microns. Based on particle size distribution, composition and rounding, Townsend concluded that this material was loess, of distal aeolian origin. He suggested that up to 25% of the soils in the Eastern Highlands and Macquarie Plain have an aeolian content.

Young et al. (2002) published results of geomorphological studies on the Namoi Alluvial Plain in north-western NSW. They found that almost 60% of sediment samples analysed had over 10% of their grain size distribution in the 20 to 50 micron range, indicating an aeolian origin. From thermoluminescence dating, Young et al. (2002) concluded that there had been significant aeolian input to that area throughout the late Quaternary.

3.1.4 Defining and Identifying Aeolian Materials

Mean grain size of a sediment is a function firstly, of the size range of available materials, and secondly the amount of energy imparted to the sediment, which depends on current velocity or turbulence of the transporting medium. It does not necessarily depend on distance from source (Folk 1980).

Sorting (range of grain sizes) depends on the size range of material supplied, the type of deposition and working, current characteristics, and rate of supply of material compared with the efficiency of the sorting agent (Folk 1980).

Single source sediments tend to have normal grain size distribution curves, while sediments from multiple sources show pronounced skewness and kurtosis. Aeolian deflation sediments are commonly bimodal (Folk 1980).

In 1974, Butler refined his description of parna, proposing that the complex subdivisions of aeolian materials were related to provenance, with aeolian clays having their origin in regions with a high proportion of clay, whereas coarser grained aeolian materials, termed loess, originated in regions low in clay but high in 25 to 30 micron (medium silt) sized material. He indicated that aeolian clay was composed of greater than 30% clay particles aggregated into silt to fine sand sized particles.

Butler (1974) noted that a discrete mineral "companion" grain of similar size to the clay aggregate often occurred in the material, dependant upon its availability at the source. He concluded:

"...that absence of a companion material could not be taken as disproof of the aeolian nature of a clay, and that the lithologic and stratigraphic relations of the aeolian clays is their adequate proof, namely a generally uniform layer of clay material overlying a variety of topographic and lithological situations."

Dare-Edwards (1984) proposed that loessic clay was characterised by a bimodal particle size with a peak in the clay-sized fraction (< 2 micron) and another in the silt-sized fraction.

Townsend (1997) recognises that dust is derived from many sources from proximal to distal, and that the source dictates dust composition and size, highlighting the difficulties with identifying aeolian additions to soils. This is because soil classification schemes generalise and minimise dust processes, and tend to rely on morphological soil descriptions, rather than use of grain size analysis techniques and examination of soil formation history (Townsend 1997). The micro-size of aeolian dust (which has usually been amalgamated with local soils) limits direct field identification, unless detailed grain size analyses, requiring painstaking preparation, are conducted.

Townsend (1997) presented a model for identifying aeolian dust. He concluded that a mode of 30 to 40 micron (silt-size), consisting > 10% quartz grains, was definitive of aeolian materials in the Eastern Highlands and Macquarie River plain. Using the terminology of Butler (1974), this material might also be interpreted as a 'companion' silt.

A notable point with the conclusion of Townsend (1997) is that all of his samples were collected from hilltops. Exposure of aeolian materials after deposition, but prior to entrainment, would almost certainly

Table 3.2: Generalised Late Quaternary Piedmont Stratigraphy in the Belarbon-Nulchara Lake Region, Showing Major Phases of Aeolian Dust Influx to the Area

Deposit	Age Estimation (years BP)	Major Environmental Influences
Alluvial sands and gullyng	<150	European occupation, climatic events
Alluvial and aeolian sands	400 - 3,800	Aboriginal fires
	7,100 - 7,500	High lake levels
Pedogenic carbonate	13,500 - 15,500	Calcareous dust
Alluvial and aeolian sands	16,000 - 18,000	Deflation, and gypsiferous lunette construction
Pedogenic carbonate	24,000 - 32,000	Calcareous dust
Alluvial and aeolian sands	>32,000	

have further modified their grain size characteristics. The effects of wind and surface water winnowing of fines from hilltops is unknown, but highly probable. Aeolian materials in valleys might be expected to have different characteristics to those preserved on hilltops.

3.1.5 Soil Formation Processes

Over large areas of Australia, successive stable soil forming phases have alternated with fluvial or aeolian depositional and erosional episodes (Butler 1974). It is clear that aeolian dust processes have played a major role in the evolution of the Australian landscape (Butler 1974; McTainsh 1989; Williams et al. 1991; Williams et al. 1993; Knight et al. 1995).

Numerous workers have suggested an association of calcrete (a carbonate-cemented crust) with aeolian deposits in eastern Australia. The evidence is summarised in Milnes & Hutton (1983) and includes contributions from many workers in the field.

Based on lithostratigraphic mapping, Williams et al. (1991, p. 276) present a summary of late Quaternary stratigraphy and major erosional, depositional and pedogenic events in central western NSW. These events are partially dated by radiocarbon and thermoluminescence techniques. A summary of the units defined by Williams et al. (1991) and Williams et al. (1991) is presented in Table 3.2.

Williams et al. (1991) determined that deposition of aeolian materials around 45 ka, was followed by an influx of calcareous dust and development of calcareous soils. The source of the dust was further west or southwest from the Nullabor Plain, playa floors, calcareous desert soils and possibly the continental shelf. Solution and reprecipitation of this dust was responsible for the development of massive calcretes and calcareous B soil horizons containing rhizcretions and nodules in a variety of prior sediments.

Active deflation during the last Glacial Maximum resulted in lunette construction towards 18 - 16 ka. Erosion was widely prevalent thereafter until about 5.5 ka, when strong unidirectional winds, sparse riparian vegetation, and a steady supply of channel sand resulted in source-bordering dunes. Mid to late Holocene, dune development continued relatively constantly until about 0.6 ka, after which the supply of quartz sand was curtailed, and erosion of pre-existing dunes and sand sheets began (Williams et al. 1993).

Williams et al. (1991) found that present stream beds were adjacent but not immediately coinciding with position of prior streams. They also observed that during the last hundred or so years, many previously shallow channels have become deeply incised by narrow, steep-walled gullies. They believe that this episode of vertical erosion coincided with the advent of European settlement in the region, and might be genetically linked to early pastoralism and associated clearing of native trees and a change in fire regime. Equally, they concluded that it might reflect a change in drought frequency, or in the seasonal influence of rainfall.

Table 3.3: Age and Sequence of Cainozoic Deposits in Upper Dicks Creek, Yass

Unit	Age Estimation (years BP)	Palaeoclimate	Description	Possible K cycle
Unit One (silts and sands)	<250	Humid moist interglacial	Contemporary alluvial	-
Unit Two (sandy silty loam)	250 - 1,200	Drier, cooler, interglacial interlude	Debris flow (plus alluvial)	K2
Unit Three (clayey silts and sands)	26,000 - 34,000	Dry, arid, windy, glacial	Debris flow	K3
Unit Four (silt)	>50,000	Unknown (possibly arid, glacial)	Basal gravity flow	K5

Downes (1954) claimed that salinisation and subsequent desalinisation during the wetter conditions between arid periods have produced solods, solodic, and solonized soils over large areas of south-eastern Australia.

In the vicinity of Canberra, van Dijk. (1959) described a number of depositional beds in the soil profile, which he related to the 'K cycles' of Butler (1959). The K cycles represent phases of erosion and deposition caused by alternating periods of landscape stability and instability.

Beds which van Dijk. (1959) equated with the Kurrumbene K2, Piallago K3 and Gundaroo K4 cycles contained extensive unsorted hill-wash and mud-flow material. He described the lowest Mugga K5 cycle material as being stable in water, forming deep erosion ravines and stream beds, non-cracking, variably calcareous, and containing voids.

Strongly developed soil features were noted by van Dijk. (1959) separating the various K cycle beds, giving evidence of long periods of quiescence between the phases of vigorous erosion and deposition. He concluded that five main cycles of landscape instability and soil formation had occurred, and that the cycles were initiated by past climatic fluctuations.

Broughton (1992) conducted salinity and geological studies in the Dicks Creek and Spring Creek "Begalia" sub catchments in the southern Tablelands of NSW. She indicated that montmorillinitic silt-sized quartz-rich sediments mantled a diversity of Palaeozoic basement rocks.

Based on mineralogy, Broughton (1992) suggested that these montmorillonite rich deposits could not have been derived from in-situ weathering of the siliceous Ordovician basement rocks. From sedimentological studies, Broughton concluded that the deposits possessed an aeolian component that had later been redeposited by debris flows.

Acworth et al. (1997) supported the hypothesis of Broughton (1992) that reworking of aeolian material as debris flows played a part in the formation of colluvial units occurring in the Yass River catchment. Acworth et al. (1997) suggested that the debris flow emplacements might correlate with climatic variations in the Pleistocene.

Melis (1998) and Melis & Acworth (2001) described four unconsolidated sedimentary units resulting from erosional/depositional cycles at Dicks Creek, Yass. These units form a sequence and were numbered from Unit One (the youngest) to Unit Four (the oldest and lowest). The units are spatially discontinuous, and are separated from each other by erosional unconformities. Melis (1998) suggests that Units Two, Three and Four might relate to the K cycle units observed by (van Dijk. 1959).

Melis (1998) determined that Unit Three was highly dispersive, and obtained radiocarbon dates for Unit Two from dispersed charcoal. A summary of the unconsolidated sedimentary units described by Melis (1998) and Melis & Acworth (2001) is given in Table 3.3.

Melis & Acworth (2001) suggested that Units Two, Three and Four have an aeolian component based on clay mineralogy contrasts with basement, and a grain size modality of fine sand to very fine silt. They calculated a simple sediment budget for Unit Two that suggested aeolian deposition in the order of 4 - 8 t/km²/yr.

3.1.6 Links of Aeolian Material With Salinity

Many studies have been conducted which infer or demonstrate a connection between aeolian materials and salinity processes (Downes 1954; Butler 1956; van Dijk 1969; Broughton 1992; Nicoll & Scowan 1993; Acworth et al. 1997; Jankowski & Acworth 1997; Evans 1998; Melis 1998; Melis & Acworth 2001; Ladanay-Bell & Acworth 2002).

Downes (1954) proposed that during arid periods of the Quaternary, interludes of low rainfall enabled salt to be accumulated in areas in south-eastern Australia. He regarded the majority of these salts to be cyclic and oceanic sourced, but acknowledged that salts were also brought in by southerly and south-westerly winds. In his classic work defining *parna*, Butler (1956) noted that this clayey aeolian material could be high in salts.

During soil studies in the Yass Valley, van Dijk (1969) noted a high percentage of salting had developed in elevated positions on hillslopes well beyond the influence of the groundwater bodies in the valleys. He believed this to indicate a major upland source of salt. He observed that most of the recent salting seemed to be caused by redistribution of relict salts that originally accumulated on ancient strath floors. He concluded that subsequent landscape dissection had left the salts stranded in the present elevated sites, from which they were released in large quantities during periods of sudden heavy rainfall following prolonged severe drought.

Evans (1998) supported, and further explored, the hypothesis that salts in the Murray-Darling Basin Uplands have been derived from accession of wind borne salts derived by groundwater deflationary processes over 300,000 years in the geological Murray Basin. He highlighted that the abundance of chloride in present day landscapes was orders of magnitude greater than what could be supplied from the chloride concentrations of Palaeozoic rocks. In addition, extensive ³⁶Cl analyses (which has a half life of 300,000 years) showed that the chloride found in the groundwater systems of the Lachlan Fold Belt were greater than zero. He indicated that this was at odds if the chloride were in fact Palaeozoic in origin and many millions of years old. Consequently, (Evans 1998) proposed that rock weathering supplied little salt to a catchment's total salt mass.

Broughton (1992) found high levels of chloride in shallow groundwaters within unconsolidated sediments formed by debris flows at Dicks Creek and Spring Creek "Begalia", Yass. Broughton proposed that chloride salts were introduced from the aeolian component of these sediments.

Nicoll & Scowan (1993) mapped the distribution of the debris flow deposits identified by Broughton (1992) throughout the Yass catchment, and concluded that these were the main source of salts in many areas, consequently those areas containing aeolian derived debris flows were predisposed to dryland salinity.

Melis & Acworth (2001) reported 1:5 extract fluid conductivities in excess of 4.7 dS/m irregularly distributed throughout Unit Two, and variable 1:5 extract fluid conductivities up to 1 dS/m from Unit Three.

Melis (1998) showed that electrical resistivity imaging successfully distinguished Ordovician bedrock from overlying conductive clay rich Cainozoic deposits. He determined, however, that this technique could not identify individual units, and indicated that accurate contact depths required confirmation by drilling. Typically, the Cainozoic deposits contained conductivities in the range 20 mS/m to 60 mS/m, with background bedrock conductivities generally less than 10 mS/m. This corresponded with electrical conductivity of aqueous 1:5 extracts, and that measured by resistivity imaging.

Acworth et al. (1997) and Jankowski & Acworth (1997) proposed an alternative model of salt accumulation for Yass, in which salt was imported into catchments with silt during dust storms in the arid and

windy conditions of the last glacial.

Acworth & Jankowski (2001) published results of a detailed salinity study at Dicks Creek, Yass, NSW. The study involved drilling, geophysics, hydrogeochemistry and groundwater monitoring over a ten year period. Based on the results, they further refined the model proposed earlier (Acworth et al. 1997). They found a highly heterogeneous distribution of salt, mostly related to swelling clay, and that dispersion of the clay caused the surface features commonly associated with dryland salinity. They reported that hydrogeochemical evidence did not suggest evaporative or transpirative concentration of salt in the groundwater, and the short flow path from the top of the catchment could not provide a significant source of salt from bedrock weathering.

Ladanay-Bell & Acworth (2002) presented results from hydrogeological and hydrogeochemical investigations in the Coleambally Irrigation Area, NSW. They suggested that salinisation of the shallow groundwater system is associated with dissolution of significant salt stores in the previously unsaturated Shepparton Formation via rising groundwater table levels. Salt balance modelling did not support evaporative concentration of rainfall or applied irrigation water as a model for salinity in the area. They hypothesised that the salts result from dust activity and aeolian deposition of salt-laden parna, sourced from saline lakes and playas in the Mallee Plain during the Quaternary.

Hydrogeochemical modelling (Ladanay-Bell & Acworth 2002) indicated that chemical reactions occurring include dissolution of halite, calcium and gypsum, and ion exchange. They proposed that these were consistent with a model of saturation of sediments composed of alluvial and salt-laden aeolian derived materials.

3.1.7 The Role of Groundwater in Salinisation

Broughton (1992) indicated that the parna-rich debris flow deposit confined the bedrock aquifer, causing an increase in hydraulic head, and penetration of the artesian water through cracks in the parna-rich deposit brought salts stored in the saturated clay layer to the surface.

Jankowski & Acworth (1997) described the impact of the parna rich debris flow deposits at Yass on salinity processes. They established that groundwater in the underlying fractured bedrock was dominated by Mg and SO_4 ions, was relatively fresh, and discharged slowly upwards through the debris flow clays. They also demonstrated that the deep discharging groundwater reacted with the clay material and that ion-exchange reactions, redox reactions, and the dissolution of entrained salts occurred. These authors noted that the absence of a constant ratio between sodium and chloride, as total dissolved solids (TDS) increased, indicated that concentration by evaporation or transpiration was not a significant process in groundwaters throughout the area.

Jankowski & Acworth (1997) determined that, in areas where groundwater maintained clay soil saturation without effectively discharging, evaporative concentration was occurring at the soil surface. This acted to further increase TDS concentrations until precipitation of salts occurred on the soil surface during dry weather. They explained that the toxic levels of bicarbonate, magnesium, sulphate, sodium, and chloride produced by these processes caused vegetation death.

Acworth et al. (1997) observed that in the absence of clay, or where well defined discharge pathways existed, bedrock groundwater discharged without significant deterioration in water quality, and dryland salinity did not develop.

It was concluded by Jankowski & Acworth (1997) that the high levels of sodium in the groundwater created an extreme sodium hazard, which caused dispersion of the clays contained in the debris flow deposits. In addition, they indicated that the sodic clays decreased the hydraulic conductivity of the deposits, reducing drainage, increasing runoff, and enhancing erosion. Acworth et al. (1997) added that dispersion of the clay and silt in the debris flows and the subsequent release of entrained salt was a major source of salts (and sediments) entering the drainage system.

3.1.8 Conclusions

The distribution of aeolian derived materials and debris flow type deposits within the Macquarie River catchment of NSW is unknown, but sodic dispersive duplex soils are mapped and reported across the catchment (Murphy & Lawrie 1998a; Murphy & Lawrie 1998b) and C. Raine (2001, pers. comm., 19 Oct.); J Lees (2001, pers. comm., 23 Oct.); B Christie (2001, pers. comm., 24 Oct.); A Nicholson (2001, pers. comm., 11 Nov).

Work by Townsend (1997) demonstrates aeolian accretion has occurred in soils on hilltops in the Macquarie catchment. Osborne (2001) suggests an aeolian source for the red clay sediments that partially fill the Miocene age (Frank 1971) Wellington Caves and contain significant fragmented Quaternary megafauna bones. The existence of high-angle talus cones below cave openings is consistent with deposition by gravity and rain-wash (Osborne 2001). This evidence suggests that aeolian and debris flow processes were actively contributing to soils in the Macquarie catchment, throughout the Quaternary.

Clearly, the implications of palaeoclimate, and aeolian dust as a sediment source are considerable with respect to salinity processes. Dust can potentially provide a major source of salt including carbonates and sodium chloride. The clayey nature and low hydraulic conductivity of this material has also been shown to strongly limit discharge of regional groundwater systems in valleys. This can result in a build up of groundwater pressure causing water tables to rise. This saturates previously dry salt stores and mobilises them to the ground surface and into surface water systems.

If soils and unconsolidated sedimentary units in the Macquarie River catchment have a significant aeolian component, then they may also be a major source of salt; this has significant implications for salinity management in the region.

3.2 LANDSCAPE CHANGE AND SALINITY IN THE SNAKE GULLY CATCHMENT

Landowners in the Snake Gully catchment were interviewed to record their recollections of the effects of climate and natural events, land management, and the development of salinity in the catchment. Key findings from these interviews have been incorporated into the following sections.

3.2.1 Landscape Change Since Human Occupation

Humans have occupied Australia (and presumably the Snake Gully catchment) for at least 40,000 years and possibly 60,000 or 120,000 years (Lines 1991; Flannery 1994; White 1994). These first human inhabitants, the Aboriginal people, modified the environment by their use of fire, to encourage new vegetation growth and increase hunting prospects (Lines 1991; Flannery 1994; White 1994).

In south-eastern Australia, European settlement around 180 years ago brought huge changes to the landscape. The clearing of forests, the introduction of grazing stock, the drainage of valley bottoms and the clearing of riparian vegetation caused a massive increase in erosion (Olley & Wasson 2003).

European settlement of the Mid Talbragar district commenced in the 1860's, although it is suggested that squatters may have come to the area as early as the 1820's (McKenzie 2002, unpublished, p.6). Following World Wars I and II a number of properties in the area were selected for soldier settlements including the properties "Murrewega" and "Randwick" (L Yeo 2002, pers. comm., 29 March).

Land laws in the first half of the 1800's stated that for every 2,000 acres occupied, 120 of those had to be cultivated (King 1957). Drought in 1841 to 1843 led to "clearing of a lot of dead wood" to increase the pasture area for starving stock (King 1957). Sheep numbers in NSW peaked in 1891, but wheat farming expanded rapidly in the 1890's due to drought, plentiful labour, global wheat shortages and

the development of agricultural machinery such as the "jump stump plough" in 1876 (McKenzie 2002). Subsequent periods of drought in the early 1900's reinforced the move from grazing to cropping, and the advent of motorised tractors in the 1930's greatly increased the area of land that could be worked in a day (McKenzie 2002).

Olley & Wasson (2003) studied changes in sediment flux in the upper Murrumbidgee catchment since European settlement 180 years ago. They report that the introduction of grazing stock triggered widespread gully erosion, increasing sediment flux by more than 150 times, compared with variations in rainfall which caused a less than two fold increase. In the second half of the 1800's, erosion rates increased by a factor of 245, and about 43,000,000 tonnes of sediment was generated, at about 480,000 tonnes per year (Olley & Wasson 2003).

As gully networks reached maximum extension, sediment yield declined to about six times the pre-European rates; however, sediment yield declined by only a factor of two, to about 100 times the pre-European rates of 250,000 tonnes per year (Olley & Wasson 2003). They attribute this to an increase in the efficiency of sediment delivery through the stream network, which in pre-European times contained swampy meadows and 'chains-of-ponds' (Scott 2001) that acted as efficient sediment traps (Olley & Wasson 2003).

In the Snake Gully catchment, settlement, climate, and grazing patterns have been similar to those in the Murrumbidgee, so gully erosion and sediment flux patterns are also expected to have been similar to those reported by Olley & Wasson (2003).

In the 1940's, plague rabbit numbers in the Snake Gully catchment denuded the landscape of much of its groundcover and left the ground susceptible to erosion. Severe gulying and salinisation developed in the catchment after several years of high and prolonged rainfall in the early 1950's (L Yeo and D Yeo 2002, pers. comm., 29 March; R and J Yeo 2002, pers. comm., 3 April; M and R Simpson 2002, pers. comm., 3 April and 10 June).

Lower in the Snake Gully catchment, during flood periods in the 1970's, turbid water reached over one metre deep on the floodplain, and sheets of sediment were deposited (R Simpson 2002, pers. comm., 3 April).

From the mid-1960's onwards the NSW Soil Conservation Service (later to become NSW Department of Land and Water Conservation, DLWC) modified the landscape with bulldozers. Numerous contour banks were constructed in the catchment to control soil erosion and loss, and existing gullies were filled-in.

At the upstream boundary of "Murrawega" and on the downstream boundary of "Mindawanda", flumes were constructed to control water flow and minimise erosion (R and J Yeo 2002, pers. comm., 3 April).

Clearly, land use has exacerbated salinity, and current European-style land management practices may not be suitable in controlling the problem.

3.2.2 Salinity Investigation and Management

Prior to 1990, some tree planting had been conducted by individual landowners. In 1990, the Snake Gully community formed the Snake Gully Landcare Group. Salinity and erosion were the key issues for the group. The main activities conducted by the Landcare group since the 1990's included salt bush (*Atriplex nummularia*) trials, planting of tree strips, piezometer installation, and fencing of riparian and salt affected land (L and D Yeo 2002, pers. comm., 29 March; R and J Yeo 2002, pers. comm., 3 April; M and R Simpson 2002, pers. comm., 3 April and 10 June). The level of salinity management activities conducted, and the strong commitment of the Landcare group, has seen the catchment become a focus for salinity investigation and management, and it is frequently visited by groups interested in salinity.

As part of a joint Murray Darling Basin Commission (MDBC) and DLWC initiative into salinity management, native grass improvement, riparian management (including fencing), sowing of perennial and saline pastures, interception tree planting, and replanting of trees in existing tree lines (C Schneider 2002,

pers. comm., 10 July) have been undertaken during 2001 and 2002. This project included examination of the social and economic barriers to achieving land use change. A monitoring component of the study involved construction of three nested groundwater monitoring bore sites (including one at the study site), and an event based surface water flow and EC gauging station in the Snake Gully catchment.

With the introduction of the new Catchment Management Boards in 2000, and Catchment Blueprints in 2002, the NSW Government proposes to conduct planning and targeted actions for salinity management in the Central West Region under a 'groundwater flow system' framework (Coram et al. 2001). This framework is being developed regionally and is based on geology and slope. It classifies and describes groundwater systems that have similar salinity attributes and responses to management and is based on broadly mapped geological boundaries. Suites of salinity management options are being developed for each Groundwater Flow System, however, this framework may not be effective if system boundaries do not correctly represent the extent of the units that cause the problem.

3.2.3 Previous Studies

A study of regional groundwater trends in fractured rock areas of the middle and upper Macquarie catchment was conducted by Smithson (2002). This study took a second water level reading from bores that had been measured 11 years previously. Although there are many inherent limitations with this type of study, the results showed a broad rising groundwater trend of 13 cm per year. Three of the private water supply bores used for this study are located in the Spicers Creek catchment, with one located a kilometre upstream from the study site in Snake Gully. All of these bores showed a relatively shallow depth to groundwater (7.8 to 1.84 metres), and a rising trend of between 3.45 and 5.15 metres over 11 years.

Work by Salas & Smithson (2002) on the dataset developed in Smithson (2002) showed that depth to groundwater has a close correlation (0.74) with rainfall trends over the last 120 years. Contrary to popular salinity theories, this study concluded that groundwater has not been rising constantly over the last century, but rather, in periods of long term rainfall excess it rises, and in periods of long term rainfall deficit it falls.

Several hydrogeological salinity studies have been completed in the Snake Gully catchment. These propose a variety of models for groundwater processes and sources of salt contributing to the salinity problem.

Mahamed (1999b) and Mahamed (1999a) conducted studies of the hydrogeology and dryland salinity in the Spicers Creek catchment. He mapped two groundwater flow systems in the area based on groundwater level measurements in deep and shallow bores: a shallow system and a deep system. He described the shallow groundwater system as being mainly an unconfined local flow system that was sensitive to rainfall, having up to half a metre change in head after rain events. The shallow groundwater system occurs in clay rich colluvium deposits between 3 and 10 metres thick. He describes the deep groundwater system as being formed in fractured and weathered hard rocks, mainly confined, and with flow ranging from local to regional in scale. Groundwater level contours indicated that deep groundwater flow for the Spicers Creek area was in a northwest direction, with a recharge area north of Mount Bodangora extending eastwards, and that Spicers Creek was the likely focus for deep groundwater discharge. He suggested that groundwater flow for the shallow system in Snake Gully was westwards, and that flow in the deep system was in a very similar direction in this catchment. Mahamed (1999b) concluded that recharge for the shallow groundwater system in Snake Gully occurred in the hills east of the property "Ben Hoden", and that discharge occurred at break of slope and areas of lower elevation.

Deep and shallow groundwater systems in the Snake Gully catchment were sampled by Mahamed (1999b) and analysed for major ions. This work showed that the deep groundwater system is predominantly a Mg-Cl type water, and that the shallow groundwater system is a Na-Mg-Cl type water. These are slightly different to the water types suggested by Schofield (1998) for the wider Ballimore region; in particular, no HCO₃ water type was evident in Snake Gully. Mahamed (1999b) observed that the concentration of dissolved ions in groundwater increased in the direction of flow, but that the increase was not gradual. Geochemical modelling indicated ion exchange and aluminosilicate weathering reactions were the major processes affecting groundwater chemistry, and that evaporation alone could not explain observed ionic

concentrations.

Chlorofluorocarbon (CFC) age dating of shallow groundwaters returned an age of 36 years Mahamed (1999a). He concluded that locally recharged groundwater was mixing with older groundwater resulting in the discontinuity of EC readings along the groundwater flow path. Hydraulic slug testing of the shallow groundwater system indicated hydraulic conductivities in the order of 0.002 to 0.3 metres per day. He calculated a groundwater gradient down Snake Gully of between 0.01 and 0.02. Using a maximum hydraulic conductivity of 1 metre per day Mahamed (1999a) obtained a groundwater flow velocity of between 0.05 and 0.4 metres per day (or 18.25 to 146 metres per year). Based on a catchment length of ten kilometres, he estimated groundwater travel times of 68 to 550 years for groundwater to travel the entire length of the catchment.

These are relevant flow rates if groundwater flow paths are in the order of ten kilometres, and water is moving via mass transfer. However, local groundwater systems have been described in the Snake Gully area (Schofield 1998; Mahamed 1999b; Mahamed 1999a) and these are expected to have flow paths much shorter than 5 kilometres. They may have a significant component of hydraulic pressure transfer that would produce a very rapid groundwater response. These hypotheses are explored further by this thesis. Mahamed (1999b) suggested that factors controlling dryland salinity were variations in geology, slope morphology and soil types of varying permeability, and that groundwater discharge, in conjunction with these factors localised salt scald sites. To stabilise dryland salinity in the Snake Gully catchment, Mahamed (1999a) recommended planting deep rooted species on recharge areas and topographic highs, and salt tolerant species in discharge areas.

A hydrogeological study of the Spicers Creek area by McElroy (2000) was commissioned by the Spicers Creek / Talbragar Catchment Management Group. He observed that dryland salinity in the Spicers Creek area seemed to occur in four main situations: within clay dominated alluvial filled gullies; within clay dominated rocks such as the Napperby and Purlawaugh Formations; at the contact between two geological units; and along major regional fault structures. He further noted that many of the affected areas occurred in narrow constrictions of the topography and explained this as hydraulic back up of groundwater flow causing shallow watertables.

Based on knowledge of the topography, distribution of soil and rock types, and deep-rooted vegetation coverage, McElroy (2000) defined recharge areas for many of the dryland salinity sites fed by shallow groundwater. In the Snake Gully catchment, he believed these to be upper hillslopes and ridges not covered with deep rooted vegetation.

Morgan & Jankowski (2004) studied salinity at a site of groundwater seepage on a hillslope in the lower Snake Gully catchment. They observed a transition from non-sodic to sodic soils with increasing distance downslope from the saline seepage zone. Unconsolidated colluvial and alluvial sediments are reported from four sites of nested piezometers up to 12 metres deep constructed down the hillslope. These sediments are at least 12 metres thick and are described as consisting of clay rich alternating gravel, clay and sand, containing angular fragments of quartz and limestone. The hole lowest on the slope is reported to contain hard impermeable clay layers that separate water bearing colluvium and alluvium. This hole displayed the highest values of soil salinity and sodicity.

Groundwater levels in the unconsolidated sediments are deeper with a downwards hydraulic gradient at the top of the slope, and are shallow with an upwards hydraulic gradient at the middle and bottom of the slope (Morgan & Jankowski 2002). They interpreted this to indicate a basement fault in the mid-slope that allows deep Palaeozoic groundwater to discharge into the shallow unconsolidated sediments.

Morgan & Jankowski (2004) reported on chemistry of 25 deep and shallow groundwater samples collected from a variety of bores in the Spicers Creek area. This included five Na-HCO₃ and six Mg-Na-Cl type Palaeozoic basement groundwater analyses, summarised as Mg-Na-Cl-HCO₃ type waters, from the Bal-limore region (Schofield 1998). The proximity of these bores to the study site is unclear. Sedimentary rock and alluvial/colluvial groundwaters are reported together, ranging from Na-Cl to mixed Mg-Na-Cl and Na-Cl-HCO₃ type waters. (Schofield 1998) assigned groundwaters from the Triassic Napperby Formation and all overlying sequences as Na-Cl type waters, but observed that groundwaters in the underlying Triassic Boulderwood Formation and Permian Dunedoo Formation were Na-HCO₃ type waters.



Figure 3.7: Upper Snake Gully Landscape

In shallow bores studied (Morgan & Jankowski 2002; Morgan & Jankowski 2004) at a site in Snake Gully, EC increased from $2750 \mu\text{S}/\text{cm}$ at the top of the slope, through $4280 \mu\text{S}/\text{cm}$ mid slope, to $10,680 \mu\text{S}/\text{cm}$ at the bottom of the slope. It was noted that groundwaters in the mid- and lower slope have strongly negative redox potential's of less than -200 mV .

It was concluded (Morgan & Jankowski 2002; Morgan & Jankowski 2004) that deep, strongly reduced, magnesium-rich groundwater was flowing via a basement fault up through shallow sodium-rich sediments, causing the development of sodic soils due to ion exchange processes. They believe deep groundwater to be the source of salt responsible for the high ionic concentrations observed in shallow bores, even though they also observe that shallow evaporative concentration is not a significant process.

Alternatively, the results Morgan & Jankowski (2002, Morgan & Jankowski (2004) also support a shallow salt source and local groundwater system processes, a model which is further developed in this thesis.

3.2.4 Salinity Models for the Snake Gully Catchment

Based on literature review of salinity studies in unconsolidated sediments, and previous studies conducted in the Snake Gully catchment, three main models appear possible to explain salinity in this catchment. These are:

1. Deep saline groundwater discharge via basement faults.
2. Mass water transfer and evaporative concentration of shallow groundwaters.
3. A shallow salt source mobilised by a shallow watertable predominantly as a hydraulic pressure response.

The validity of these models will be assessed from the findings of this research project.

Chapter 4

INVESTIGATION METHODS

4.1 GEOLOGY OF SEDIMENTARY UNITS

Unconsolidated sedimentary units are distributed across the floor of the Snake Gully valley. These are exposed in eroded creek walls and platforms over one kilometre at the study site. The geology and stratigraphic relationships of these units was mapped, in order to establish their characteristics and spatial variability, and gain some insight to their origin and mode of deposition.

4.2 BOREHOLE DRILLING AND GEOLOGICAL LOGGING

Four groundwater monitoring and investigation bores were completed at the study site. These consist of a series of three nested monitoring bores, and a shallow cored hole that was completed as a monitoring bore. Bore locations are shown on Figure 4.1.

4.2.1 Cored Hole CH1

A shallow cored hole (CH1) was completed in January 2002. The location of the hole was selected to be adjacent to a clearly exposed 1.5 metre deep eroded section of the creek, to enable correlation between recovered core and in-situ units.

The hole was drilled by the DLWC Salinity Unit, under the supervision of the author, using a Proline soils rotary drilling rig (Figure 4.2). Hole advancement and sampling were carried out using a 1 metre long, 6 inch diameter hollow steel barrel containing two steel splits with welded flight augers, held in place by a detachable coring bit (Plate 10).

The core was recovered in runs of one metre or less. Several zones of core loss occurred owing to sample falling from the end of the core barrel during retrieval from the hole between runs. Drilling continued until refusal on large angular clasts of pink shale. Basement was not encountered in sample retrieved.

The cored hole was completed as a shallow monitoring bore with 65 mm diameter PVC casing and an end cap glued to the bottom. The bottom one metre of the PVC casing was hand slotted to act as a screen. The annulus around the screen was filled with gravel pack to 0.5 m above the screen, and the remainder of the annulus backfilled with basalt dust. One metre of PVC casing was left protruding above ground level and a cap was placed onto this. The total bore depth was 4.33 metres from top of casing.

Each core was transferred into two 6 inch PVC splits, these were taped closed over the sample to form a "tube". The ends of the PVC were sealed with packing materials and taped to prevent the core breaking

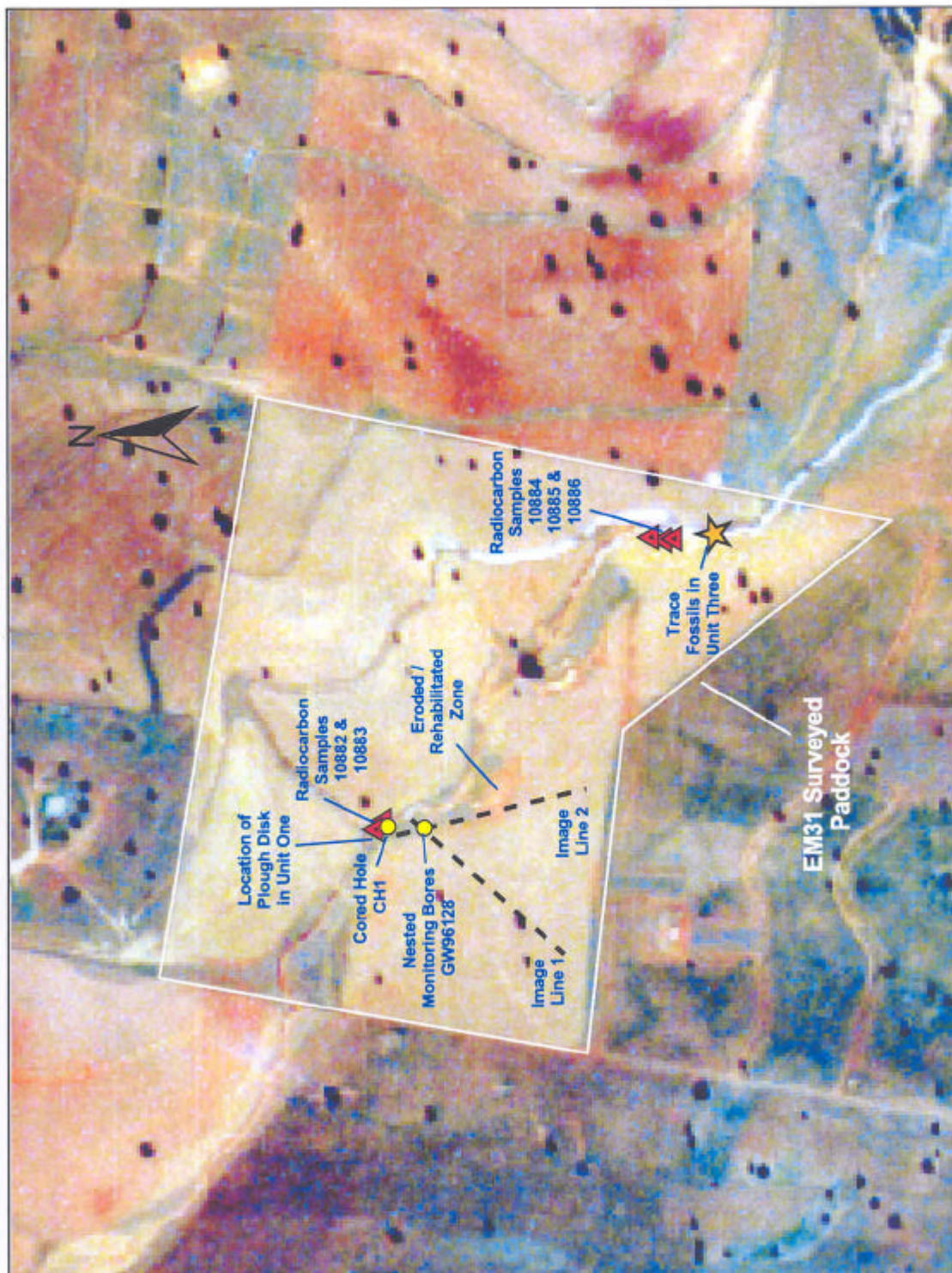


Figure 4.1: Airphoto Showing Bores and Sample Locations at the Study Site



Figure 4.2: Drilling Cored Hole CH1 (January 2001)



Figure 4.3: First Metre of Core From CH1



Figure 4.4: Sampling Core From CH1



Figure 4.5: Drilling Nested Monitoring Bore Site GW96128

up during transport. The cores were transferred to the Wellington Research Station laboratory, where they were logged, photographed, and then cut into 10 cm samples for further analysis (Figure 4.4).

4.2.2 Nested Bore Site GW96128

Three nested monitoring bores (GW96128/1, GW96128/2, and GW96128/3) were drilled and completed by the DLWC Drilling Unit in October 2001 (Figure 4.5 and Figure 4.6).

The bores were drilled using compressed air and a 6.5 inch percussion hammer. No additives or fluids were used during drilling. Bores were cased with glued lengths of 75 mm diameter Class 12 PVC. A sump was placed below the screened section and completed with a glued PVC cap at the bottom of the casing. Screened sections were chosen based on water bearing zones encountered during drilling. Screens were constructed of horizontally machine slotted PVC (2 mm aperture at 40 mm spacing).

The annulus was filled with rounded 3-5 mm graded gravel pack. A one metre bentonite plug was placed above the screened length in the two deeper holes, to prevent leakage of groundwater into the bore from other water bearing zones. Bores were completed with headworks consisting of a 6 inch diameter 4 mm wall steel casing protector cemented into the ground and finished with a locked cover.

On completion, each bore was developed by airlift for three hours. During drilling of the deepest hole GW96128/3, samples were collected at one metre intervals for logging and further analysis.

A summary of the completed construction of these bores is presented in Table 4.1.



Figure 4.6: Nested Monitoring Bore Site GW96128

Table 4.1: Construction Details For GW96128 Nested Monitoring Bores

	GW96128/1	GW96128/2	GW96128/3
Total depth (m bgl)	3	15	31
Screens (m bgl)	1 - 2.5	11 - 14	27 - 29
Screened lithology	Sedimentary	Weathered bedrock	Fresh bedrock
Cemented (m bgl)	0 - 1	0 - 1	0 - 1
Bentonite plug (m bgl)	-	4 - 5	21 - 22
Gravel Pack (m bgl)	1 - 3	1 - 4, 5 - 15	1 - 21, 22 - 31
Sump (m bgl)	2.5 - 3	14 - 15	29 - 31



Figure 4.7: Trace Fossils In Unit Three

4.3 DATING OF UNITS

Dating of the sedimentary units at the study site would allow a chronology to be established, and enable links to be made with palaeoclimate from which inferences about provenance, mode of transport, and deposition mechanisms might be made.

4.3.1 Circumstantial Evidence

The sedimentary units were examined for circumstantial evidence of their age, with stratigraphic relationships, clast component and other unusual features of each unit being appraised.

4.3.2 Trace Fossils

Trace fossils (Figure 4.7) occur in Unit Three at the location shown on Figure 4.1. The organisms that created the trace fossils in Unit Three might be identified, and from the species age range, confine the age of deposition of that unit. Photographs of the trace fossils were sent to palaeontology staff at the School of Biological Sciences UNSW, and the Australian Museum in Sydney for identification.

4.3.3 Radiocarbon Dating

The radiocarbon dating technique is the most dependable and widely applied dating technique for the late Pleistocene and Holocene periods (Radiocarbon WEB-info [online] 2001). Cainozoic units at Yass were successfully dated from entrained charcoal clasts using radiocarbon dating (Melis 1998). Charcoal clasts are randomly distributed throughout the upper part of Unit Two. In order to date the emplacement of Unit Two carbon bearing material in the unit was collected for dating by C^{14} analysis.



Figure 4.8: Radiocarbon Dating Charcoal Clast Sample 10882 Prior to Excavation



Figure 4.9: Radiocarbon Dating Charcoal Clast Sample 10882 Cavity Following Excavation

The Radiocarbon Dating Technique

Three main isotopes of carbon occur naturally in the atmosphere at about the same ratio's - C^{12} , C^{13} (both stable), and C^{14} (unstable or radioactive). C^{14} is being formed and is decaying in the atmosphere at approximately the same rate. While any organism is alive, it continues to incorporate radiocarbon from the atmosphere. Once it has died, the amount gradually declines because of radioactive decay.

The C^{14} dating method relies on comparison of the ratio of the radioactive isotope of carbon (C^{14}) to normal carbon (C^{12}) in a sample. After 5568 ± 30 years (termed the Libby-half-life), half of the C^{14} accumulated during the life of the organism has decayed, and after another 5568 years, half of that remaining C^{14} has decayed. This continues until after 10 half-lives, or about 50 - 60,000 years (the limit of the technique), there is no C^{14} left in the sample.

The residual radioactivity of a sample is measured and compared with modern levels of activity. Using the measured half-life, it becomes possible to calculate a date for the death of the sample. Radiocarbon concentrations in the atmosphere have fluctuated periodically, so a more accurate age is determined by calibration of the radiocarbon date against material of known age to give a calendar age.

In the radiometric technique, the radioactivity or decay rate of the C^{14} is measured (beta-counting method). In the Accelerated Mass Spectrometry (AMS) technique, the amount of C^{14} remaining in the sample is counted. The advantage of the AMS technique is that only small samples are required for dating (Radiocarbon WEB-info [online] 2002; Accelerator Mass Spectrometry (AMS) [online] 2001; Radiocarbon Dating [online] 2001).

Sample Collection and Preparation

Roots remain in Units One and Two from trees that no longer exist above ground. Because of this, great care was taken in selecting and excavating the samples to ensure that they were actual clasts and not burned out roots of relatively modern trees. It was assumed that if the sample was a burned out root, that the charcoal would be somewhat continuous back into the unit.

Five samples were collected for radiocarbon dating (sample no's 10882 to 10886). For charcoal samples 10882 and 10883, each phase of the excavation was photographed as a record that the clasts were indeed isolated entities entirely surrounded by the matrix (Figure 4.8 and Figure 4.9). One sample of a tree root penetrating into Unit Two was collected for comparison (sample no 10886). Sample locations are shown on Figure 4.1.

Possible sources of younger carbon contamination were considered during sampling. Care was taken to ensure that hands and equipment used during excavation were free of potential contaminants. In order to minimise possible contamination, the samples were packed and sealed in new plastic bags immediately

following their excavation. Contamination by humic acids was considered, however this does not appear to be a significant problem outside of high rainfall climates (Hogg, A. pers. comm. in Melis (1998)).

Radiocarbon dating analyses were carried out at the University of Waikato Radiocarbon Dating Laboratory, New Zealand. Samples were prepared by having possible contaminants removed. They were then washed in hot 10% *HCl*, rinsed and treated with hot 1% *NaOH*. The *NaOH* insoluble fraction was treated with hot 10% *HCl*, filtered, rinsed and dried.

Sample Analysis

Four of the samples (numbers 10883 to 10886) were of sufficient size to enable them to be analysed by the radiometric Liquid Scintillation Counting (LSC) technique (Hogg 2002a; Hogg 2002b). The remaining sample (number 10882) was less than 5 g allowing analysis by the AMS technique. Details of the AMS method are given on the web site <http://www.rlaha.ox.ac.uk/orau> (2001).

4.4 CORE ANALYSIS

4.4.1 Emerson Aggregate Testing

Dispersion testing by determination of Emerson Class Number was conducted on samples of each sedimentary unit from bores CH1 and GW96128. This was done to investigate the susceptibility of the sedimentary units to erosion, and hence their potential to contribute salts and suspended sediment to surface waters.

Sample Selection and Preparation

Emerson Aggregate Tests (EAT) were carried out on three representative air dried aggregates between 5 and 10 mm in size (Australian Standard AS 1289.3.8.1 1997).

Analysis Method

The three sample aggregates were placed equally around the side of a 250 mL beaker containing 200 mL of distilled water (Figure 4.10). Dispersion and slaking were rated after 2 and 20 hours, with the latter used for interpretive purposes (Geeves, Craze, & Hamilton 2000).

If samples did not display any dispersion after 20 hours of immersion, a few grams of air dried sample were mixed with distilled water to approximate plastic limit. Samples were worked for 2 minutes, and then shaped into 1 cm cubes and tested as for unworked aggregates. Worked samples still not displaying any dispersion were checked for calcium carbonate (calcite) using 1M *HCl*, and for calcium sulphate (gypsum) using 10% barium chloride solution.

If no calcite or gypsum were detected, a 1:5 soil water suspension was made up and observed for dispersion or flocculation. In practice this step was conducted during the 1:5 aqueous extract analysis.

4.4.2 Aqueous Extracts

The concentration of soluble salts in soil is estimated by measuring the electrical conductivity (EC 1:5) of a fluid extracted from a 1:5 soil suspension. To investigate whether the sedimentary units at the study



Figure 4.10: Emerson Aggregate Dispersion Testing

site contain salt, 1:5 aqueous soil extract tests) were carried out on samples of each sedimentary unit from bore CH1 and the top 10 metres of GW96128.

Sample Preparation

The soil water suspension was prepared by selecting a representative air dry sub-sample of approximately 60 grams. This was hand crushed using a mortar and pestle, and passed through a 2 mm sieve (Figure 4.11). A 10 gram sub-sample from the < 2 mm fraction was added to 50 mL of distilled water (a ratio of 1 to 5). Where the aqueous solution was to be analysed for major ions, the amounts were increased to 40 grams of soil and 200 mL of water. Every fifth sample was duplicated as a check. The samples were then rotated end over end at 15 rpm for one hour to dissolve the soluble salts (Figure 4.12).



Figure 4.11: Preparation of 1:5 Extracts

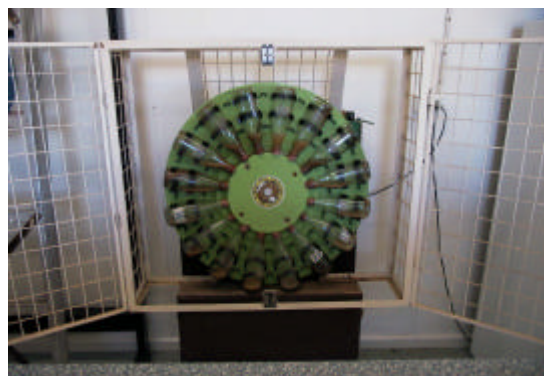


Figure 4.12: Agitation Wheel For 1:5 Extracts



Figure 4.13: Aqueous 1:5 Extracts Settling Period Prior to Measurement



Figure 4.14: Measurement of pH and EC From 1:5 Aqueous Extract

Analysis Method

After rotation, the samples were allowed to settle for 10 minutes (Figure 4.13). The aqueous solution was drawn off using a 50 mL bulb pipette, and the electrical conductivity (EC 1:5) and pH 1:5 of the aqueous solution measured (G.Rayment & Higginson 1992) (Figure 4.14).

An Orion model 130 conductivity meter with internal temperature correction was used to measure electrical conductivity. The meter was calibrated at the start of each batch of 16 extracts using 0.01M ($1413 \mu\text{S}/\text{cm}$) and 0.1M ($12900 \mu\text{S}/\text{cm}$) potassium chloride reference solutions. The probe was rinsed in distilled water and dried with a clean tissue between each reading.

The pH was measured while the solution was being stirred using the pH function of a TPS multi-parameter meter, model WP-91. The pH probe and meter function were calibrated at the start of each batch of 16 extracts using pH 4 and pH 7 buffer solutions. The probe was rinsed in distilled water and dried with a clean tissue in between each reading.

4.4.3 Aqueous Extract Major Ions

Chloride was determined by argentometric titration (as per APHA 1992) against approximately 0.02 molar AgNO_3 using a few drops of 10% K_2CrO_4 indicator solution. The silver nitrate solution was initially calibrated against a primary standard 0.02 molar NaCl solution. Three 25 mL aliquots of the same water sample were titrated against the AgNO_3 solution until the endpoint was reached. A duplicate of every sample was analysed. Due to an oversight, sample number CH21 was omitted from analysis.

Cation determination was by Inductively Coupled Plasma - Atomic Emission Spectrometry (ICP-AES) conducted at the School of Geography, University of New South Wales. Elements analysed were Na, Mg, Ca, K, Total Fe, Total S, Mn, B, and Sr.

4.4.4 Grain Size Analysis

Grain size distributions may be characteristic of sediments deposited in certain environments (Blatt, Middleton, & Murray 1980). Townsend (1997) suggests an aeolian component in soils across the Macquarie catchment. This suggestion is based on a characteristic grain size frequency peak observed at the 30 to 40 micron size in the sub-63 micron fraction of soil samples, regardless of rock type.

In order to determine whether similar characteristic aeolian peaks occur in the sedimentary units at Snake Gully, hence inferring some component of aeolian origin, particle size analyses were conducted on the sub-50 micron fraction. A sample of weathered Palaeozoic basement was also analysed to investigate the

contribution from bedrock weathering.

Analyses of the sub-50 micron fraction were conducted on nine samples from the sedimentary units in bores CH1, and on one sample of the weathered basement from bore GW96128/3 for comparison. Three duplicates and a Millipore reagent blank were included to ensure accuracy, repeatability and non-contamination.

Sample Preparation

Samples were hand crushed then passed through a 2 mm sieve. Fifty grams of the -2 mm material was added to a 250 mL sample bottle. This was topped up to approximately 225 mL with standard dispersing agent (sodium hexametaphosphate, prepared as per AS 1289.3.6.1 and diluted approximately 50%). Bottles were rotated end over end at 15 rpm for 24 hours, to ensure dispersal of clumped clay aggregates. This procedure resulted in good dispersion of the clays.

Samples were then passed progressively through 300, 150, and 50 micron sieves. Contents were washed through with distilled water and the retained fraction discarded.

The remaining sub-50 micron material was sub-sampled whilst being mixed with a magnetic stirrer to ensure even distribution of material. Between three and five drops of sample were collected using a Pasteur pipette, and added to a 150 mL vial. The vial was topped up with Millipore Q ultrapure distilled water to achieve a recommended obscuration value of approximately 30%.

Analysis Method

The laser diffraction based particle size analysis technique was selected because of its ability to differentiate and measure finer size distributions. Sieving or hydrometric determination are not precise enough techniques to show this detail.

The samples were analysed using a Malvern Laser Diffraction Particle Sizer, (model Mastersizer S), at the UNSW School of Civil and Environmental Engineering. This machine is capable of measuring particles ranging from 0.5 to 600 μ . The technique uses the principle of diffraction from the particles as the means of measurement.

The laser sizer acts on the principle that particles dispersed in a fluid will settle in accordance with Stokes Law. The technique is based on settling ratios of particles measured by the concentration changes of particles that are present at decreasing sedimentation depths in a suspension-filled cell. A finely calibrated laser beam penetrates the cell (which is continuously lowered), measuring the degree of penetration achieved through the settling suspension. The differences are measured as a function of time and height. A comparison is then made with the cell when only pure water is run through the machine (McCave & Syvitsky 1991).

During laser sizer analysis three runs were made on each sample, with 10,000 sweeps per run. Sample and machine alignments were checked if residual error exceeded 5%. Obscuration of all samples was within tolerance levels of 10 to 45%. Results for some samples had to be normalised to the sub-50 micron fraction only, as lint free tissues were not available for drying equipment between readings resulting in small amounts of plus 50-micron fibres in the sample.

4.5 GEOPHYSICAL TECHNIQUES

4.5.1 Introduction

Geophysical techniques measure variation in physical properties of the ground, and rely upon lateral or vertical contrast in the physical properties being measured. These contrasts normally coincide with geological material boundaries, or changes in groundwater saturation or quality. From a distribution map of a particular physical property, inferences are made regarding the nature of the sub-surface (Shaver 1997).

The suitability of a particular geophysical technique depends on the physical property contrasts involved, the depth of the target, and the nature and thickness of the overburden (Shaver 1997). Salinity problems are directly or indirectly related to the location of groundwater, salts, and clays. Geophysical techniques such as galvanic and induced electrical methods, and gamma ray activity can investigate these properties, and are therefore the most relevant techniques for use in salinity investigations. Techniques have been reviewed by several workers (McNeil 1980; McNeil 1986; Keys 1989; Taylor et al. 1989; Nicoll & Scowan 1993; Vogelsang 1995; Acworth & Jankowski 1997; Shaver 1997; Acworth & Beasley 1998; Melis 1998; Acworth 1999).

4.5.2 EM 31 Survey

The Electromagnetic Induction Technique

Electromagnetic (EM) ground conductivity meters map lateral variation in subsurface electrical conductivity (EC). The GEONICS EM31 maps lateral variation in the apparent bulk electrical conductivity (ECa) distribution in a horizontal plane. In vertical dipole mode, the total nominal depth of penetration for EM31 in homogeneous ground is 6 metres (McNeill 1980). Other workers (R.D.Barker 1989) have suggested a median depth of penetration of 3.2 metres. McNeil (1980) details the theory of EM31 operation.

In the electromagnetic induction technique, a transmitter coil is energised with an alternating frequency current (the EM31 operates at an audio frequency of 9600 Hz). A receiver coil is located away from the transmitter coil (3.7m in EM31). The time-varying magnetic field, arising from the alternating current in the transmitter coil, induces very small eddy currents in the earth. The eddy currents generate a secondary magnetic field that is sensed, together with the primary magnetic field, by the receiver coil.

Field Methodology

An EM31 survey was conducted in July 2002 across the paddock covering the 25 hectares around the study site and Snake Gully creek. The location of the EM31 survey is shown on Figure 4.1. Ideally, this survey would have been completed early in the project, so that anomalies could be further investigated by drilling, however, equipment availability precluded this option.

The EM31 survey was conducted using a GEONICS EM31 meter mounted in vertical dipole mode on a QUADCYCLE, which was equipped with a Trimble Global Positioning System (GPS). Survey lines were oriented west-northwest and spaced at approximately ten metres, with readings taken every second (equating to every 4 to 5 metres) along the line.

Data Processing

The data was downloaded into Geosoft's 'Oasis Montaj' processing software. Gridding was carried out using the default minimum curvature option, and a cell size one quarter of the maximum distance between

points as specified by Vogelsang (1995).

4.5.3 Electrical Imaging

The Resistivity Imaging Technique

Electrical resistivity imaging is a 2-dimensional investigation method used to determine subsurface conductivity variation in the vertical plane. Griffiths & Barker (1993) describe the resistivity imaging method, and (Acworth 1999) presents its application to salinity studies.

The resistivity imaging technique measures apparent resistivity using a four-electrode system. An electrical field is induced into the sub-surface via two electrodes. The third and fourth electrodes measure the potential difference at other locations on the surface. The potential difference is then converted to resistance. Resistance values are converted to apparent resistivities by a geometric factor. The geometric factor accounts for the volume through which the current flows.

Numerous electrode array configurations can be selected to take resistivity measurements, however, for this project the Wenner array was used. This is the most common array for environmental applications. The Wenner array was chosen due to its ability in resolving vertical variations in resistivity. This array also has an extremely high signal, compared with arrays such as the Dipole array. The geometric factor for the Wenner array is $2\pi a$ where "a" is the electrode spacing.

With the Wenner array, the electrode measurements are initially moved along the line with constant separation. The separation is changed, and the electrodes are moved along the line again. This process is continued until all of the measurements are acquired.

Field Methodology

Two electrical resistivity image lines were run at the study site. The first line started 7.5 metres east of the nested bore GW96128/3 at the edge of the creek bank, and was run 122.5 metres southwest, up slope (Figure 4.15). The second line started 35 metres north of the nested bore GW96128/3, and was run 122.5 metres southeast across a recently rehabilitated area of sheet and gully erosion, then up the slope away from the creek (Figure 4.16).

Resistance data was collected with an SAS4000 Terrameter (Figure 4.17), manufactured by ABEM (www.abem.se). Multi-core cables were connected to a LUND ES464 automatic switching unit, also manufactured by ABEM. Two multi-core cables are laid out together but offset by 2.5 metres. The connectors on alternating cables were joined to stainless steel electrodes, driven into the ground surface at 2.5 metre intervals. Each cable consists of 25 connectors at 5 metre intervals giving a net result of 50 connections at 2.5 metres.

The Wenner array has a depth of investigation equal to approximately half the maximum electrode spacing. The maximum electrode spacing in these two surveys was 40 metres, so the maximum depth of investigation was approximately 20 metres. The resolving power of surface resistivity measurements decreases exponentially with depth, and the location of near surface features is mapped with increased accuracy compared to deep features.

Data Processing

Apparent resistivity values were stored by the SAS4000 Terrameter in digital form. These were downloaded and displayed in pseudo-section. The x locations of the apparent resistivity values were plotted according to the array's midpoint. The y locations were plotted according to the "n" separation of the electrodes. Many electrical geophysical techniques rely on inversion of the physical property measure-



Figure 4.15: Electrical Resistivity Image Line One and Borehole Geophysical Logging at GW96128



Figure 4.16: Electrical Resistivity Image Line Two

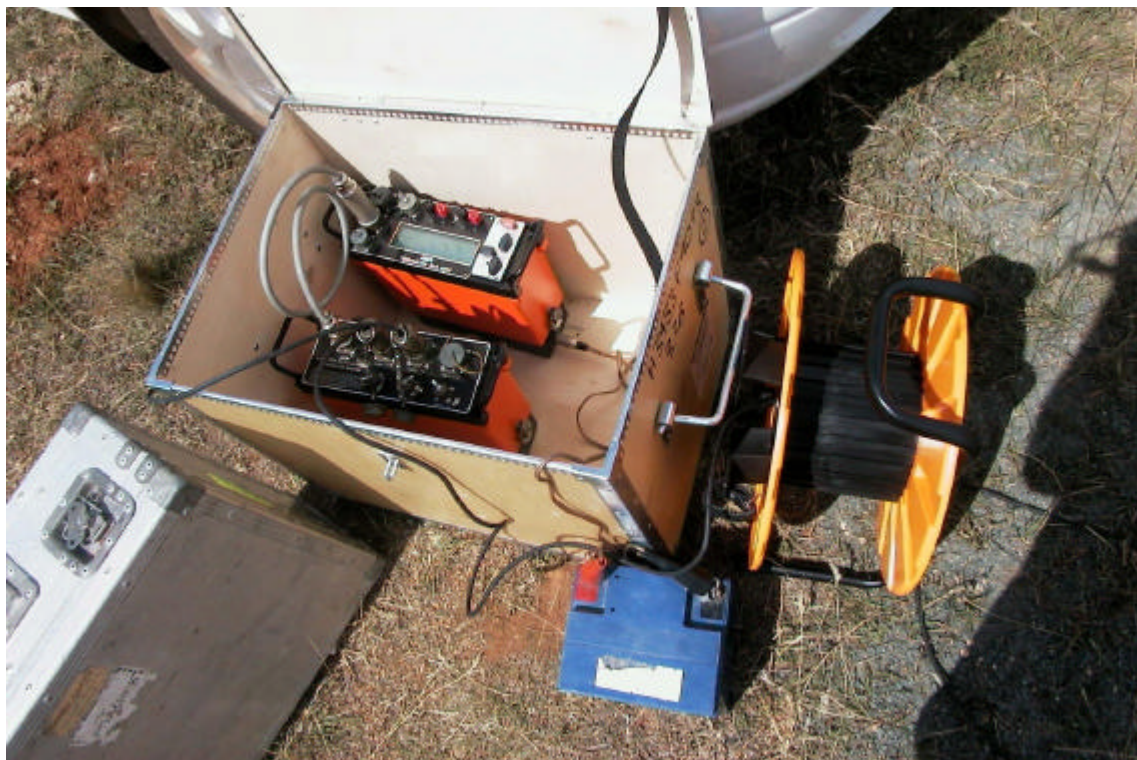


Figure 4.17: ABEM SAS4000 Terrameter Used For Electrical Resistivity Imaging

ments to model the nature of the sub-surface conditions. Inversion allows the profile apparent electrical resistivity data to be interpreted in terms of different layer depths and real distribution of resistivity values. The method takes the apparent electrical resistivity distribution and inverts it to produce a true 2-dimensional model of resistivity distributions.

The apparent electrical resistivity data was inverted using RES2DINV automated inversion software (Loke & Barker 1995; Loke & Barker 1996; Loke 1999). The inversion method is based upon a smoothness-constrained least squares deconvolution of the apparent electrical resistivity image data.

Prior to inversion, data was checked for "bad" points. The sub-surface was divided into model blocks, and the apparent resistivity of these blocks was altered to match the survey data. The data was topographically corrected, and standard default settings were used to invert the image lines. The results of the inversion are displayed on screen, along with the forward model and the original apparent resistivity pseudo-section. The root mean square (RMS) error between the pseudosections and the calculated forward model gives an indication of the validity of the final inversion model.

4.5.4 Borehole Geophysical Logging

Downhole geophysical logging allows detailed vertical resolution of a number of physical properties. Two of the most useful properties in salinity studies are apparent bulk conductivity and gamma ray activity.

Logging tools are lowered into the hole by an electrically powered variable speed winch. The winch cable passes over a pulley supported by a tripod. The logging speed is measured by a shaft encoder mounted adjacent to the pulley. Individual sondes measure gamma-ray activity and bulk electrical conductivity. At surface, data is recorded and directly plotted, by connection to a lap-top computer. Details of borehole geophysical techniques are given by Keys (1989).

Downhole Electromagnetic Induction

The GEONICS EM39 has a sonde that measures apparent bulk electrical conductivity as a function of depth in boreholes, using an electromagnetic induction technique based on exactly the same physical principles as the EM31. The apparent bulk electrical conductivity can be measured through the PVC casing in boreholes, and is not affected by the fluid conductivity inside the bore (Acworth & Beasley 1998).

The nominal depth of penetration into formation is 500 mm due to the inter-coil spacing of 0.5 metres. The operating frequency for the EM39 is 39,200 Hz. McNeil (1986) details the theoretical basis behind the EM39, and (Taylor et al. 1989) provide a review of the application of this equipment to groundwater studies.

Downhole Gamma Ray Activity

Gamma rays are produced by the spontaneous decay of unstable isotopes in geologic materials. As these unstable isotopes decay, they emit gamma photons. The gamma radiation released by the decay of an unstable isotope can be captured and converted to an electronic pulse. The pulses that are detected in the logging sonde are transmitted to the surface, counted by a rate meter, and recorded as gamma ray activity (in counts per second). Further details of the gamma method are given by Keys (1989) and Acworth (1998).

Naturally occurring unstable isotopes are Potassium-40, Uranium-238, and Thorium-232. Potassium is abundant in some feldspars and micas, which decompose to clay. Uranium and thorium are concentrated in clay by the processes of adsorption and ion exchange (Acworth & Beasley 1998). A log of gamma-ray activity indicates variations of clay content in the geological formation with depth; therefore, the gamma log is useful in identifying clayey versus sandy layers.



Figure 4.18: Borehole Geophysical Logging At GW96128 Site

Field Methodology

The EM39 and gamma tools were run down boreholes GW96128/3 and CH1 (Figure 4.18). The gamma ray activity log was run first in each hole at a speed of 0.05 m/s using a time constant of 8 seconds. The EM39 induction tool was then run at a speed of 0.5 m/s to produce an apparent bulk electrical conductivity log. In borehole CH1, the EM39 was run twice as a check. Readings were made at 25 mm depth increments.

Location of the sensor on the individual sonde dictates the final depth to which readings can be obtained for each method. For the gamma tool, this is about 10 cm above base of hole, and for the EM39 tool, it is about 78 cm.



Figure 4.19: Pumping Bore GW96128/3 With Grundfos Pump



Figure 4.20: Pumping Shallow Bores With Amazon Pump, Measurement of Unstable Parameters, and Sample Collection

4.6 HYDROGEOCHEMISTRY

4.6.1 Introduction

Over a period of five days in May 2002, thirty two water samples were collected from deep and shallow bores, groundwater seepages, and surface waters in the Snake Gully catchment for hydrogeochemical analysis. A sample was collected for comparison from Spicers Creek immediately downstream of the Snake Gully confluence. Sampling locations are shown on Figure 4.21.

4.6.2 Field Measurements and Sample Collection

Surface waters were sampled directly, and groundwaters were sampled by pumping. Shallow bores (less than ten metres) were pumped using a plastic 40 mm diameter submersible inline "Amazon" pump. Bores deeper than ten metres were pumped using a stainless steel GRUNDFOS submersible 48 mm diameter pump (Figure 4.19). Shallow bores with low specific capacity were pumped to discard stagnant water and allowed a twenty-four hour recovery period before being pumped again for water sampling. Bores with better recovery were pumped until unstable groundwater parameters (ToC, EC, pH, Eh, and O_2) had stabilised, to ensure that all stagnant casing water had been removed, and that representative groundwater samples were obtained before samples were collected (Figure 4.20).

Unstable parameters were measured by placing the probes for all meters into a jar through which water from the bore was pumped. Electrical conductivity and temperature were measured using an Orion model 130 conductivity meter with internal temperature correction. The meter was calibrated daily using 0.01M ($1413 \mu\text{S}/\text{cm}$) and 0.1M ($12900 \mu\text{S}/\text{cm}$) potassium chloride reference solutions. The probe was rinsed in distilled water and dried with a clean tissue between each reading.

The pH, Eh, and dissolved oxygen were measured using a TPS model WP-91 multi-parameter meter. The pH probe and meter function were calibrated daily using pH 4 and pH 7 buffer solutions. Redox potential (Eh) and dissolved oxygen were measured in a separate electrode. Calibration of dissolved oxygen was conducted in air, and using 2% sodium sulphite oxygen-free solution. The Eh function was factory calibrated and there is no user calibration facility for this mode. The probes were rinsed in distilled water, dried with a clean tissue, and capped between each reading.

All water samples were collected for chemical analyses using one-litre polyethylene bottles, which were filled to the brim to exclude as much air as possible. These were kept cool and transferred as quickly as possible to the on-site laboratory for analysis, or preservation and refrigeration.

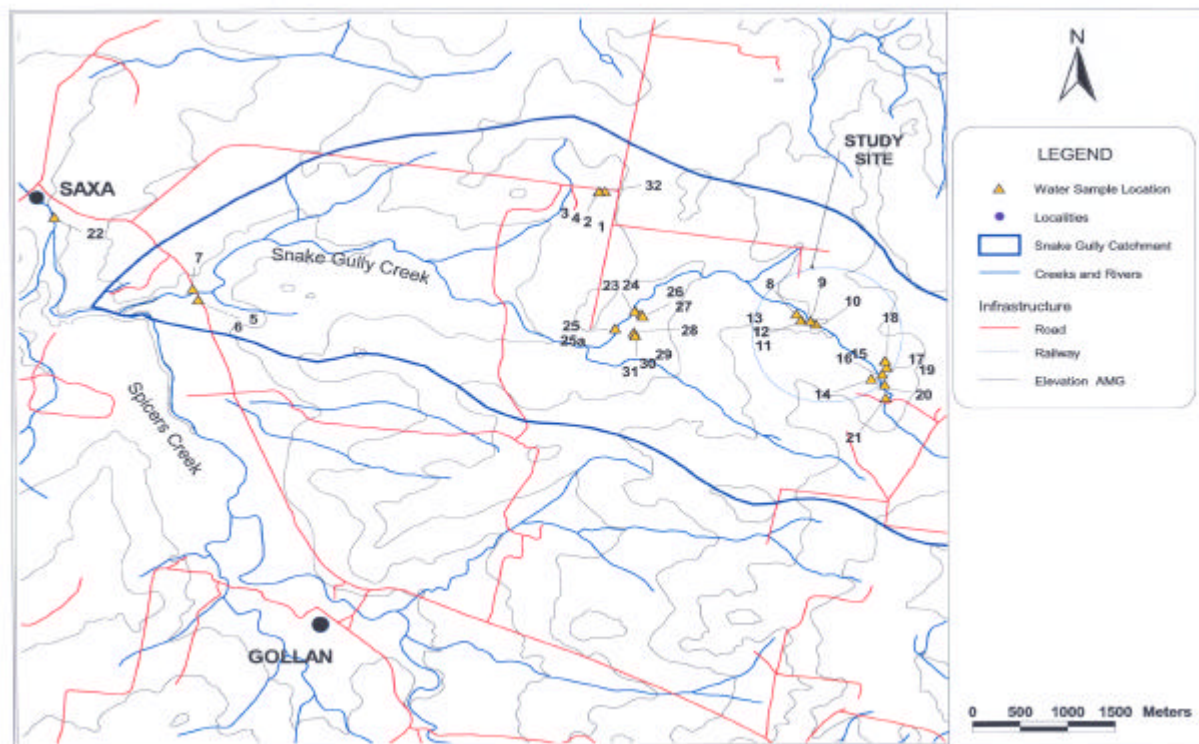


Figure 4.21: Surface Water and Groundwater Sampling Locations

4.6.3 Laboratory Measurements

Sample Preparation and Preservation

In the mobile laboratory, approximately 150 mL of water was passed through a 45-micron cellulose fibre filter and acidified with 10 molar HCl to give pH 1 - 2 for cation determination. A similar amount was transferred directly to another container for anion determination and refrigerated (Figure 4.22).

Major Ion Analysis

Inorganic carbon species were determined immediately on site in the mobile laboratory by acid/base titration as per American Public Health Association (1992). Bicarbonate alkalinity was determined by titrating two aliquots of approximately 30 mL of unfiltered water sample against 0.01 molar HCl until endpoint was reached at pH 4.3. Endpoint was detected using a pH electrode (Figure 4.23).

For waters with pH above 8.3, carbonate alkalinity was determined by titrating two aliquots of approximately 100 mL of unfiltered water sample against 0.01 molar HCl until endpoint was reached at pH 8.3. Endpoint was detected using a pH electrode.

For waters with pH above 4.3, carbon dioxide acidity was determined by titrating two aliquots of approximately 100 mL of unfiltered water sample against 0.02 molar NaOH until endpoint was reached at pH 8.3. Endpoint was detected using a pH electrode.

Ferrous iron was determined by colorimetric technique by treating 10 mL of filtered water with 2 mL of PPDT-DAS colour complexing reagent, followed by a 2 mL of buffer solution. The resulting colour was compared with a series of prepared standards.

Sulfide was determined by colorimetric technique by treating 20 mL of unfiltered water with 20 mL of



Figure 4.22: Filtering and Preservation of Water Samples



Figure 4.23: Field Titration For Unstable Parameters

Cu/DMP colour complexing reagent. The resulting colour was compared with a series of prepared standards.

Chloride was determined by argentometric titration (as per APHA 1992) against approximately 0.02 molar $AgNO_3$ using a few drops of 10% K_2CrO_4 indicator solution. The silver nitrate solution was initially calibrated against a primary standard 0.02 molar NaCl solution. Prior to determination, the water samples were diluted with Millipore Q ultrapure distilled water as per Beck (1998), and a dilution duplicate was made for every sample. Two aliquots of between 10 and 20 mL of the same water sample were titrated against the $AgNO_3$ solution until the endpoint was reached. Aliquot volume was guided by the diluted water salinity.

Cation determination was by Inductively Coupled Plasma - Atomic Emission Spectrometry (ICP-AES) conducted at the School of Geography, University of New South Wales. As all samples had relatively high EC, they were diluted prior to analysis with Millipore Q ultrapure distilled water as per Beck (1998). Two Millipore Q reagent blanks and two repeats were included with the batch as a quality check. Elements analysed by ICP-AES were Na, Mg, Ca, K, Total Fe, Total S, Mn, B, and Sr.

4.7 ENVIRONMENTAL ISOTOPES

4.7.1 Introduction

Environmental isotopes are the naturally occurring isotopes of elements found in abundance in our environment, and are the principle elements of hydrological, geological and biological systems. Oxygen and hydrogen are the constituents of the water molecule so these elements are effective tracers of the origin and history of water (Clarke & Fritz 1997).

The variation in numbers of neutrons in an element provides different isotopes with different atomic masses. The stable isotopes oxygen-18 ($\delta^{18}O$) and deuterium (δ^2H) are isotopically light and since molecules with differences in mass have different reaction rates, this leads to isotopic partitioning or fractionation. During evaporation of water, the vapour becomes isotopically lighter due to fractionation processes. Conversely, when water vapour condenses to form rain, fractionation takes place in the reverse direction with the liquid being isotopically heavier than the vapour. This process (called Rayleigh Fractionation) causes rain to become progressively lighter in $\delta^{18}O$ and δ^2H as it occurs further from the ocean source. In addition, rain becomes isotopically lighter from the equator toward the poles and from

lower to higher elevations.

Stable environmental isotopes are measured as the ratio of the two most abundant isotopes of a given element. Fractionation processes modify this ratio. Ratios of deuterium and oxygen-18 in water samples provide a useful tool for investigating processes that have affected surface and groundwater systems (Leaney 2001).

4.7.2 Sample Collection

Six groundwater and surface water samples were collected from the study site for stable isotope analysis. Samples were collected in 28 mL glass bottles that were filled to the rim to exclude as much air as possible, and then tightly screwed shut. The lids on the bottles were periodically tightened.

4.7.3 Sample Analysis

Samples were delivered to CSIRO Adelaide for $\delta^{18}O$ and δ^2H (deuterium) analysis. Because all six samples had salinity above 3000 mg/L, they required distillation prior to analysis. Analysis was by gas source isotope ratio mass spectrometer (IRMS).

4.8 GROUNDWATER LEVELS

On 4th January 2002, a Hydrokit CTL 200 series groundwater level logger, equipped with DRUCK pressure transducer, was installed in each of the nested bores GW96128/1, GW96128/2 and GW96128/3. Readings were taken every 15 minutes. Manual water level readings were taken at least monthly in each of the GW96128 series bores, as a calibration check against the loggers. The water level in cored hole CH1 was measured on 4 May 2002. Data from the dataloggers was downloaded on 5 May 2002.

Barometric pressure data was available from the Bureau of Meteorology for Dubbo Airport, which is the nearest meteorological station recording this information. Three hourly data was acquired for the period January to May 2002; the period of continuous water level measurement. Daily rainfall data was available for "Binginbar" approximately 3 km away.

The loggers were replaced at the beginning of August 2002 and monitored hourly through to the middle of March 2003. Atmospheric pressure was also measured at the site using a separate atmospheric pressure data logger



Figure 4.24: View South From 'Binginbar" Across Upper Snake Gully Catchment

Chapter 5

RESULTS

5.1 GEOLOGY OF SEDIMENTARY UNITS

Three unconsolidated sedimentary units are exposed in the erosional section of the creek line at the study site. These unconformably overlie Palaeozoic basement. From uppermost to lowermost in the sequence the units are Unit One, Unit Two, and Unit Three (Figure 5.2)

A stratigraphic column summarising the main features of the unconsolidated sedimentary sequence is presented in Figure 8. The main characteristics of each unit are presented in Table 5.1.

5.1.1 Unit One

Unit One is stratigraphically the uppermost and therefore the youngest unit in the unconsolidated sedimentary sequence. It ranges in thickness from 20 cm to 1.1 m. Internal structures and clast arrangement in this unit are consistent with water-borne deposition (Blatt et al. 1980).

The unit consists of loose to moderately dense, or friable, light-medium orange to light-medium brown, 1 to 50% fine to medium gravelly (2 to 80 mm), 20 to 40% fine to coarse sandy, silt.

Clasts consist of charcoal, ironstone, quartz, and Palaeozoic bedrock (Figures 5.3 and 5.4). A significant clast component is sub-rounded calcrete, which has been reworked from underlying sedimentary units and its original horizon of deposition (Figure 5.3). Clasts range in size from fine to medium (2 to 80 mm) gravel. They vary in shape from angular to sub-rounded and are moderately to poorly sorted. Gravelly bands are clast supported, however, clasts are matrix supported in finer grained parts of the unit.

Bands of larger flatter clasts (predominantly siltstone) display upstream imbrication angles relative to bedding of 10 to 35 degrees (Figure 5.5), confirming deposition aqueous under flow (Blatt et al. 1980), in a direction from east to west.

Unit One is very thinly to moderately bedded (1 to 30 cm). Cycles of graded beds commonly occur, these often being truncated or scoured, indicating several phases of relatively high energy deposition, followed by periods of lower energy deposition (Figure 5.6). Bed composition and structure change rapidly with lateral position; a characteristic of channel deposits.

Unit One is most coarsely grained along the central creek line; with grain size and unit thickness decreasing rapidly away from the creek. A facies variation of Unit One is exposed in the eroded wall of a tributary three hundred metres upstream of monitoring bore GW96128. Here, it is still over one metre thick, but is composed of finely laminated silts and clays (Figures 5.6 and 5.7). This facies clearly represents lower energy floodplain or overbank deposits, rather than deposition in the main high energy channel. Unit



Figure 5.1: Eroded Creek Section in Snake Gully Exposing Units One, Two, and Three

Table 5.1: Summary Geological Characteristics of Unconsolidated Sedimentary Units at Study Site

	Unit 1	Unit 2	Unit 3	Unit 4
Colour	Light to medium orange and brown	Medium to dark orange-red brown	Medium to dark orange-red brown	Medium orange-grey brown
Consistency	Loose to moderately dense or friable	Friable to firm	Sti® to very sti®, compacted	Sti® to very sti®, compacted
Material Description	Gravelly sandy SILT	Clayey SILT	Gravelly silty CLAY	Sandy clayey SILT
Key Features	Graded bedding, Scour and fill, Pebble imbrication, Lamination	Randomly oriented matrix supported gravels, Strongly bimodal	Randomly oriented matrix supported gravels, Strongly bimodal	Randomly oriented matrix supported gravels
Unique Features	Graded bedding, Scour and fill, Pebble imbrication, Lamination	Palaeosol, Charcoal, Bleaching	Calcrete, Trace fossils, Relict carbonate stringers, Bleaching, Pores	Massive
Bedding	Very thinly to moderately bedded	Massive to very thickly bedded	Massive to thickly bedded	Massive
Carbonates	Calcareous	Non-calcareous	Non-calcareous	Slightly calcareous
Deposition	Alluvial	Mud/Debris Flow	Debris Flow	Mud/Debris Flow

UNIT ONE

Loose to friable, 0.2 to 1.1m thick, orange-brown, non-dispersive, 1 to 50% fine to medium gravelly, 20 to 40% fine to coarse sandy SILT.









UNIT TWO


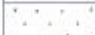
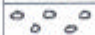


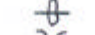

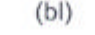
Firm, 0.2 to 2.7 m thick, dark red-brown, dispersive, 1 to 5% fine sandy to fine gravelly, 30% clayey, SILT.

UNIT THREE

Compacted, 0.5 to >1.5m thick, dark orange-red brown, dispersive, 10 to 25% coarse sandy to coarse gravelly, 30% silty, CLAY.

LEGEND

-  Erosional unconformity
-  Gradational contact
-  Nature of contact unknown
-  Internal bedding
-  Lateral variation/facies change
-  Palaeosol
-  Graded bedding
-  Imbricated clasts

-  Clay
-  Silt
-  Sand
-  Gravel
-  Calcrete
-  Bioturbation
-  Relict carbonate stringers
-  Bleached

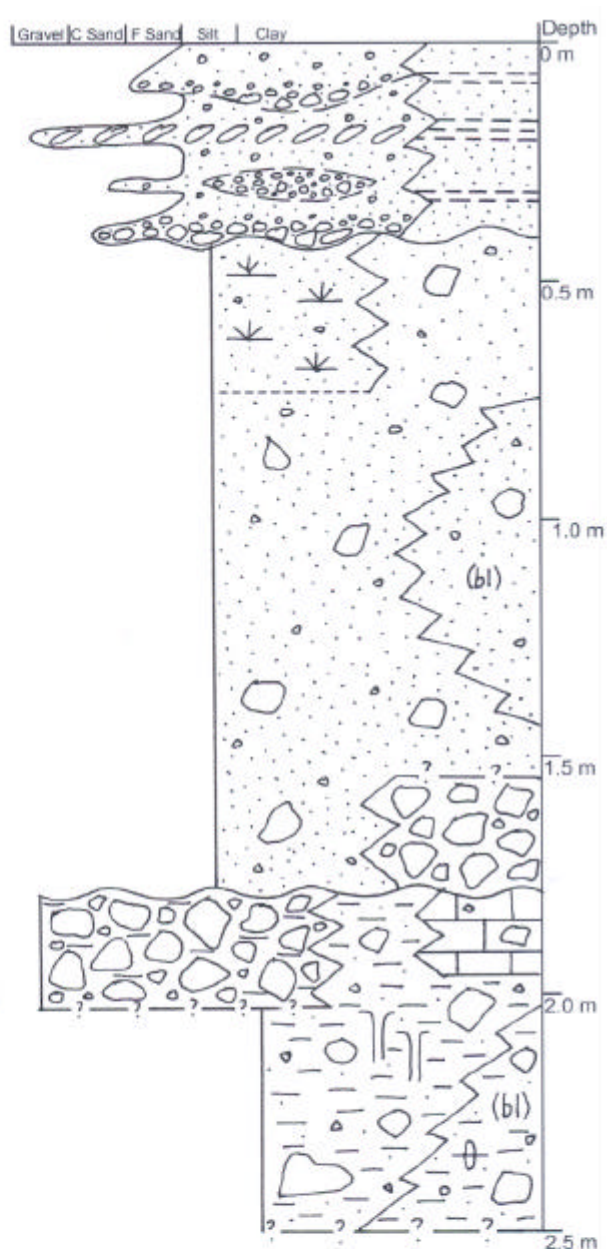


Figure 5.2: Representative Stratigraphic Column For Unconsolidated Sedimentary Units Mapped in Eroded Creek Section in Upper Snake Gully



Figure 5.3: Beds of Calcrete Clasts in Unit One



Figure 5.4: Lenses of Charcoal and Calcrete Clasts in Unit One



Figure 5.5: Clast Imbrication in Unit One



Figure 5.6: Scour and Fill Structure in Unit One

One is penetrated by several slightly carbonised tree stumps and roots, from trees no longer existing above ground.

The unit is not visibly erodible or dispersive. In the paddock adjacent to the creek, the vegetation over Unit One is healthy, and there are no signs of soil salinity or erosion unless the Unit One soils have been disturbed or mixed with Unit Two. In the finer grained facies of this unit, salts accumulate at the top of the capillary zone (Figure 5.7).

Where it occurs, this unit always overlies Unit Two and has an abrupt, planar, erosional, and unconformable basal contact. At several places on equivalent north and south sides of the eroded creek gully, Unit One is slightly thicker by a few centimetres in the southern bank. Adjacent to monitoring bore CH1 is a north branching tributary of the creek. Fifty metres upslope in this tributary, the bank has been eroded to one metre, exposing a clear section. Unit One does not occur at this location (Figure 5.8).

5.1.2 Unit Two

Unit Two is stratigraphically the second unit down, lying below Unit One and above Unit Three in the unconsolidated sedimentary sequence. It ranges in thickness from 0.2 to 2.7 m. The unit is massive, slightly gravelly, silt matrix supported, and strongly bimodal at the hand specimen scale. The features of this unit are consistent with deposition as a liquefied debris flow (Blatt et al. 1980).

The unit consists of friable to firm, medium to dark orange-red brown, 1 to 5% slightly fine sandy to fine gravelly, 30% clayey, silt. Orange mottling is sometimes present. Up to 1% black manganese and iron nodules and concentrations from 1 to 5 mm occur throughout the unit. Clasts consist of quartz, ironstone, ferruginised sandstone, charcoal, calcrete, and minor Palaeozoic siltstone (Figure 5.9).



Figure 5.7: Salt Concentrating at the Top of the Capillary Zone in Unit One



Figure 5.8: Unit Two Exposed in North Branching Tributary of Snake Gully Creek (100m N of CH1), Note: Unit one not present at this location



Figure 5.9: Clast Detail Unit Two



Figure 5.10: Large Angular Clast of Basement Siltstone Entirely Supported by Matrix, Showing the Strong Bimodality of Unit Two

Clast sizes are predominantly coarse sand to fine gravel (2 to 16 mm), and these are matrix supported. They vary in shape from angular to sub-rounded, however, calcrete is always sub-rounded, and Palaeozoic siltstone is always angular to sub-angular. The clasts are randomly oriented and distributed, and are very poorly sorted.

Although the main body of this unit is massive, a half metre thick, coarse basal silty gravel was observed at one location. This is composed of up to 70% randomly oriented angular coarse gravel clasts up to 300 mm, sourced from outcropping Palaeozoic basement tens of metres upstream.

Other large clasts consist of quartz, ironstone, and ferruginised sandstone. Clasts are entirely floating within the silt-clay matrix (Figure 5.10), or are partially clast supported. This infers that, at time of deposition, the muddy matrix must have been sufficiently dense to enable it to support such large clasts, as would occur in a debris flow (Blatt et al. 1980).

Near monitoring bore GW96128, Unit Two grades laterally into a ten metre long pale greyish-cream and orange mottled zone that has been leached of ferromagnesian minerals. This bleached zone is a result of selective redox conditions occurring after deposition (Figure 5.11).

Trees were, at one time, growing in the top of this unit. Now, slightly carbonised roots and stumps are all that remain (Figure 5.12). At several locations at the top of Unit Two, a very dark brown fossil soil horizon exists. It ranges in thickness from 10 to 50 cm. This palaeosol may have been spatially extensive throughout the area, formed in a period of moist warm climate, and subsequently eroded from all but those areas in the gully where it was preserved by further deposition. Alternatively, the palaeosol may have formed in swampy areas of low gradient during periods of comparative climatic stability (chain-of



Figure 5.11: Bleaching in Unit Two Adjacent To GW96128 Bore Site



Figure 5.12: Relict Tree Roots In Unit Two



Figure 5.13: Palaeosol at Top of Unit Two



Figure 5.14: Hexagonal Shrinkage Cracks and Surface Frittering In Unit Two

ponds scenario). Whatever the case, some erosion on the top of this layer has occurred since its deposition (Figure 5.13).

Analysis of palaeosol material returned an organic carbon content of 1.55%. This was lower than expected given the very dark colour, and it is suggested that much of the organic matter has already decomposed (Lawrie, J. 2001, pers. comm., 26 Nov.).

Unit Two is highly dispersive, even where bleached. It displays significant hexagonal and columnar shrink-swell cracking, indicating a significant component of expandable lattice clays. Wetting and drying of this unit causes frittering of its surface (Figure 5.14). This, combined with its highly dispersive properties, results in rapid erosion of the unit once exposed. Rill, gully, and tunnel erosion are all prominent features of this unit.

During late July 2001, a dark area of soil 30 m by 20 m, with poor or no crop germination was observed close to the creek line at the study site (Figure 5.15). Closer inspection showed that this area was not damp (groundwater seepage) but indicated where the darker subsoil had been incorporated into the topsoil by ploughing. This dark subsoil was sedimentary Unit Two, exposed in the eroded creek face 20m away. Observation of this low germination area during the following 12 months showed that these mixed soils have a propensity to disperse and lose their structure due to raindrop impact. Consequently, little vegetation establishes on these areas. The net result is reduced infiltration and increased surface runoff from this area and may eventually lead to erosion.

During dry periods, salts effloresce on the surface of Unit Two (Figure 5.16). Groundwater seepage occurs at the contact with Unit Three, possibly a result of a permeability contrast between units.

In thicker sections, Unit Two is well developed and reaches a maximum thickness of over 2.5m. At these locations, it always overlies Unit Three, and the contact between the units is a parallel erosional



Figure 5.15: Area of crop germination failure due to entrainment of Unit 2 material



Figure 5.16: Columnar Shrinkage Cracks and Salt Efflorescence on Surface of Unit Two



Figure 5.17: Manganese Nodules and Relict Carbonate Stringers in Unit Three



Figure 5.18: Clasts In Unit Three Exposed In Creek Platform

unconformity. Where the sequence is not well developed (eg 400 m upstream from the monitoring bores) it is much thinner and the contact with Palaeozoic basement is an erosional angular unconformity. This unit is not always overlain by Unit One, as is seen in the north branching tributary near monitoring bore CH1 (Figure 5.8).

5.1.3 Unit Three

Unit Three is stratigraphically the third unit down, lying below Unit Two in the unconsolidated sedimentary sequence. The base of Unit Three is not visible, however, the exposed part of the unit ranges in thickness from 0.5 to 1.5 m. The unit is significantly more compacted and coarse (gravelly) than Unit Two. It is thickly bedded to massive, clay matrix supported, and strongly bimodal at the hand specimen scale. The features of this unit are consistent with deposition as a liquefied debris flow (Blatt et al. 1980).

The unit consists of well compacted, stiff to very stiff, medium to dark orange-red brown, 10 to 25% coarse sandy to coarse gravelly (2 mm to 300 mm), 30% silty, clay. Orange and tan mottling is common. Angular pores up to 1.5 mm are sometimes present, indicating post-compaction leaching of some component. Up to 2% black manganese and iron nodules and concentrations up to 15 mm occur throughout the unit (Figure 5.17). Clasts consist of quartz, silicified siltstone, ironstone, ferruginised sandstone, and angular to sub-angular Palaeozoic siltstone (Figures 5.18 and 5.19).

Clast range in size from fine to medium gravel (5 to 75 mm), and are matrix supported consistent with deposition as a mud-flow (Blatt et al. 1980). Clasts vary in shape from angular to sub-rounded, randomly oriented and distributed and are very poorly sorted.



Figure 5.19: Matrix Supported Clasts In Unit Three



Figure 5.20: Incised Channel in Unit Three

The unit is generally massive, but thick (0.5 to 1 m) matrix supported beds within the unit contain up to 40% randomly oriented clasts which range in size from 20 to 300 mm and are dominantly composed of angular Palaeozoic siltstone.

Unit Three grades laterally into a ten metre zone of cream and orange mottled bleaching 300 m upstream of the monitoring bores. This bleached zone indicates ferromagnesian mineral leaching due to selective redox conditions occurring after deposition.

The unbleached surfaces of Unit Three have developed a thin (<5 mm) non-dispersive crust that has a "waxy" indurated appearance (Figure 5.19). This crust was probably formed by weathering, salt precipitation, and chemical modification of the exposed face, and appears to be composed of ferrous oxyhydroxides and clays.

At several locations at the top of Unit Three, a 10 to 30 cm band of flaggy, weak to moderate well cemented calcareous duricrust occurs. This calcrete appears to be in-situ, and is the source for calcrete clasts in overlying units. A calcrete horizon may have been well developed across the area, or alternatively, it was locally developed in the gully only. It is clear, however, from the amount of this material comprising overlying units, that significant erosion of the calcrete occurred prior to deposition of Unit Two.

Vertical and sub-vertical cream and light grey 10 to 20 mm wide tubular structures filled with non-calcareous clay are present at several locations. These are believed to be relict carbonate stringers (Figure 5.17).

Fossil burrows are observed in the bleached zone of the creek platform in Unit Three. The contrast between the unit matrix and the burrow fill material is highlighted in the bleached zone, probably owing to slight differences in chemical composition between the two, making them easily visible at this location. The burrows are up to 1 cm wide and are branched. One example (Figure 4.7) exhibits backfilling meniscus. This evidence of bioturbation indicates that, at some stage in the past, Unit Three was much less compacted, and had a soft mud consistency.

Unit Three is highly dispersive, even where bleached, however, the degree of compaction combined with the protective surface crust, means that this unit is much less prone to erosion. Instead, it forms a solid pavement through which the creek cuts a deep narrow channel (Figure 5.20).

During dry periods, salts effloresce on the surface of this unit (Frontispiece and Figure 2.9). Groundwater seepage and salt accumulation are associated with the top of Unit Three. This may be coincident with the top of the capillary zone, or is more likely related to some hydraulic property contrast with overlying Unit Two (Figure 5.1).

Although the contact between Unit Three and Palaeozoic basement is not exposed, an angular erosional unconformity is implied by stratigraphic relationships. Unit Three is absent where basement is shallow and the sequence is thin and poorly developed. Either, it was never deposited in these locations, or it was totally eroded prior to deposition of Unit Two (Figure 5.21 and Figure 5.22 with Unit Two only 0.5 m



Figure 5.21: Unconformable Angular Contact of Sedimentary Units With Basement

thick). Given the variation in thickness of overlying sedimentary units, and depth to basement along the creek line, basement topography appears to be highly irregular.

5.2 BOREHOLE DRILLING AND GEOLOGICAL LOGGING

Site and location details for bores completed at the study site are shown on Figure 4.1 and 4.21.

5.2.1 Cored Hole CH1

A cored hole was successfully completed to a depth of 3.3 metres. Core samples from CH1 were logged in detail and four unconsolidated sedimentary units were identified. Main characteristics of each unit are presented above in Table 5.1.



Figure 5.22: Unconformable Angular Contact With Basement

Table 5.2: Summary Lithology in Bore GW96238/3

Depth	Lithology
0 - 4.5 m	Sandy clay and silt
4.5 - 11 m	Weathered bedrock
11 - 31 m	Fresh, felsic to intermediate volcanic

5.2.2 Nested Bore Site GW96128

Three nested monitoring bores were completed at the study site. A summary of lithology encountered in the deepest borehole, GW96128/3, is presented in Table 5.2.

5.3 DATING OF UNITS

5.3.1 Circumstantial Evidence

An upright buried plough disc is exposed in an eroded face of Unit One. There is very little possibility that the disc was ripped loose whilst this unit was being ploughed (L Yeo 2002, pers. comm., 29 March). More likely, the disc was removed from the plough and left lying adjacent to the creek, where it has been incorporated into this unit during a phase of recent alluvial deposition. This evidence implies an age of deposition for Unit One within the era of the disc plough. Cropping and the use of disc ploughs in the Snake Gully district commenced around 1850 (L Yeo 2002, pers. comm., 29 March). Unit One has been dissected by severe gullyng at this location. Gully development did not commence until after the rabbit plague, during the early 1950's rainfall events (L Yeo and D Yeo 2002, pers. comm., 29 March; R and



Figure 5.23: Plough Disc Entrained During Deposition of Unit One

J Yeo 2002, pers. comm., 3 April; M and R Simpson 2002, pers. comm., 3 April and 10 June). Thus, stratigraphic and historical evidence suggest an age of deposition for Unit One of between 50 and 150 years ago (1850's to 1950's).

5.3.2 Trace Fossils

The species that created the trace fossils in Unit Three was not able to be determined, which precluded these as a dating method.

5.3.3 Radiocarbon Dating

Radiocarbon dating results for samples from Unit Two are given in Table 5.3.

Results are reported as percent Modern when the conventional (uncalibrated) C^{14} age is younger than 200 yr BP or younger than ca 1750 AD in calendar years. Samples assigned a result of "Modern" cannot be calibrated (Hogg, A. 2002, pers. comm., 31 May).

5.4 CORE ANALYSIS

A summary of results derived from tests conducted on unconsolidated sedimentary units in cored hole CH1 is given in Table 5.4.

Table 5.3: Radiocarbon Dating Results for Unit Two at Snake Gully

Location	Sample Number	C ¹⁴ Date	Calibrated Date of Deposition in Years AD (% probability)	Material Dated
1	10882	Modern < ca 1750 AD	-	Charcoal clast <5 grams
2	10883	Modern < ca 1750 AD	-	Charcoal clast
3	10884	277 ± 50 BP	1480 - 1690 (67.9%) 1620 - 1680 (30.6%)	Charcoal clast
4	10885	229 ± 54 BP	1630 - 1960 (92.5%) 1620 - 1680 (30.6%) 1640 - 1690 (19.7%)	Charcoal clast
5	10886	Modern < ca 1750 AD	-	Tree root

Table 5.4: Mean 1:5 Extract and Emerson Aggregate Test Data - Cored Hole CH1

Cored Hole	N	PH	EC	Salinity Class	Emerson Class Number Range	Average Dispersibility	Sodicity
Unit 1	5	8.47	144	Non-saline	4 to 2(1)	Negligible (top 10 cm) to high	May be sodic
Unit 2	6	8.36	461	Moderately to highly saline	2 (1) to 2 (2)	High to moderate	Highly likely to be sodic (to may be sodic)
Unit 3	10	8.28	301	Moderately saline	3(3) to 2(1)	High to moderate	May be sodic
Unit 4	8	8.28	346	Moderately saline	2(1) to 2(2)	High to moderate	Highly likely to be sodic (to may be sodic)

Table 5.5: Relationship of Emerson Aggregate Class Number With Dispersibility

Emerson Aggregate Classes	Dispersibility
1 and 2 (3)	Very High
2 (2)	High
2 (1)	High to Moderate
3 (4) and 3 (3)	Moderate
3 (2), 3 (1), and 5	Slight
4, 6, 7, 8	Negligible/Aggregated

Table 5.6: Relationship Between Emerson Class Number and Sodicity

EAT Class	Sodicity
Class 1 and 2 (3)	Almost certainly sodic
Class 2 (2)	Highly likely to be sodic
Class 2 (1)	May be sodic
Classes 3 (4), 3 (3)	May be sodic
Classes 3 (2), 3 (1)	Unlikely to be sodic
Class 4	May be sodic
Class 5	Unlikely to be sodic
Class 6	Almost certainly non-sodic

5.4.1 Emerson Aggregate Testing

Emerson Aggregate Test Class Numbers (EAT) were determined by the procedure described by Smithson (2002). EAT numbers are related to dispersibility by Charman (1978) in Table 5.5. A summary of the average dispersibility for each sedimentary unit presented above is given in Table 5.4. A general guide to the relationship between sodicity and Emerson Aggregate Class is given by Hazelton & Murphy (1992) and is presented in Table 5.6.

Results from Emerson Aggregate testing show that, except for the top 10 cm, Unit One has a high susceptibility to dispersion. Units Two, Three and Four all have a moderate to high susceptibility to dispersion.

5.4.2 Aqueous Extracts

The results are reported as soil 1:5 extract conductivity (EC1:5) read directly from the soil solution. Variation in EC1:5 with depth is presented in Figure 5.24.

A summary of the average EC1:5 for each unit is presented below in Table 5.9. Unit One contains far less soluble salts than the underlying three sedimentary units. The top 40 cm of Unit One has an average salinity of $110 \mu\text{S}/\text{cm}$. Soluble salts are variably distributed within Units Two, Three, and Four, with EC1:5 ranging between 200 and $600 \mu\text{S}/\text{cm}$. Unit Two is the most salty, with the highest EC1:5 value of $620 \mu\text{S}/\text{cm}$.

A salinity classification for soils based on 1:5 extract conductivity (adapted from Nicoll & Scowan (1993)) is given in Table 5.7.

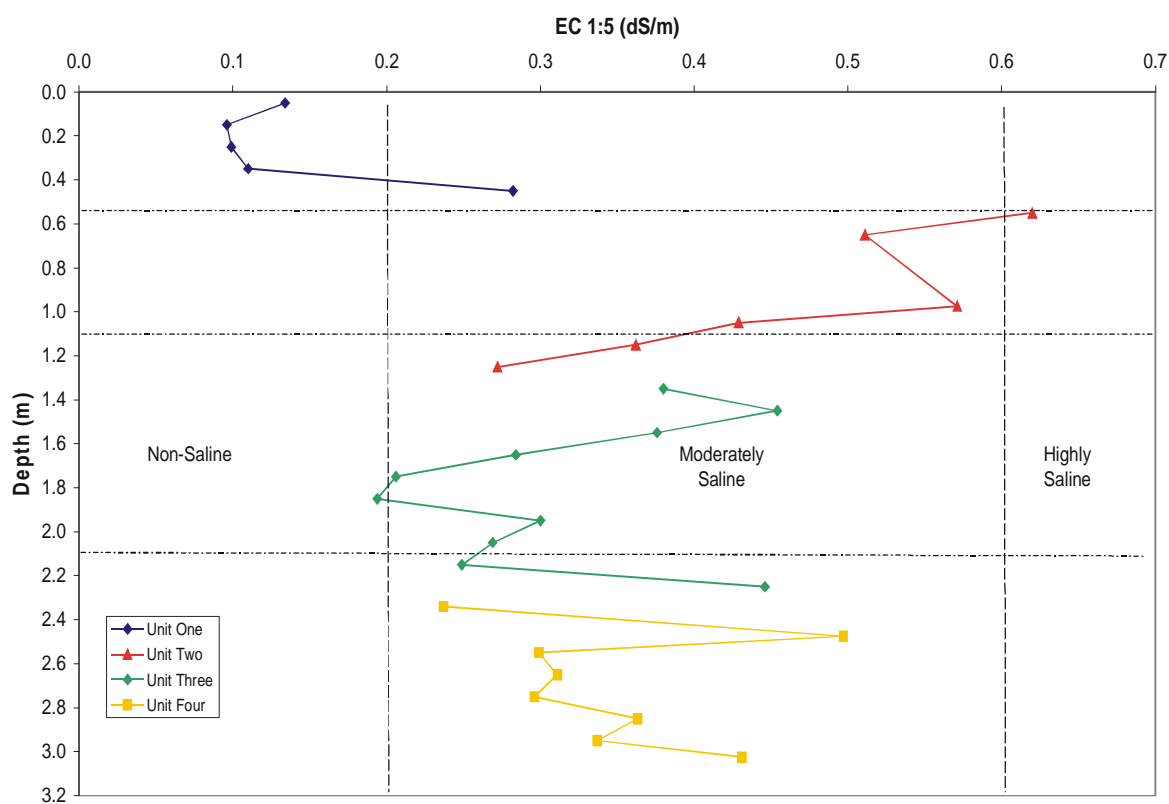


Figure 5.24: Variation in EC1:5 With Depth for CH1

Table 5.7: Salinity Classification of Soils Based on Aqueous Extract Conductivity

Electrical Conductivity 1:5 Soil Solution $\mu\text{S}/\text{cm}$)	Salinity Classification
< 200	Non-saline
200 - 600	Moderately saline
600 - 2000	Highly saline
>2000	Extremely saline

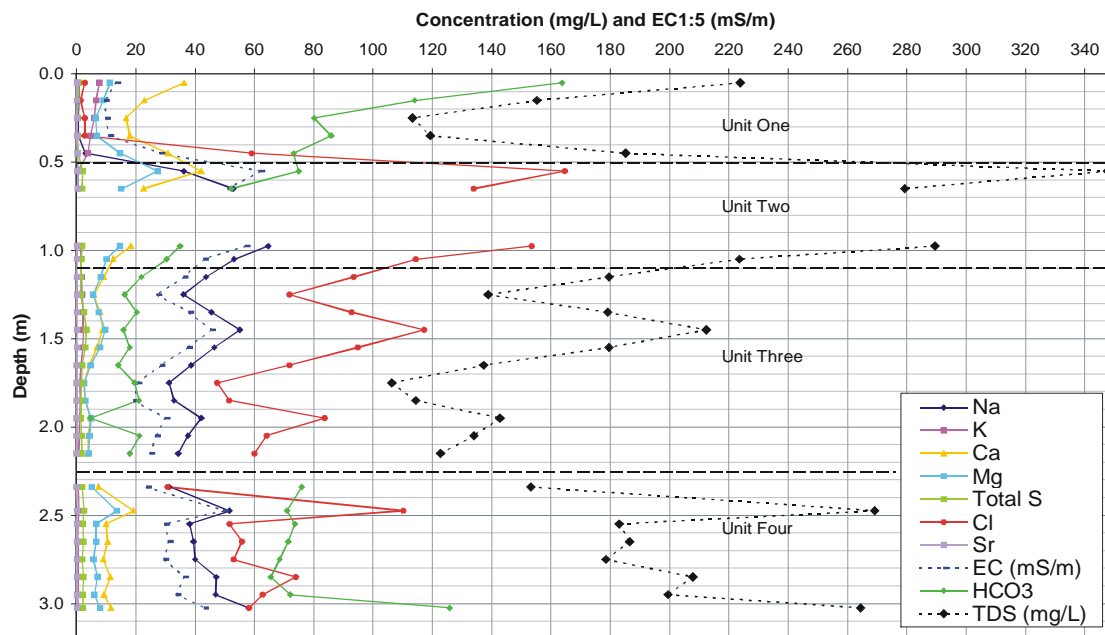


Figure 5.25: Major Ions, TDS, and EC with Depth in CH1

5.4.3 Aqueous Extract Major Ions

Major ion analysis results for all CH1 samples are shown on Figure 5.25 and are given in Table 5.8. Mean data for the 4 units is shown in Table 5.9.

A piper diagram of major ions for the extract waters is presented in Figure 5.26.

Unit One is dominated by calcium, magnesium, and bicarbonate ions, but has a lower ionic concentration than underlying units with a mean TDS of 159 mg/L. The deepest sample in Unit One displays geochemical characteristics averaging between Unit One and Two.

Units Two, Three and Four are dominated by sodium and chloride. In Unit Four, calcium and magnesium are both higher than in Units Two and Three, however sodium is still the major cation. Bicarbonate content is distinctly higher in Unit Four than in Units Two and Three, and is the major anion, followed by chloride. The mean TDS for Units Two, Three and Four combined is 193 mg/L.

The distinctly different chemical nature of the soluble salts in the four sedimentary units is evident by the groupings formed on the piper diagram. Unit One is clearly quite different in salt composition (being calcium and bicarbonate dominated) compared with the three other units (which are sodium-chloride dominated).

5.4.4 Grain Size Analysis

A summary of sub-50 micron particle size frequency for representative units is presented in Figure 5.27.

Results indicate that the majority of the sub-50 material is very fine silt and clay, with no peaks at the expected 30 to 40 micron size as suggested by Townsend (1997). Instead, all samples display characteristic peaks at 2 microns (clay), and between 6 and 8 microns (fine silt).

Sedimentary Unit One displays subdued peaks at 2 and 7 microns, while these peaks are much more pronounced in Units Two, Three, and Four. These characteristic peaks also occur in the sample of

Table 5.8: Groundwater related studies at the Hudson site.

ID	Depth	Na mg/l	K mg/l	Ca mg/l	Mg mg/l	SO ₄ mg/l	Sr mg/l	Cl mg/l	HCO ₃ mg/l	pH mg/l	EC μS/cm
Unit 1											
CH1	0.05	0.92	7.75	36.30	11.30	0.87	0.24	2.79	163.76	8.35	134
CH2	0.15	0.69	6.58	22.80	9.14	0.55	0.18	1.40	114.00	8.48	96
CH3	0.25	0.62	6.04	16.73	6.53	0.35	0.13	2.79	80.11	8.58	99
CH4	0.35	0.67	4.69	18.00	6.88	0.34	0.14	2.79	85.87	8.56	110
CH5	0.45	3.07	3.81	30.75	14.70	0.54	0.30	59.06	73.22	8.4	282
Unit 2											
CH6	0.55	36.20	0.48	42.00	27.30	2.13	0.51	164.63	74.94	8.31	620
CH7	0.65	52.85	0.65	22.60	15.15	1.86	0.29	133.94	52.24	8.46	511
	0.75										
	0.85										
CH8	0.97	64.70	1.37	18.40	14.70	1.93	0.26	153.47	34.95	8.29	571
CH9	1.05	53.10	1.46	12.40	10.10	1.58	0.19	114.40	30.46	8.37	429
CH10	1.15	43.70	1.68	9.17	8.12	1.46	0.15	93.48	21.92	8.35	362
CH11	1.25	36.10	1.82	5.89	5.56	1.38	0.10	71.85	16.24	8.37	272
Unit 3											
CH12	1.35	45.50	2.35	7.97	7.62	2.53	0.14	92.78	20.38	8.35	380
CH13	1.45	55.10	2.37	8.84	9.68	3.30	0.17	117.20	15.84	8.18	454
CH14	1.55	46.50	2.14	6.98	8.06	3.06	0.14	94.87	17.96	8.2	376
CH15	1.65	38.70	1.59	4.42	4.78	1.94	0.08	71.85	14.04	8.27	284
CH16	1.75	31.20	1.15	2.51	2.60	1.72	0.05	47.44	19.67	8.37	206
CH17	1.85	32.87	1.20	2.91	3.09	1.55	0.05	51.45	21.09	8.42	194
CH18	1.95	42.10	1.03	4.78	4.87	1.52	0.08	83.71	4.74	8.27	300
CH19	2.05	37.60	0.97	3.93	4.39	1.63	0.07	64.18	21.26	8.27	269
CH20	2.15	34.30	0.74	3.86	4.11	1.76	0.07	59.99	17.93	8.21	249
	2.25										
Unit 4											
CH22	2.34	31.40	0.58	7.40	5.08	2.01	0.09	30.69	75.99	8.16	237
CH23	2.47	51.60	0.89	19.30	13.60	2.60	0.24	110.22	70.97	8.1	497
CH24	2.55	38.20	0.65	10.00	6.66	2.18	0.12	51.62	73.64	8.07	99
CH25	2.65	39.45	0.44	10.50	6.71	2.31	0.12	55.81	71.36	8.3	311
CH26	2.75	40.00	0.36	9.01	5.71	1.96	0.10	53.02	68.51	8.41	296
CH27	2.85	47.10	0.38	11.40	7.17	2.31	0.13	73.94	65.51	8.24	363
CH28	2.95	46.90	0.43	9.23	6.02	2.09	0.10	62.78	72.08	8.4	337
CH29	3.02	58.00	0.59	11.60	7.91	2.26	0.13	58.25	125.82	8.38	431

Table 5.9: Mean Geochemical Data For Cored Hole CH1

Cored Hole 1:5 Ex- tracts	No of Samples	TDS	Na	Mg	Ca	K	Cl	HCO ₃	Total S	Total Fe
Unit 1	5	154	1.2	10	25	0.15	14	103	1	0.06
Unit 2	6	241	48	13	18	0.03	122	38	2	0.004
Unit 3	10	145	40	5	5	0.04	76	17	2	0.05
Unit 4	8	204	44	7	11	0.01	62	78	2	0

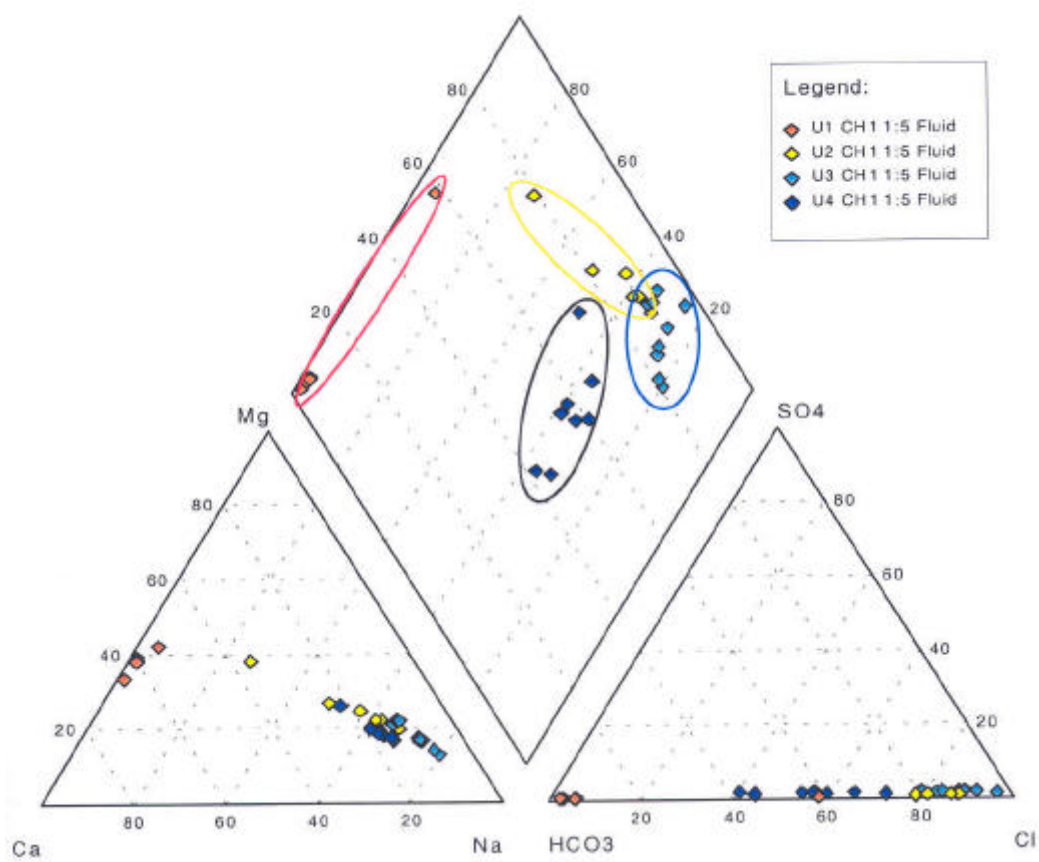


Figure 5.26: Piper Diagram of 1:5 Extract Fluids for CH1 at Study Site in Snake Gully Catchment

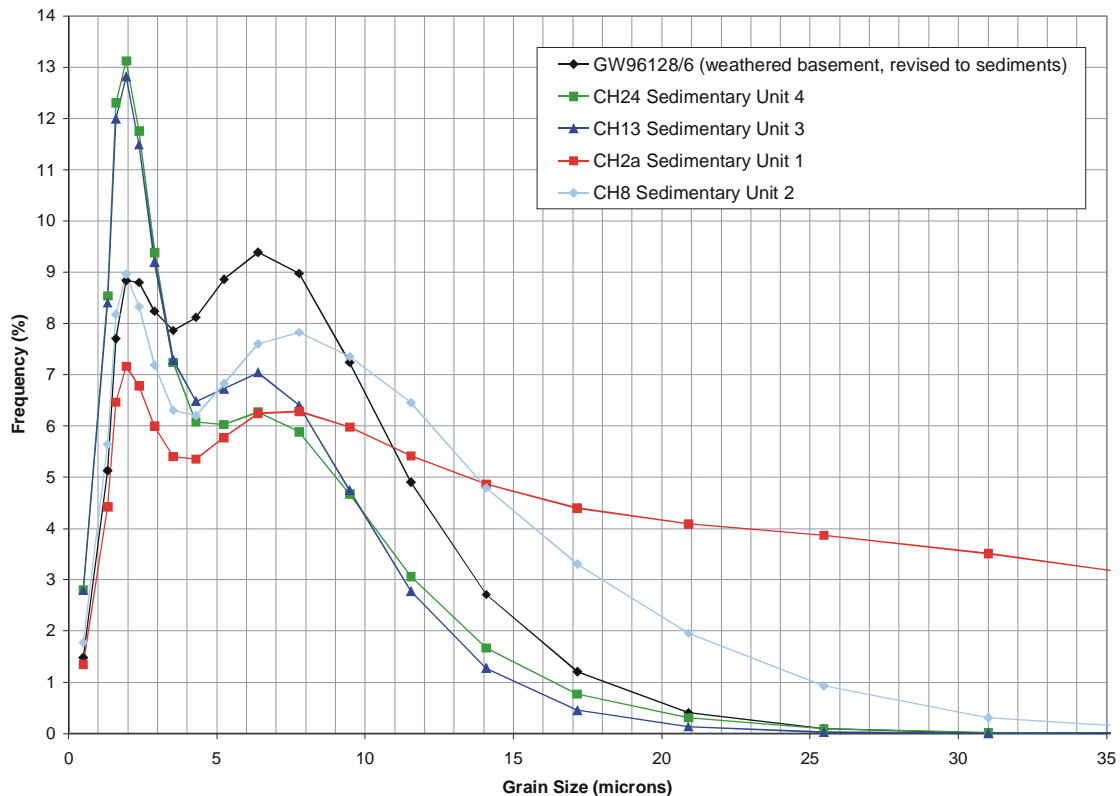


Figure 5.27: Sub-50 Micron Particle Size Frequency for Selected Samples from CH1 and GW96128

weathered basement, however, the 7 micron peak is much more prominent than the 2 micron peak.

5.5 GEOPHYSICAL TECHNIQUES

5.5.1 Introduction

Resistivity is the ratio of electric field to current density and is the inverse of conductivity. It represents the "difficulty with which current flows through the ground". Convention dictates that measurements made using galvanic techniques (electrodes and wire) are recorded as resistances (Ohms) whereas measurements made using inductive techniques (EMI) are recorded as conductances (Siemens) even though the physical property being measured is the same. Measurements of electrical conductivity are presented with the units millisiemens per metre (mS/m). Measurements of electrical resistivity are presented as ohm metres (ohm m) (Acworth 1999).

The electrical conductivity or resistivity of a homogeneous volume of material is a function of many variables, including porosity, saturation, clay content, grain size and shape, and the total dissolved solids in the saturating fluid. Changes in any one of these variables may cause the electrical conductivity to change. The apparent electrical conductivity over ground containing zones of differing electrical conductivity, represents a weighted average electrical conductivity value that is influenced by the values of electrical conductivity in the various zones (Acworth 1999).

In all electrical geophysical techniques, a variety of ground conditions can contribute to the measured values. As a result of this, these surveys are best interpreted in conjunction with information about the geological material and water quality. Additional information about ground conditions from geological logging, sample analyses, water level observations, and fluid conductivity measurements, should be used

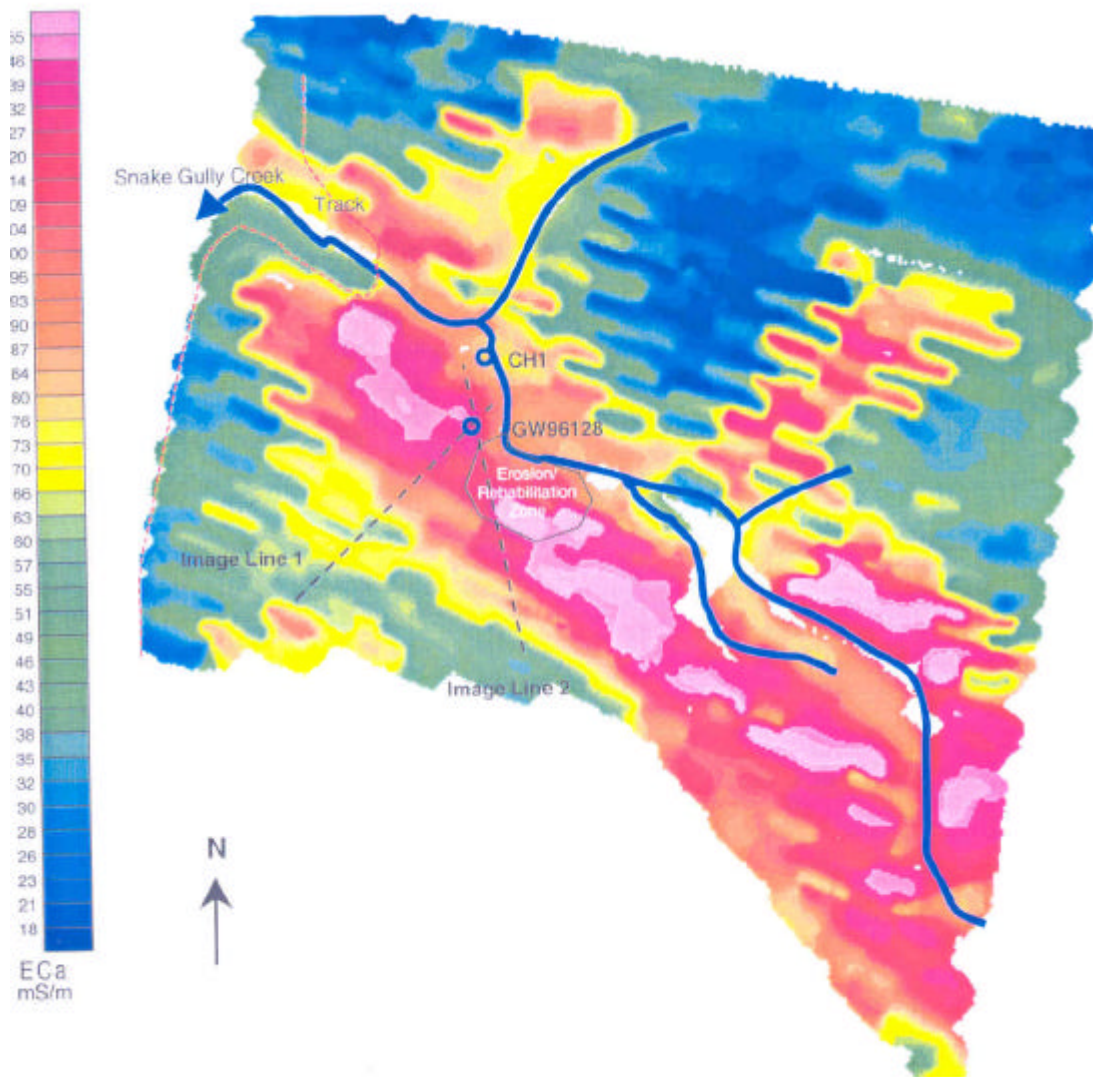


Figure 5.28: EM31 Image For Study Site Paddock at "Murrawega"

to arrive at an interpretation closest to the real ground conditions (Griffiths & King 1981; Kearey & Brooks 1991; Shaver 1997).

5.5.2 EM31 Survey

The location of the EM31 survey is shown on Figure 4.1 (airphoto). The results of the EM31 survey are presented in Figure 5.28. In addition, a three-dimensional surface was created from the GPS co-ordinates collected during the survey, and the EM31 image was draped over this surface (Figure 5.29). Areas of white indicate that no data was collected at those locations due to gullies restricting access.

Near the monitoring bores, the EM31 shows a 60 metre wide, highly (apparent) conductive linear zone, in the order of 150 mS/m. This zone is oriented the same as the drainage line, but the creek lies along its northern margin. Bore CH1 is located at the margin of this zone, whereas GW96128 is closer to the centre. At the top end of the area surveyed, the area of high apparent conductivity broadens. High apparent conductivity arms are indicated lying parallel with, but offset west of the two northeast trending creek tributaries. Away from these zones, conductivity diminishes rapidly upslope to apparent conductivities of less than 20 mS/m.

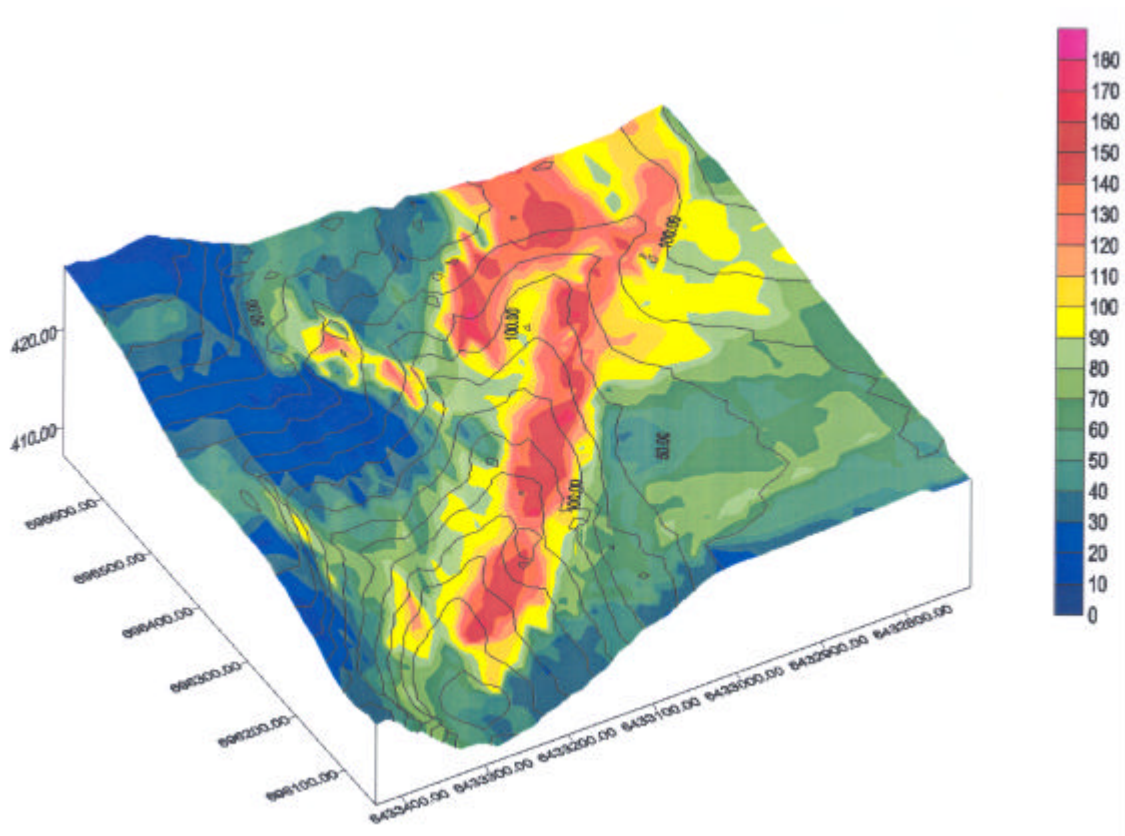


Figure 5.29: EM31 Survey Draped Over Elevation Data

5.5.3 Electrical Imaging

The location of the two image lines are shown on Figure 4.1 and Figure 5.28. The field data was used to construct a theoretical 2-dimensional cross section of measured apparent resistivity. Inversion techniques were then applied to derive a modelled true resistivity distribution. The mean square of the errors for inversion of image lines was 3.2% and 1.05%, these are considered acceptable, and indicate that a good match was achieved between modelled and observed values.

Colour pseudo-sections of the final inversion derived model, are presented for Line 1 in Figure 5.30 and for Line 2 in Figure 5.31.

Results for line one show a relatively consistent, low resistivity layer of less than 5 ohm m, that is between 3 and 8 m deep, and thickens upslope. Below this, there is a rapid transition into a much higher resistivity zone, which has apparent resistivities up to 200 ohm m. Results for line two indicate a similar resistivity distribution; however, at about 65 metres along the line, the very low resistivity layer lenses out sharply. Further upslope, near the end of the line, is a lower resistivity zone of about 10 ohm m, which has a thickness of about five metres.

To provide a comparison with the data from the study site, an electrical image taken adjacent to the road at Binginbah (Figure 4.21 sample site 22) and passing through the deep bore GW96122 is shown in Figure 5.32 and an image measured across the lower part of the valley at Mindawanda (Figure 4.21 sample site 23 - 27) is shown in Figure 5.33.

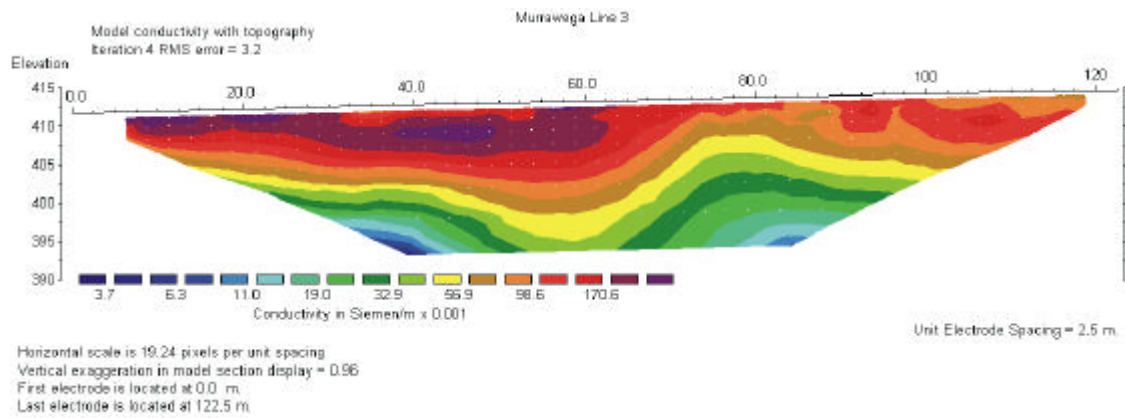


Figure 5.30: Electrical Resistivity Image Line One

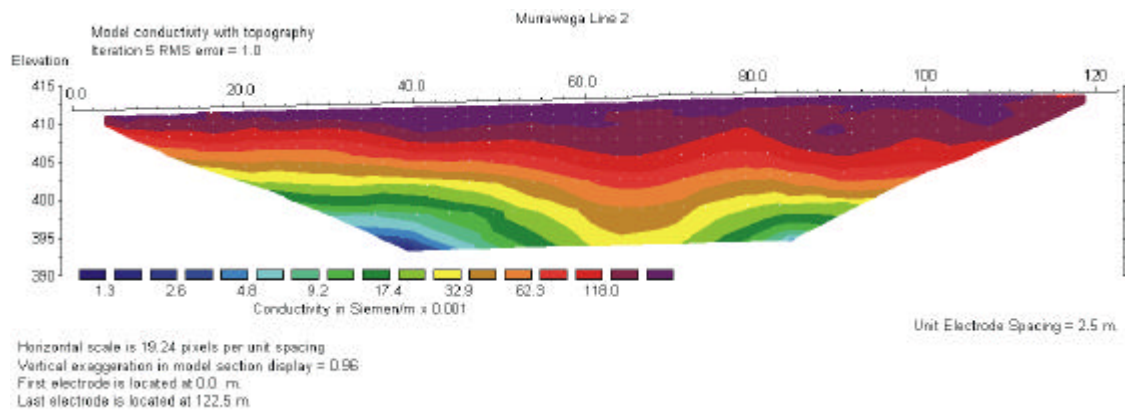


Figure 5.31: Electrical Resistivity Image Line Two

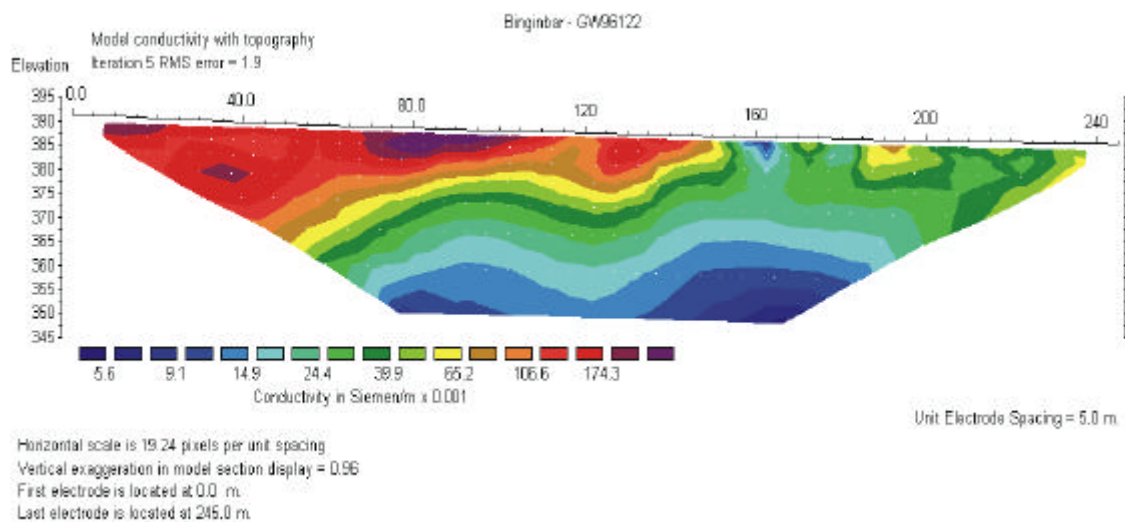


Figure 5.32: Electrical Resistivity Image Line passing through GW96122

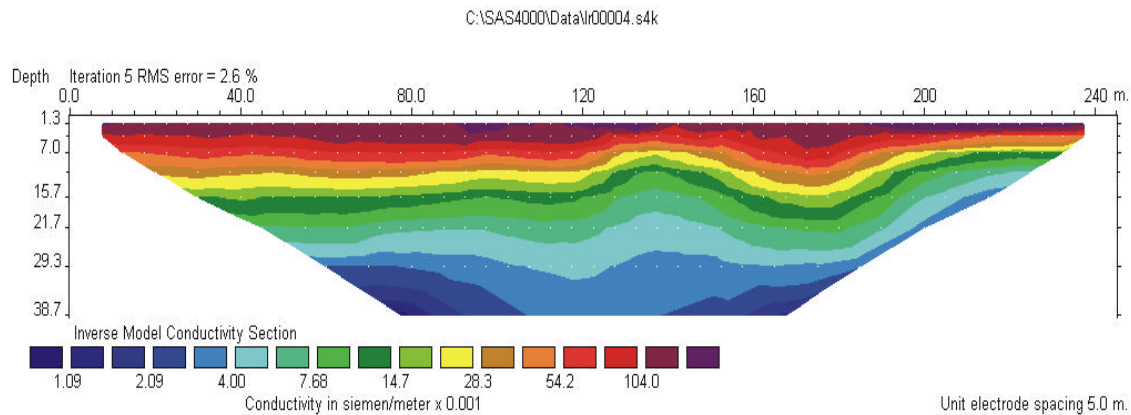


Figure 5.33: Electrical Resistivity Image Line over the valley at Mindawanda

5.5.4 Borehole Geophysical Logging

Results are presented in Figure 5.34 for deep bore GW96128/3, and in Figure 5.35 for shallow cored hole CH1. Aqueous extract EC1:5 is plotted for samples from the bores for comparison with downhole bulk EC. Data is also presented in Figure 5.36 for the deep (>100 m) bore at Binginbar Farm adjacent to the access road.

The deep bore GW96128/3 has steel casing installed to one metre, so initial bulk EC readings are discounted from interpretation because of casing effects. Bulk EC below the steel casing in GW96128/3 is high, at over 200 mS/m, but by 5 metres this drops to just over 100 mS/m. Geological logging of cuttings from this hole suggested that the contact with weathered basement was at about 4.5 metres. The bulk EC of the basement is very uniform at about 6 to 7 mS/m. This confirms the much higher bulk electrical conductivity of the unconsolidated sedimentary units compared with basement.

A peak in conductivity at 6 metres may indicate a saline horizon in the weathered rocks, alternatively, the top of the basement may have been incorrectly determined in the geological logging and could be around 7 metres. Since this hole was originally logged, it has been discovered that coarse basement clasts occur in the lower sedimentary units. It is possible that chips of coarse basement gravels recovered in samples from 4.5 to 7 metres, caused the assumption of weathered basement.

Gamma-ray activity, which is unaffected by the steel casing, shows that the top 0.5 metres are sandier than the rest of the hole. The remainder of the gamma log indicates a relatively uniform clayey composition to end of hole, however, small gamma peaks occur from 7.5 to 8 metres and 18 to 23 metres, indicating more clay rich zones. The first zone is most probably the highly weathered upper basement, supporting the idea that top of basement may be deeper than originally interpreted. The second zone could be due to fracture facilitated basement weathering.

Run one of the EM39 in bore CH1 shows an initially low bulk EC which increases rapidly down to 0.5 metre, whereas run two has a number of peaks in the top 0.3 m of this hole, but from then parallels run one for the rest of the hole. The variability in the top of run two is regarded as spurious, confirmed by the values from the first run and the EC1:5 conductivities.

In run one, conductivity increases from about 35 mS/m at surface to about 85 mS/m at the base of Unit One. At the top of Unit Two, in the palaeosol layer, the bulk EC drops sharply.

Bulk EC has a strong peak of up to 200 mS/m between 8 and 10 metres. Core loss occurred between 0.7 and 0.95 metres, so EC1:5 values are not available for comparison, but samples either side of the zone of core loss do have higher EC1:5 values. A dip down to about 140 mS/m occurs at 1.1 m, after which bulk EC is relatively constant at about 170 mS/m. All of these trends are reflected in the EC1:5 values for samples from this hole.

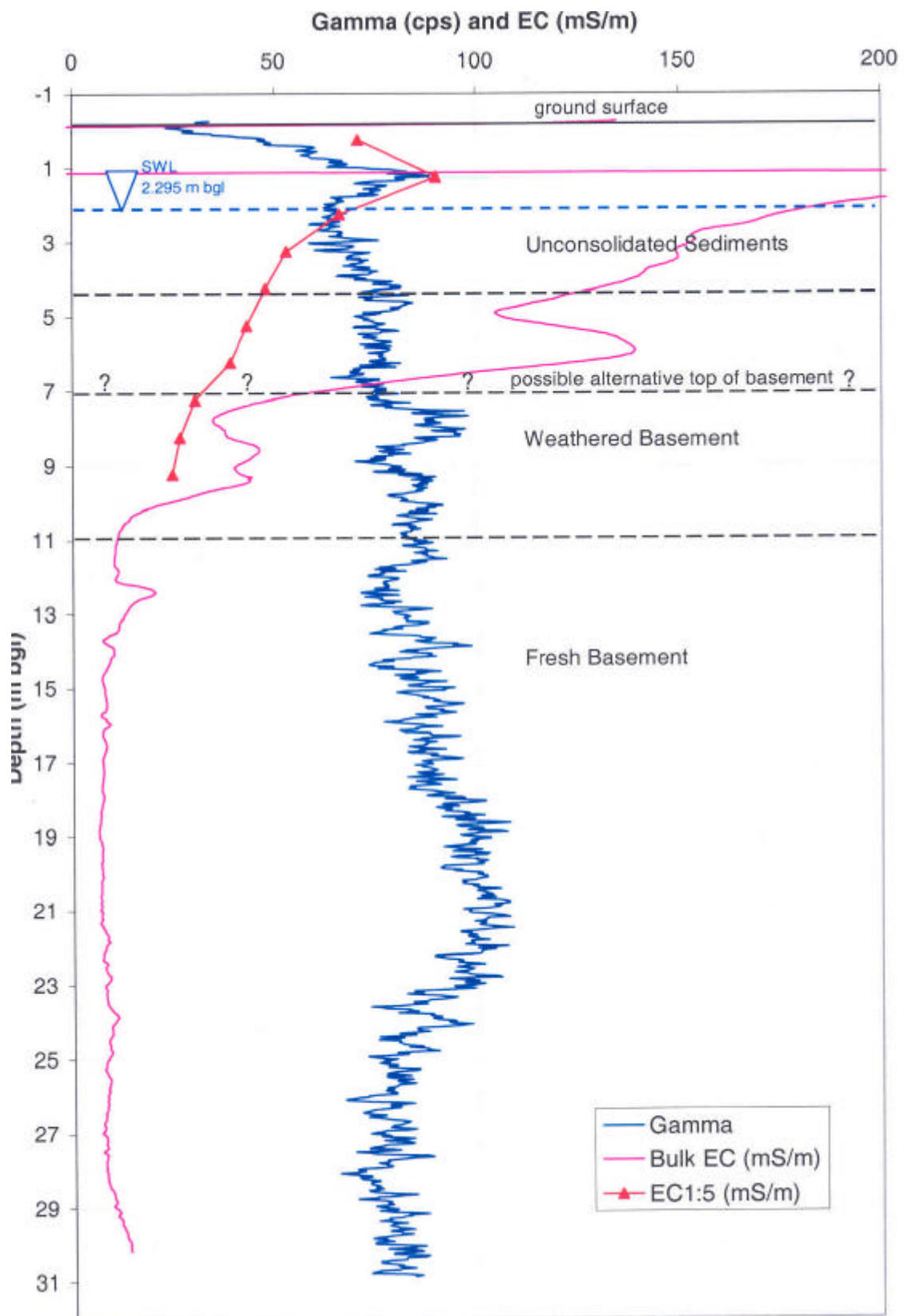


Figure 5.34: Downhole Gamma and EC for GW96128/3

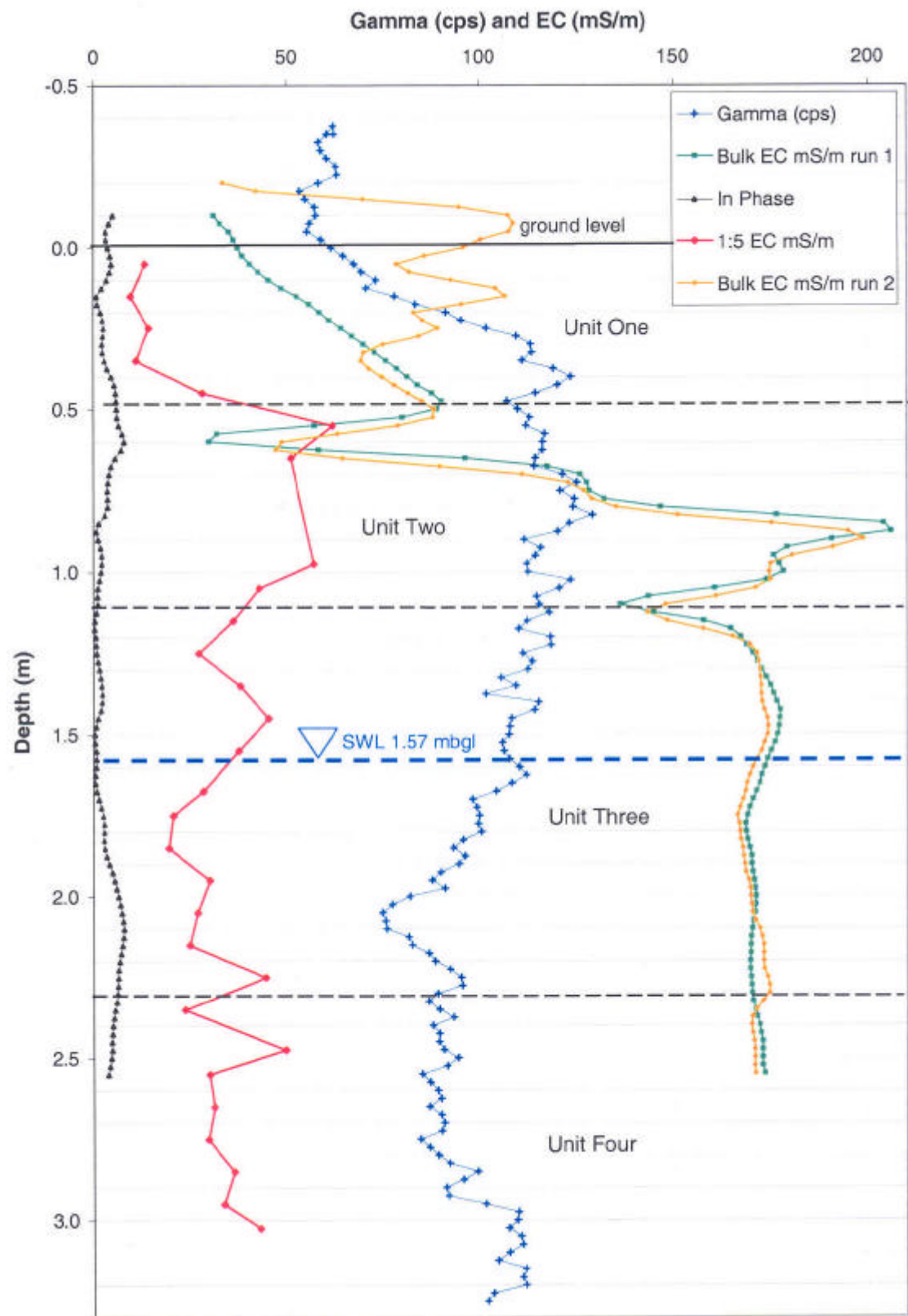


Figure 5.35: Downhole Gamma and EC for CH1

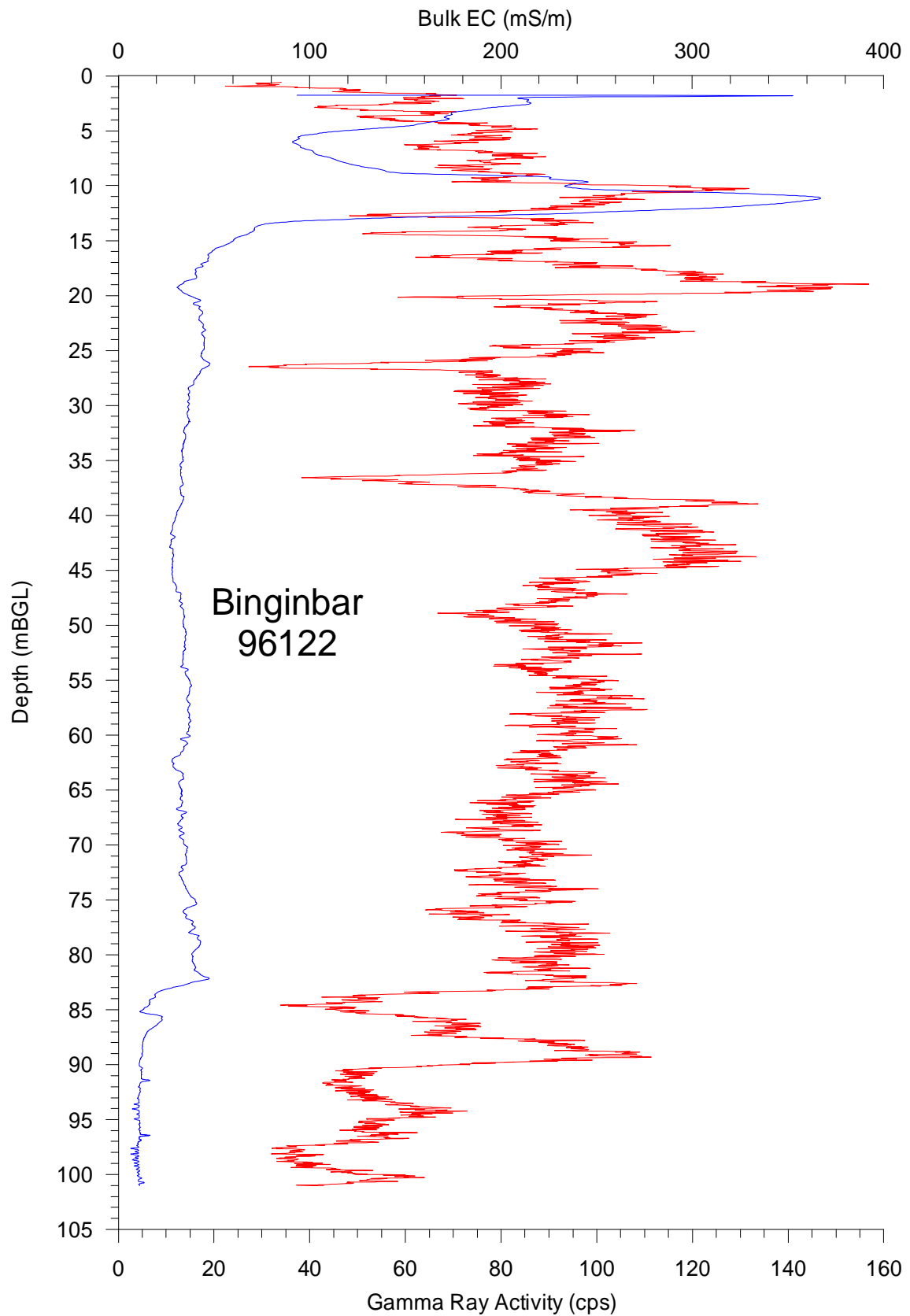


Figure 5.36: Downhole Gamma and EC for CH1

Results of the gamma log show the majority of the material intersected in the cored hole is clay, with narrow silty-sandy bands. The top of Unit One is mainly sandy silt but the bottom 20 cm of the unit has a much higher clay content. Unit Two is the most clay rich layer. The upper portion of Unit Three has a similar clay content to Unit Two, however the unit becomes more silty with depth. Unit Four is mainly silty but becomes more clayey after 3 m.

5.6 HYDROGEOCHEMISTRY

The field chemistry for 34 sample analyses is presented in Table 5.10 and the major ion analyses are presented in Table 5.11.

A summary of unstable parameter and geochemical analyses by water source, and the calculated SAR hazard for each, is presented in Table 5.12 and Table 5.13.

5.6.1 Unstable Parameters

During the first day of sampling, water leaked into the Eh probe causing spurious results for the creek water at the study site, so the value was omitted from the dataset. Throughout the sampling period, the dissolved oxygen probe was functioning erratically and so O₂ was only gathered for about one third of the sample locations.

A summary of EC results by water source and relative location in the catchment is presented in Table 5.14. Electrical conductivity in surface and shallow groundwaters increases from the top to the bottom of the catchment. All waters in Snake Gully catchment have a higher EC than the water in Spicers Creek.

In the GW96128 nested bores at the main study site, periodic measurements since bore construction show that groundwater EC is consistently lowest in the intermediate bore and consistently highest in the shallowest bore.

At the main study site, redox potential gradually decreases with depth, from -4 mV in GW96128/3 to -40 mV in GW96128/1. Redox potential is strongly negative in the deep GW96122 bores (>40 m) located further down catchment but on a hillside.

5.6.2 Major Ions

Error between duplicate chloride titrations was less than 0.3% which is acceptable. Field testing for reduced iron and sulphur, indicated very minor amounts, so sulphur and iron were assumed to exist completely as oxidised species, and results are presented as Total Fe and Total S. The ICP-AES results were corrected for dilution factors. The mean anion-cation charge balance error was 0.6%, with the highest error at 2.42%, indicating the analytical results are well within acceptable limits. Major ions are presented on a piper diagram in Figure 5.37. Ionic ratios were plotted to determine geochemical processes that might be occurring in the waters. These are presented on Figure 5.38.

5.6.3 Sodium Adsorption Ratio

The sodium adsorption ratio (SAR) represents the relative amount of sodium in water compared to calcium and magnesium. This ratio predicts the degree to which water tends to enter into cation-exchange reactions in soil. High values of SAR imply a hazard of sodium replacing adsorbed calcium and magnesium (Hem 1985), which may lead to soil dispersion (Hazelton & Murphy 1992), a situation ultimately damaging to soil structure (Hem 1985). The lower the ionic strength of the solution, the

Table 5.10: Hydrogeochemistry - Field Measurements

No	Location	pH	Eh	T	DO	EC μS/cm
9	S4 Creek	8.63	-74	17.7		6580
20	S5 Creek S Branch	7.66	101	18.8		5340
18	S5 Creek N Branch	8.72	120	24.9		7780
22	Spicers Creek	7.55	97	11.8		5680
25	S3 Creek	8.26	112	20.7		8930
25a	25 repeat	8.26	112	20.7		8930
32	S2 Seep	8.39	85	17.1		11400
10	S4 Seep	6.96	-13.2	19.1		8800
19	S5 Seep	7.09	142	16.3		5360
1	GW96122/1	7.12	-9	21.9		9870
5	GW96133/1	6.88	-8.1	18.1		8020
7	GW98037	7.13	-22.4	19.0		12490
8	CH1	6.92	-10.1	20.5	11.3	7890
11	GW96128/1	7.46	-40.8	22.4		9400
14	GW98034	7.36	288	20.4		6660
15	GW98035a	6.84	332	18.8		3700
16	GW98035b	7.40	-	-		3570
17	GW98036	7.15	105	21.2		9890
21	Piezo 60	7.63	78	19.8		7660
23	Piezo 12a	7.57	-149	19.8	2.04	5980
24	Piezo 12b	7.20	77	19.9		5390
26	Piezo 15a	7.59	-117	20.3	2.98	5600
27	Piezo 15b	7.35	42	20.4	2.42	6950
28	Piezo 5	7.26	79	20.9	4.9	8920
29	Piezo 13a	7.81	-143	20.0	3.05	6170
30	Piezo 13b	8.03	-202	20.0	3.17	5700
31	Piezo 13c	7.35	-60	20.6		13670
2	GW96122/2	7.30	-20	19.9		13790
6	GW96133/2	6.82	-5.6	20.1		7111
12	GW96128/2	6.97	-13.4	19.5		6410
13	GW96128/3	6.81	-4.5	20.3		7070
3	GW96122/4	7.06	-283	22.2		3940
4	GW96122/3	6.76	-195	20.6		4920

Table 5.11: Groundwater related studies at the site.

No	Location	Na (mg/l)	K (mg/l)	Ca (mg/l)	Mg (mg/l)	SO ₄ (mg/l)	Cl (mg/l)	CO ₂ (mg/l)	HCO ₃ (mg/l)
9	S4 Creek	711	9.14	67	430	38.8	1838	0.00	1052
20	S5 Creek S Branch	460	14.15	77	423	19.4	1415	4.12	1167
18	S5 Creek N Branch	955	9.05	42	448	48.9	2409	0.00	789
22	Spicers Creek	597	8.22	129	225	52.8	1387	23.50	683
25	S3 Creek	736	8.52	124	700	64.6	2874	25.25	851
25a	25 repeat	721	8.73	121	688	63.8	2874	0.00	826
32	S2 Seep	1564	17.7	113	572	160.1	3527	0.00	1155
10	S4 Seep	623	15.97	169	696	141.3	2700	0.00	964
19	S5 Seep	262	4.74	176	441	23.4	1406	134.25	1077
1	GW96122/1	794	39.68	101	789	149.3	3094	102.63	983
5	GW96133/1	203	28.67	550	521	34.5	2653	65.02	411
7	GW98037	1287	4.73	142	855	277.7	4040	0.00	589
8	CH1	671	7.78	398	415	105.3	2348	0.00	907
11	GW96128/1	1726	15.28	61	193	109.7	2674	0.00	1026
14	GW98034	833	3.62	68	360	57.1	1821	61.42	1031
15	GW98035a	163	1.14	185	273	26.7	9081	0.00	785
16	GW98035b	180	2.38	140	307	14.9	9311	0.00	837
17	GW98036	1338	7.22	113	481	103.4	2943	101.23	1135
21	Piezo 60	1411	1.74	4	234	42.6	1801	39.50	1772
23	Piezo 12a	738	2.57	75	299	59.1	1602	51.07	886
24	Piezo 12b	891	2.08	54	242	93.1	1579	73.79	863
26	Piezo 15a	890	1.63	59	259	107.7	1704	78.04	840
27	Piezo 15b	1367	1.45	46	203	167.5	2130	66.82	912
28	Piezo 5	1138	1.93	49	481	124.3	2702	55.17	886
29	Piezo 13a	642	7.18	106	358	14.5	1840	21.25	694
30	Piezo 13b	648	6.75	116	334	12.3	1583	16.68	890
31	Piezo 13c	3287	32.31	587	1302	271.6	9341	0.00	403
2	GW96122/2	1600	31.24	22	899	258.5	4151	109.75	1562
6	GW96128/2	748	3.6	106	338	96.1	1732	128.31	893
13	GW96128/3	730	3.16	122	426	102.0	1957	170.29	976
3	GW96122/4	427	15.03	88	227	120.6	932	93.47	936
4	GW96122/3	487	20.16	67	351	96.1	1219	198.80	1141

Table 5.12: Mean Unstable Parameters By Water Source

Water Source	No. Samples	pH	Eh (mV)	T °C	EC μS/cm	TDS	Water Type
Creeks	6	8.18	108	19.1	7207	4366	Mg-Na-Cl-(HCO ₃)
Seeps	3	7.48	71	17.5	8520	5270	Mg-Na-Cl-(HCO ₃)
Bores in Sediments	18	7.34	14	20.2	7641	5137	Na-Mg-Cl-(HCO ₃)
Shallow Bores (<40m)	4	6.98	-11	20.0	8595	5202	Mg-Na-Cl-(HCO ₃)
Deep Bores (>40m)	2	6.91	-239	21.4	4430	3064	Mg-Na-Cl-HCO ₃

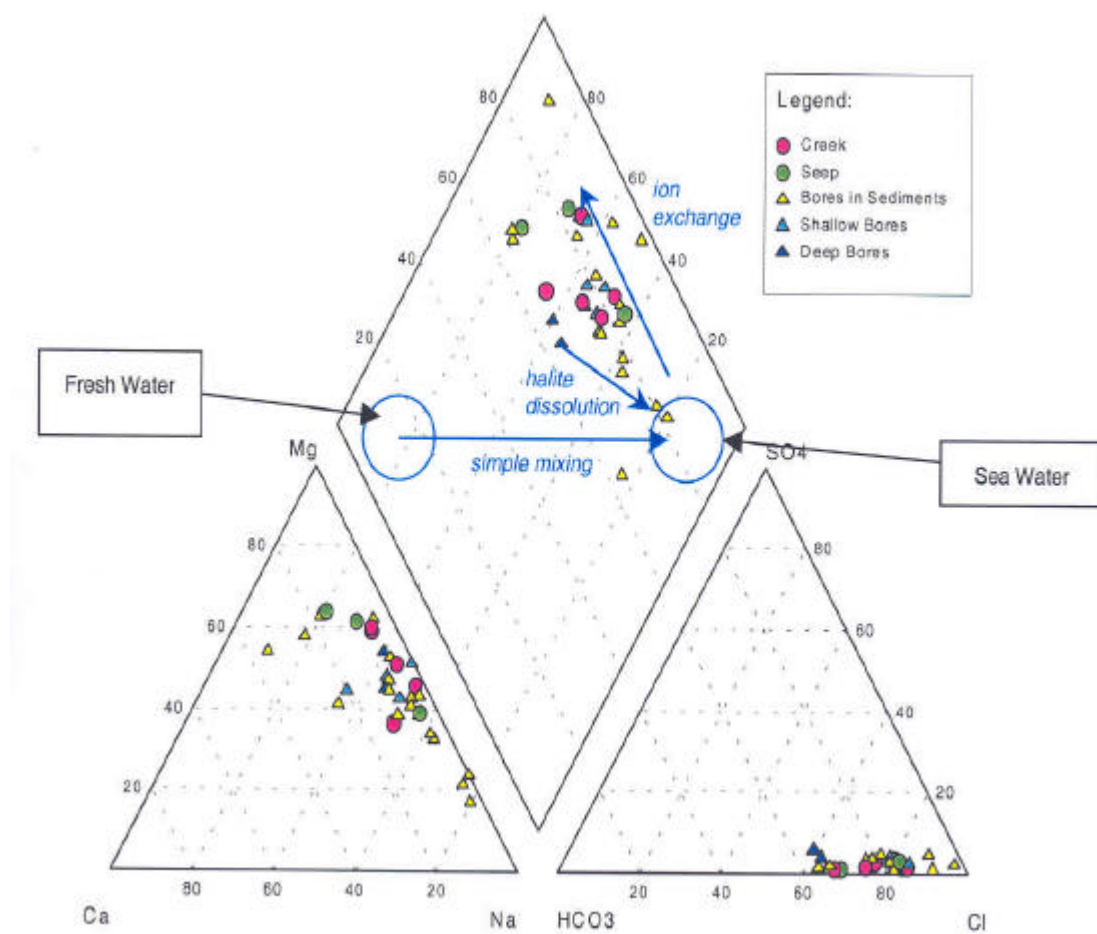


Figure 5.37: Piper Diagram of Groundwaters and Surface Waters From the Snake Gully Catchment

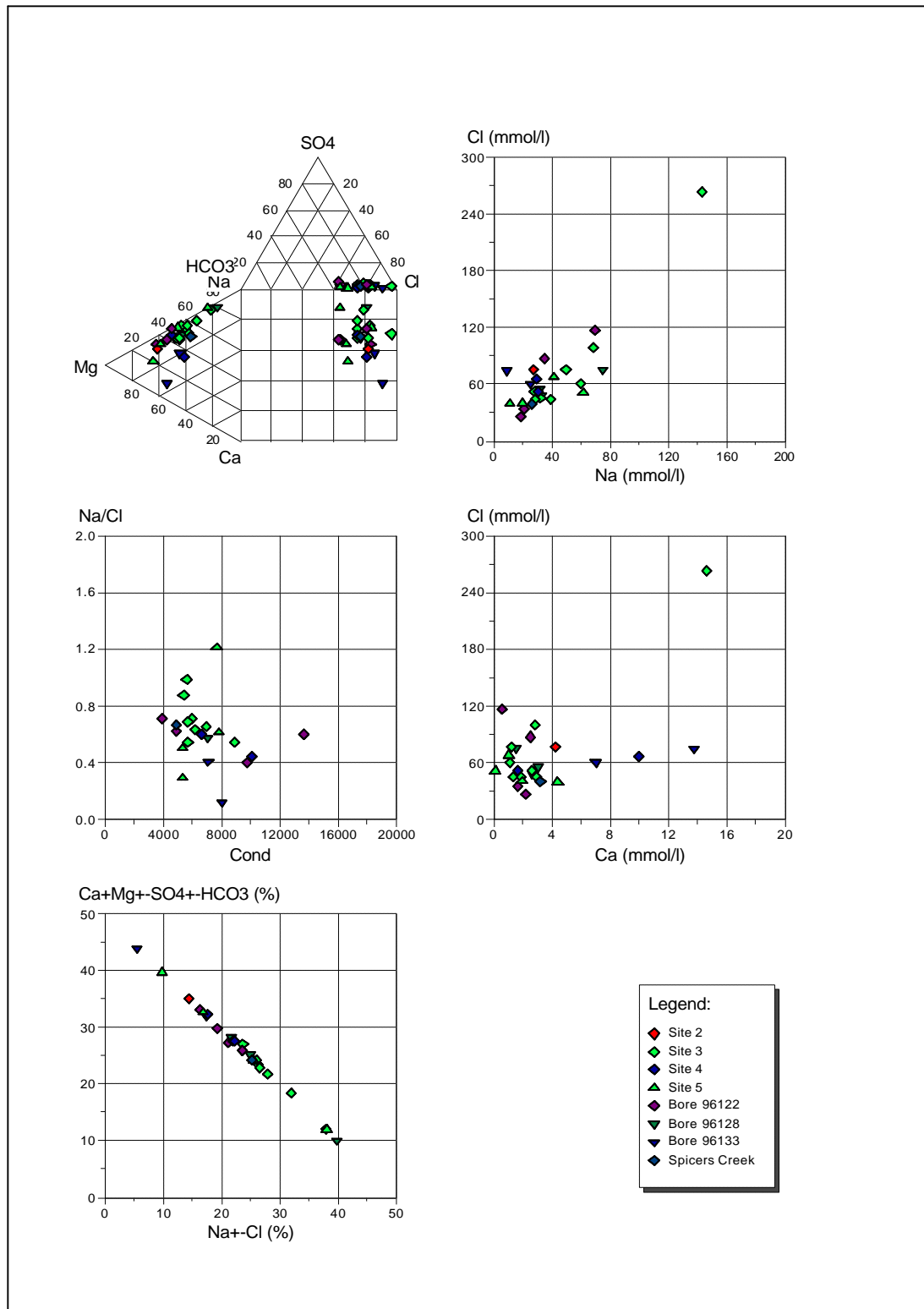


Figure 5.38: Ionic ratios for waters from the study site

Table 5.13: Geochemical Analyses By Water Source

Water Source	Na	Mg	Ca	K	Cl	HCO ₃	CO ₃ Fe	Total	Total Hazard	SAR Na:Cl
Creeks	697	486	94	0.25	2133	895	4	48	0.06	6.6
Seeps	817	570	153	0.33	2544	1065	0	108	0.07	6.8
Bores in Sediments	1012	439	159	0.24	2539	881	0	98	0.12	10.2
Shallow Bores (<40 m)	912	510	133	0.35	2497	1003	0	133	0.09	7.9
Deep Bores (>40 m)	457	289	78	0.45	1076	1039	0	108	0.07	5.4

Table 5.14: Mean EC (μ S/cm) By Catchment Location and Water Source in Snake Gully

Water Source	Site 5 Top of Catchment	Site 4	Site 3 Mid Catchment	Site 2	Site 1 Bottom of Catchment	Spicers Creek
Creeks	6560	6580	8930	-	-	5680
Seeps	5360	8800	-	11400	-	-
Sediments	6977	8645	8018	-	10255	-
Shallow Basement (<40 m)	-	6740	-	9870	7111	-
Deep Basement (>40 m)	-	-	-	4430	-	-

greater the sodium hazard for a given SAR (Fetter 1994). SAR is calculated by Equation 5.1:

$$SAR = \frac{Na^+}{0.5(Ca^{2+} + Mg^{2+})} \quad (5.1)$$

where ion concentrations of Na^+ , Ca^{2+} and Mg^{2+} are expressed as meq/L (Hem 1985).

A summary of SAR by water source is presented above in Table 5.15. The sodium hazard rating based on SAR is given in Table 5.15. Sodium hazard for each major water source is presented above in Table 5.13.

5.7 ENVIRONMENTAL ISOTOPES

The alteration of the oxygen-18 and deuterium composition of water gives an insight into its history. For surface water this includes meteoric processes and for groundwater includes subsurface history and geochemical reactions (Clarke & Fritz 1997).

The variation in stable environmental isotope concentrations is indicated using the delta (δ) notation

Table 5.15: Sodium Hazard Rating Based on SAR

SAR	Hazard
2 - 10	Low
7 - 18	Medium
11 - 26	High
> 26	Very high

because of the difficulty in measuring the absolute isotope ratio or abundance (Clarke & Fritz 1997). The delta notation represents the relative difference in parts per thousand or permil (‰) between the isotopic ratio in the sample and the ratio in some standard (Clarke & Fritz 1997).

The oxygen-18 and deuterium values in precipitation and hence in fresh waters generally plot close to a straight meteoric water line. The position along this line, of a particular rainfall, indicates the amount of fractionation that has occurred since the water molecule left the ocean.

An equation for the relationship between oxygen-18 and deuterium in worldwide fresh surface waters, was developed by Craig (1961) in Clarke & Fritz (1997, p. 36). This global meteoric water line (GMWL) was modified by further stable isotope analyses of global precipitation, collected by IAEA (the Global Network for Isotopes in Precipitation - GNIP) (Clarke & Fritz 1997) to give Equation 5.2:

$$\delta^2H = 8.13\delta^{18}O + 10.8 \quad (5.2)$$

Detection limits for isotope concentration by the CSIRO laboratory (Leaney 2001) are:

$\delta^{18}O$ - 0.15‰ (natural abundance) 0.4 (enriched)
 δ^2H - 1‰ (natural abundance) 3‰ (enriched)

Results for stable isotopes oxygen-18 and deuterium collected in waters at the study site are given in Table 5.16 and are presented in Figure 5.39. Data from recent studies by Schofield (1998) and Timms et al. (2002) are included for comparison. Rainfall data from (Timms et al. 2002) is presented in Table 5.17 and included in Figure 5.39.

Oxygen-18 and deuterium results for 59 groundwaters and two rainwaters were published by Schofield (1998) for the Ballimore region, NSW. Timms et al. (2002) reported oxygen-18 and deuterium in 17 rainfall samples at Gunnedah, NSW. Results from both studies these studies are also presented in Table 5.16 for comparison.

Timms et al. (2002) constructed a local meteoric water line from their rainfall oxygen-18 and deuterium results, which has the equation: $\delta^2H = 8.41\delta^{18}O + 15.99$.

The global meteoric water line presented by IAEA has been used to compare the relationship of oxygen-18 and deuterium at the Snake Gully study site. The groundwater oxygen-18 and deuterium results from (Schofield 1998) were plotted as a comparison of waters at the study site with regional waters.

Oxygen-18 and deuterium isotope compositions for seep and creek water in Snake Gully are shifted to the right of the GMWL and plot along the evaporation trend. The Snake Gully groundwaters are enriched in oxygen-18 and deuterium relative to rainfall at Gunnedah and Ballimore but are isotopically heavier than the soda waters reported by Schofield (1998).

The Snake Gully groundwaters plot close to but slightly to the right of the GMWL. This group falls within the Na-Cl water type of Schofield (1998). He explains that evaporation would enrich the isotopic composition of the isotopically heavy (Na-Cl type) group through the preferential loss of light isotopes (via processes such as Rayleigh Fractionation, but judges it unlikely that the overall regional Na-Cl trend reflects the influence of pervasive evaporative concentration.

The soda waters reported by (Schofield 1998) from Ballimore are isotopically the lightest waters. These waters plot slightly to the left of the GMWL due to isotopic exchange between groundwater and magmatic derived CO₂.

5.8 GROUNDWATER LEVELS

Groundwater level readings for the nested GW96128 series bores were downloaded from the data loggers on several occasions during 2002 and 2003. Extracts from this data set are presented below.

Table 5.16: Oxygen-18 and Deuterium Stable Isotope Data for Study Site, Snake Gully. Data for the Ballimore (Schofield 1998) included for comparison

Sample Number	Bore Location	$\delta^{18}\text{O}$ ‰/‰ SMOW	$\delta^2\text{H}$ ‰/‰ SMOW	Sample Number	Bore Location	$\delta^{18}\text{O}$ ‰/‰ SMOW	$\delta^2\text{H}$ ‰/‰ SMOW
Snake Gully sampled in early May 2002							
Seep	39850	-2.88	-23.5	Creek	39846	-4.32	-28.5
CH1	39845	-4.98	-32.7	GW96128/1	39847	-5.19	-34.5
GW96128/2	39848	-5.16	-33.1	GW96128/3	39849	-5.09	-33.3
Ballimore Data (Schofield 1988)							
UNSW-001	268	-4.02	-26.9	UNSW-002	287	-7.86	-47.1
UNSW-006	332	-6.05	-42.8	UNSW-008	1620	-5.94	-39.3
UNSW-009	1626	-5.08	-33.6	UNSW-010	1636	-5.16	-33.9
UNSW-012	1663	-7.05	-42.9	UNSW-013	2453	-4.97	-34.9
UNSW-014	2594	-5.53	-37.2	UNSW-015	2734	-5.82	-46.1
UNSW-016	5261	-4.75	-32.5	UNSW-018	7711	-7.49	-44.7
UNSW-022	7827	-5.19	-36.1	UNSW-023	8268	-5.21	-37.9
UNSW-024	9119	-5.98	-39.6	UNSW-025	9121	-5.21	-34.7
UNSW-026	19822	-4.88	-32.6	UNSW-030	22202	-4.31	-29.9
UNSW-031	23336	-7.51	-47.1	UNSW-033	23737	-7.55	-47.3
UNSW-037	23752	-6.75	-43.8	UNSW-038	24363	-4.23	-32.7
UNSW-039	25024	-6.26	-39.7	UNSW-040	26988	-5.08	-32.5
UNSW-042	27865	-5.08	-36.3	UNSW-043	30694	-7.19	-47.7
UNSW-045	30873	-5.06	-31.4	UNSW-046	31334	-8.24	-49.5
UNSW-052	38148	-7.16	-44.9	UNSW-053	38721	-4.83	-33.6
UNSW-057	44700	-5.14	-32.8	UNSW-058	44924	-5.16	-32.8
UNSW-059	45979	-6.54	-41.3	UNSW-060	46772	-5.70	-38.1
UNSW-061	50926	-7.39	-47.5	UNSW-065	51209	-5.26	-37.4
UNSW-066	51472	-7.63	-46.6	UNSW-067	51655	-4.32	-27.5
UNSW-068	52521	-7.38	-45.6	UNSW-069	52522	-7.49	-46.9
UNSW-070	54474	-6.96	-46.0	UNSW-071	56320	-7.40	-48.4
UNSW-073	57140	-5.67	-36.9	UNSW-075	62567	-7.10	-46.3
UNSW-078	62584	-5.04	-38.7	UNSW-079	62929	-7.08	-46.8
UNSW-080	65909	-7.59	-47.3	UNSW-087	71085	-7.69	-49.7
UNSW-089	Unreg-1	-5.88	-40.3	UNSW-090	Unreg-2	-5.61	-41.1
UNSW-091	Unreg-3	-6.58	-41.7	UNSW-095	Unreg-7	-7.23	-47.5
UNSW-097	Unreg-9	-6.26	-41.0	UNSW-098	Unreg-10	-5.08	-29.3
UNSW-099	Unreg-11	-5.26	-34.9	UNSW-100	Unreg-12	-5.41	-33.1
UNSW-101	Unreg-13	-3.90	-27.2	UNSW-102	Unreg-14	-4.52	-32.3
UNSW-103	Unreg-15	-5.41	-37.1				

Table 5.17: Rainfall Oxygen-18 and Deuterium Stable Isotope Data for Ballimore (Schofield 1998) and Gunnedah (Timms et al. 2002) included for comparison

Date	Rainfall (mm)	$\delta^{18}\text{O} \text{ ‰ SMOW}$	$\delta^2\text{H} \text{ ‰ SMOW}$	Fluid EC ($\mu\text{S}/\text{cm}$)
Ballimore				
		-1.3 -1.645	5.9 0.8	
Gunnedah Research Station				
31-Mar-98		-2.81	-10.5	
23-Oct-99	3.6	-4.16	-11.9	
09-Nov-99	16	-2.97	3.8	
28-Jan-00	3.6	-4.22	-14.1	20.3
09-Mar-00	38.4	-8.28	-60.9	18.8
04-May-00	8	-2.66	-11.8	14.5
09-Aug-00	9.8	-1.66	3.3	11
14-Oct-00	57.6	-2.47	-0.5	12.9
26-Oct-00	28.6	-5.14	-30.1	3.9
15-Nov-00	26.0	-4.53	-21.4	3.4
16-Nov-00	31.6	-4.76	-24.7	1.7
18-Nov-00	12.6	-3.00	-14.2	3.9
19-Nov-00	29.2	-4.06	-19.9	3.2
01-Dec-00	9.4	1.52	22.1	11.2
14-Dec-00	31.2	0.77	27.8	4.2
31-Jan-01	33.4	-10.4	-69.2	2.2
12-Jan-01	30.8	-11.04	-76.1	1.8

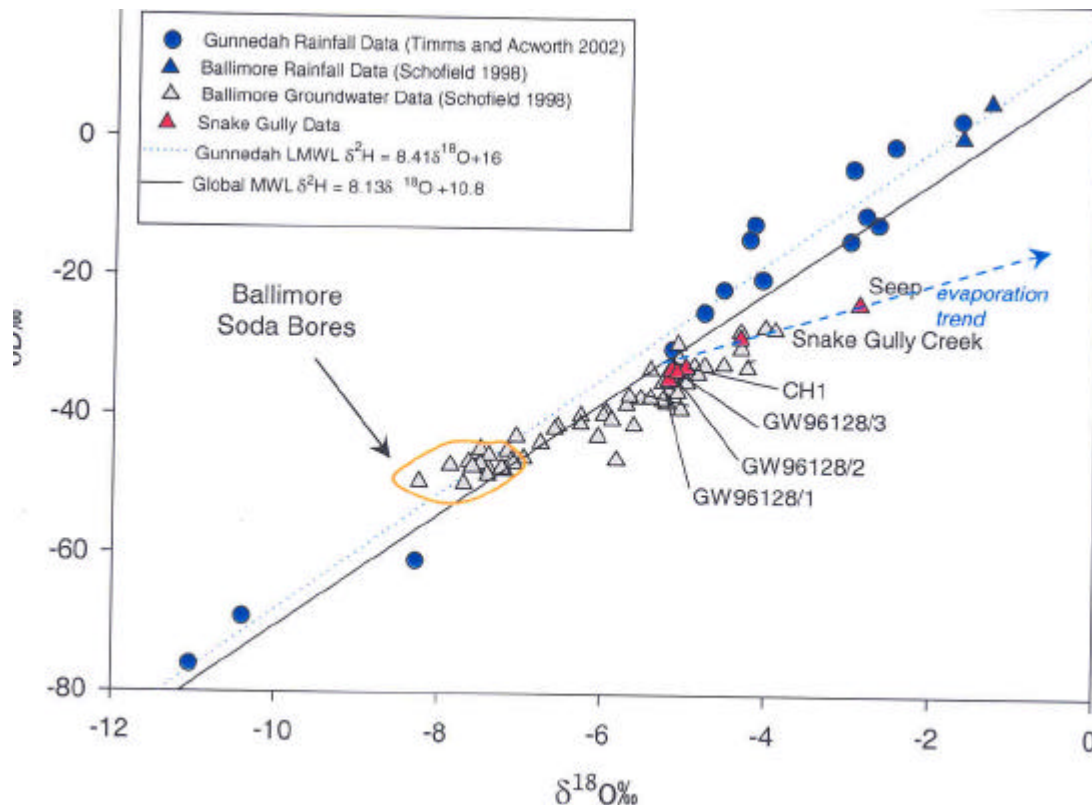


Figure 5.39: Oxygen-18 and Deuterium Isotope Data

Initial and final datalogger readings were calibrated against manual water level readings using the top of the PVC casing as a reference point. Instrument drift over the four months of reading was 8.6 mm in GW96128/2 and 13.5 mm in GW96128/3. The water level in CH1 was measured from the top of its PVC casing at 2.56 m, or approximately 1.56 m below ground level.

Manual water level readings since 8 October 2001 for all three bores at this site are presented for comparison in Figure 5.40.

Continuous water level hydrographs for two bores are presented in Figure 5.41 for the period 4 January to 5 May 2002. Data from the shallow piezometer was lost during the download procedure. The hydrographs for GW96128/2 and GW96128/3 show an almost identical pattern of water level response. At any time, there is about 66 mm difference between the water levels in the two bores. The largest change in difference is 12 mm (although there was 5 mm difference in instrument drift over the period), showing the very close correlation of response. At any time, this bore always has a water level about 30 mm greater than GW96128/3, and 30 mm less than GW96128/2. Even though the bores have different water levels, responses in all three bores are nearly identical.

There is a close association between rainfall and groundwater level response with about a two day time lag. Groundwater levels respond to rainfall above 20 mm in one event, although they do respond to lesser amounts if the ground has been saturated by previous rainfall events. The water level in the deepest bore GW96128/3 responds with slightly more magnitude (in the order of 3.5 to 5 cm).

Groundwater levels were gradually declining during January 2002, however, February was a month of unseasonal rainfall, with a total of 196 mm recorded in 28 days. This is compared with the monthly average of 41.8 mm for "Binginbar" over 64 years of collection. This was a period of significant groundwater recharge, which, in 25 days, caused an elevation in water levels of 66 cm in GW96128/3 and 57 cm in GW96128/2. From early March until early April, groundwater levels declined in both bores at about 8.5 mm per day. From early April until readings stopped in early May, water levels were declining at

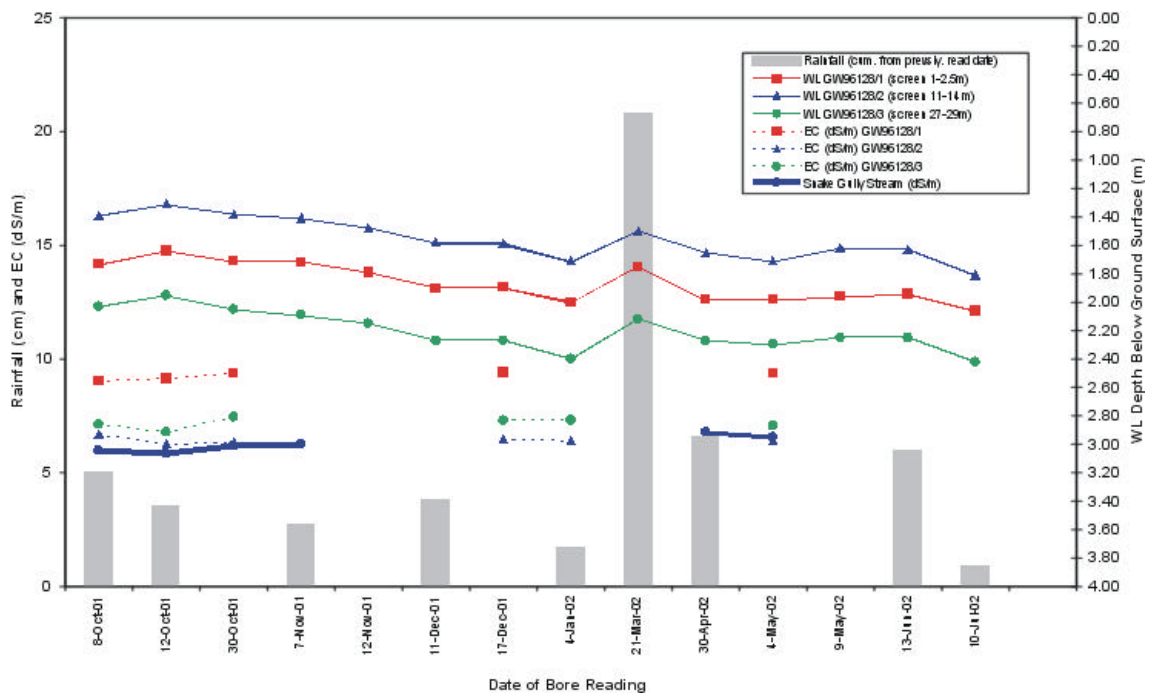


Figure 5.40: Hydrographs for Nested Bore Site GW96128 From October 2001 to July 2002 - Dip readings

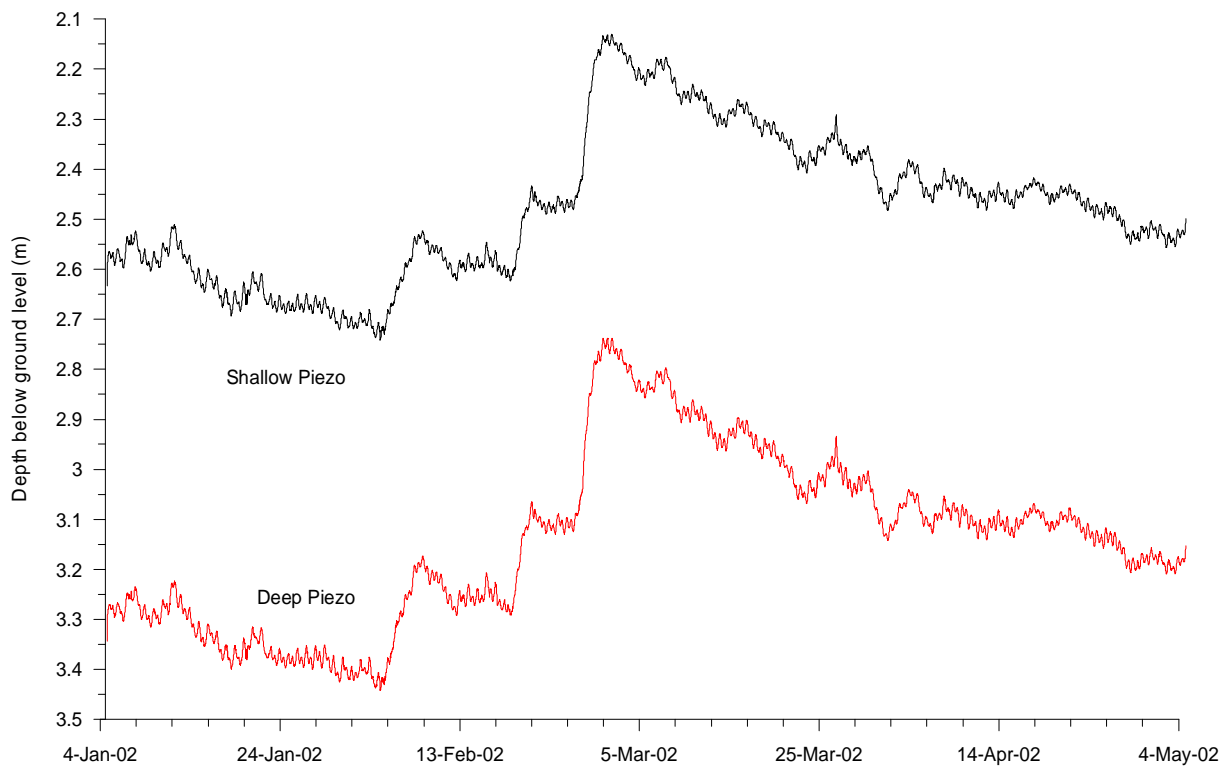


Figure 5.41: Hydrographs for GW96128/2 and GW96128/3 from 4 January to 5 May 2002

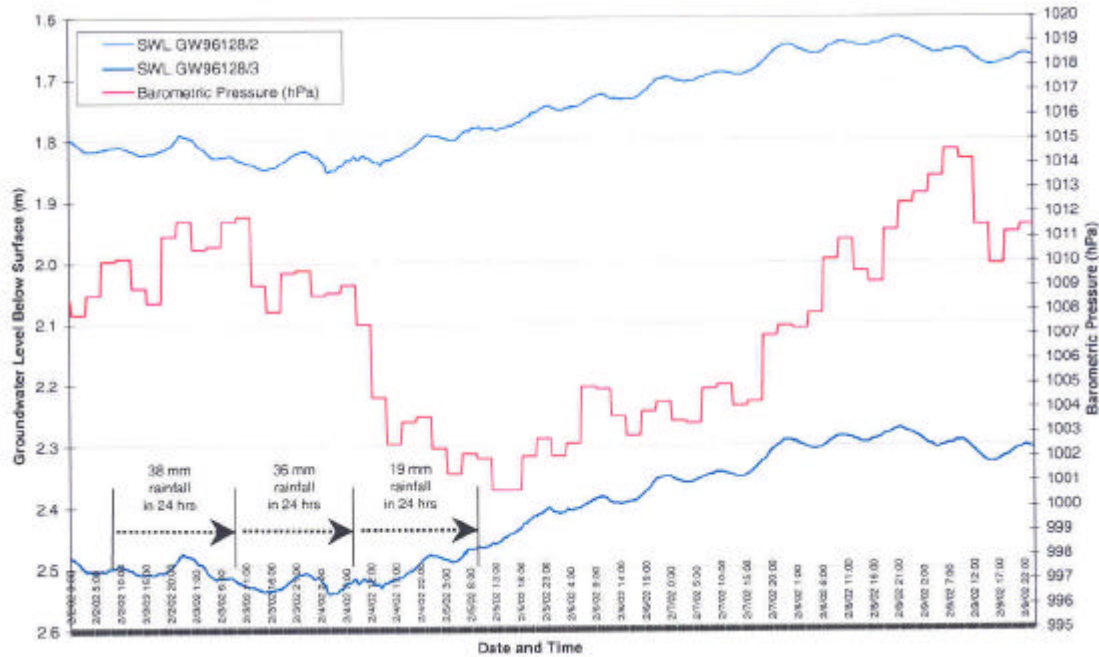


Figure 5.42: Hydrographs for GW96128/2 and GW96128/3 From 2 to 9 February, 2002

about 4.3 mm per day.

Two periods in February 2002 were examined in more detail, these being specific periods of notable groundwater recharge and water level response. These are presented on Figures 5.42 and 5.43.

During the eight day period from 2 to 9 February 2002, there was rainfall on three consecutive days totalling 93 mm, and a fall in barometric pressure of 11.2 hPa followed by a rise of 13.9 hPa. Over this period, the water level in GW96128/2 rose 21.9 cm and the water level in GW96128/3 rose with 26.9 cm (Figure 5.42).

During the nine day period from 21 February to 1 March 2002, there was rainfall on three days totalling 55 mm, and a fall in barometric pressure of 8.6 hPa followed by a rise of 10.1 hPa. Over this period, the water level in GW96128/2 rose 33.2 cm and the water level in GW96128/3 rose with 36.75 cm (Figure 5.43).

In both cases, groundwater levels in both bores were relatively static for two days after the drop in barometric pressure and the commencement of rainfall. Water levels began to rise in both bores on the third day after rain started, and continued to rise for another three days.

The relationship between the water level in the monitoring bores and barometric pressure was examined in more detail with the installation of a barometric pressure logger at the site in September 2002. Data was recorded through the latter part of the drought until the end of March in 2004. Data for the 3 loggers and barometric pressure data are shown in Figure 5.44.

There is a clear response to barometric pressure change in all 3 monitoring bores. The effect is clearly seen in Figure 5.45 where a reduced time interval is used. The confining impact of less than 2 m of clay in the shallow monitoring bore is well demonstrated by the fact that the water levels show a barometric efficiency that is not usually associated with unconfined aquifers.

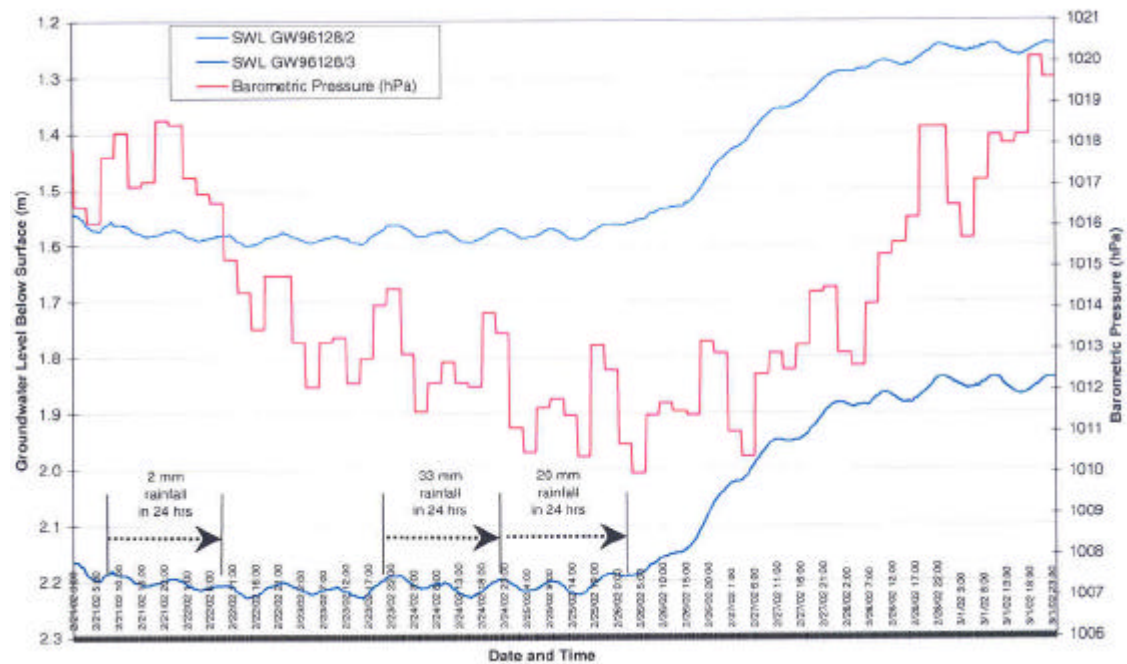


Figure 5.43: Hydrographs for GW96128/2 and GW96128/3 From 21 February to 1 March, 2002

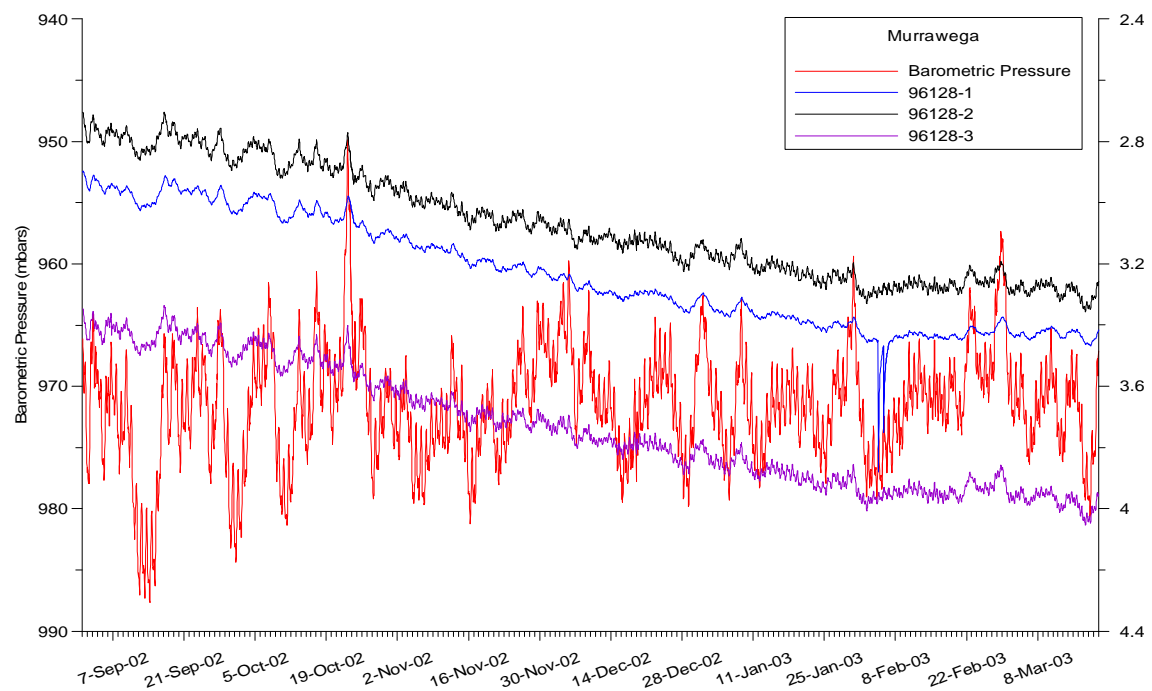


Figure 5.44: Hydrographs for all 3 GW96128 monitoring bores and barometric pressure from September 2002 to March 2003

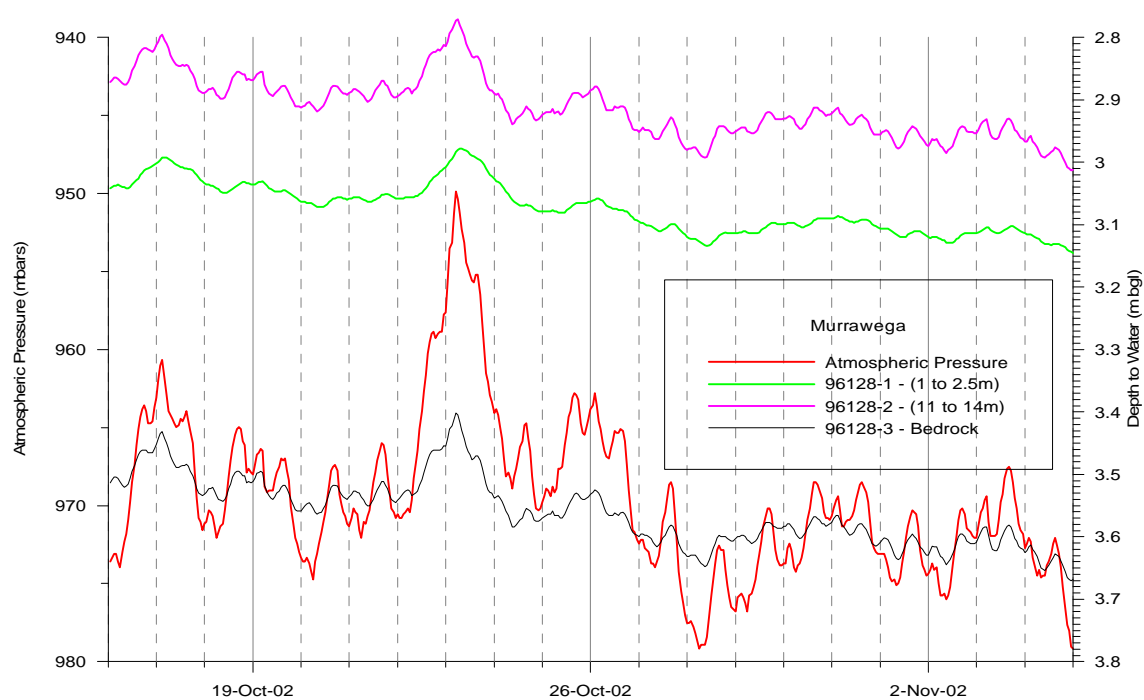


Figure 5.45: Hydrographs for 3 monitoring bores and barometric pressure from 6 October to 5 November 2002

Chapter 6

INTERPRETATION OF RESULTS

6.1 GEOLOGY OF SEDIMENTARY UNITS

A clear angular unconformity separates the unconsolidated sedimentary sequence from the underlying bedrock, and evidence for erosion of calcrete in Unit Three, and palaeosol in Unit Two suggests at least four phases of erosion and deposition have occurred.

The geological characteristics of Unit One such as pebble imbrication, graded bedding, and scour and fill structures, support alluvial deposition.

In unconsolidated sedimentary units Two, Three and Four, the presence of large angular clasts of fresh local bedrock entirely supported by the clay/silt matrix, demonstrates the strongly bi-modal grain size distribution. This grain size pattern could not have been formed by in-situ weathering of the basement, and does not support a model where all components are derived from erosion at the same locality under the same energy regime.

The most plausible explanation for the deposition of these units is by liquefied mud debris-flow. Debris flows originate when the internal friction of the material is exceeded (usually due to saturation), and the mass flows down gradient under the influence of gravity.

The flows entrain local bedrock clasts available at surface (but does not carry them far, as evidenced by lack of rounding). Very large bedrock clasts occur only where basement outcrops in the creek a short distance (within tens of metres) upstream. This implies that the coarse gravel component was probably transported as a basal lag within the mud matrix, and was deposited very close to source. Possibly, as the drainage line opened up after passing over the basement high, the debris-flow lost energy, depositing its largest components.

Unit Three appears to have been subject to post-depositional solution and replacement as suggested by the development of solution porosity, calcrete horizons, and manganese nodules.

The presence of remnant calcrete horizons in Unit Three indicates that calcrete may have been formed by Na-rich water interacting with Ca-rich clay, such as are derived locally from the weathering of calc-alkaline basalts in the region (Murphy & Lawrie 1998a). This would produce a dispersible Na-clay and add Ca^{2+} to solution, where it might react with bicarbonate to precipitate as calcrete.

Alternatively or additionally, carbonate rich dust as described by Williams et al. (1991) may have provided an exotic source of carbonate (and other salts). This is supported by evidence in Unit Three of dissolution pores that may have been crystals of halite, calcite, or gypsum.

Table 6.1: Proposed Date of Deposition For Sedimentary Units at Snake Gully

Unit	Date of Deposition
Unit One	<150 years
Unit Two	2000 - 180 years
Unit Three	25,000 - 13,000 years
Unit Four	> 50,000 years

6.2 UNIT DATING

The upper two unconsolidated sedimentary units in Snake Gully are geologically very young. Entrainment of a plough disc into Unit One dates this unit at less than 150 years, having been deposited since European settlement of the area.

Radiocarbon dating of the upper part of Unit Two, gives a date of emplacement of between 180 and 330 years before present (ie 1670 to 1820) prior to European settlement, at the end of the 'Little Ice Age'.

Accurate ages for Units Three or Four could not be determined, but a Quaternary age is implied based on dating of other depositional units in the central western region of NSW (Williams et al. 1991)), the Namoi plain (Young et al. 2002), and at Yass (Melis & Acworth 2001).

Units Three and Four have many features similar to the lower two debris flow units described at Yass by Broughton (1992) and Melis & Acworth (2001). Melis & Acworth (2001) associated these units with prior phases of glacial aridity, and assigned the higher of these an age of 26,000 to 34,000 years, and the lowest unit and age of greater than 50,000 years.

Similar dates of deposition are arrived at for Units Three and Four in the Snake Gully catchment, based on the growing body of evidence in the literature for periods of major dust generation throughout arid phases of the Quaternary. The palaeoclimatic evidence inferred from geological characteristics and mode of deposition support this conclusion. A summary of proposed date of deposition for each sedimentary unit in Snake Gully is given in Table 6.1.

6.3 CORE ANALYSIS

Emerson Aggregate testing shows that all sedimentary units, except the top 10 cm of Unit One, are prone to dispersion. The upper 10 cm of Unit One provides protection from dispersion and loss of structure in the underlying material. This upper non-dispersive material is sandier than the lower material, probably a result of downwards flushing of salts and clays by rainfall.

Based on aqueous extract electrical conductivity, Unit One is classed as non-saline, whereas Units Two, Three, and Four contain appreciable amounts of soluble salts, and are classed as moderately saline, ranging to highly saline in places.

Aqueous extract geochemistry shows that each sedimentary unit has its own distinctive chemistry, with Unit One having a different ionic composition and lower ionic concentration than the underlying units. The bottom 10 cm of Unit One is a chemical hybrid between Unit One and Unit Two, although from geological observation it is clearly part of Unit One. This is probably a result of some geochemical mixing at the contact. Units Two, Three and Four are chemically similar with much higher levels of sodium and chloride. Obviously, these units are an important source of these salts.

6.4 GRAIN SIZE ANALYSIS

The lack of correlation between results from this study and those done within 50 km of the study area by Townsend (1997), was initially very perplexing. Further consideration of Townsend's work showed that his samples were collected exclusively from hilltops, whereas those analysed in this study were valley floor deposits.

Obviously, hilltops and valley floors are places of vastly different particle transport energies and processes. Sorting processes must continue after the initial deposition of aeolian materials due to environmental exposure, with finer grained materials being transported further and more easily than coarser grained materials. In an environment of aeolian reworking by wind and rainfall, finer grained materials would be transported further from place of initial rest than coarser materials. Selective winnowing of the very fine fraction from aeolian materials on hillslopes is possible, with their eventual accumulation in flat vegetated valley floors. Certainly, these processes require further investigation.

When Butler (1974) refined his definition of parna, he concluded that no single grain size is characteristic for aeolian materials, and rather, that peaks in fine-grained materials are evidence for the high degree of sorting produced by aeolian winnowing. Dare-Edwards (1984) proposed that loessic clay is characterised by a bimodal particle size with a peak in the clay-sized fraction (<2 micron) and another in the silt-sized fraction.

Based on these grain size characteristic given by Butler (1974) and Dare-Edwards (1984), all samples analysed are interpreted to contain a component of fine aeolian material.

The 2 and 7 micron peaks are of the least magnitude in Unit One which is alluvial. They probably represent (as do other grains in this material) reworking of lower sedimentary units.

If the sample analysed for a depth of 5 to 6 metres in GW96128 was indeed weathered basement, these peaks might indicate a local origin for these particular grain sizes. However, interpretation from other investigative techniques in this study suggests that top of basement in GW96128 might actually be deeper than first thought. This would classify the materials at 5 to 6 metres as unconsolidated sediments, with an aeolian component confirmed by the characteristic peaks in particle size.

6.5 GEOPHYSICAL TECHNIQUES

The linear zone of very high apparent conductivity shown by the EM31 is confirmed in the resistivity imaging lines at between three and eight metres deep. Downhole EM39 bulk electrical conductivity logging shows that unconsolidated sedimentary units Two, Three, and Four compare closely with high bulk conductivity. This is substantiated by the EC1:5 values for those sedimentary units, although it is noted that the cored hole was drilled to the side of the highest zone of conductivity, where soluble salt content may be even higher. The zone of core loss from 0.7 to 0.95 m is indicated by the bulk EC to have the highest conductivity, and it is inferred that the average EC1:5 value for this unit would have been even higher than $461\mu\text{S}/\text{cm}$ if the core had been available for analysis.

Results from the downhole logging have caused a revision of the interpreted depth to basement in GW96128/3. This was placed at 4.5 m, but has been revised to 7 m. In combination, these provide convincing evidence that the linear anomaly in the EM31 is a palaeochannel with a maximum depth of about 8 m and which is filled with moderately saline unconsolidated clayey sediments.

Young et al. (2002) reiterate and provide further evidence from the Namoi Plain in NSW, that channel migration during the Tertiary was common, and that palaeochannels occur in many places away from present day drainage lines, making them difficult to detect.

The high conductivity anomaly in Bore 96122 (Figure 5.36) at a depth of approximately 10 m correlates with the base of the Cuga Burga volcanics overlying the Gleneski Formation that can be seen in the

electrical image (Figure 5.32). The boundary is shown on the geological map (Figure 2.6).

6.6 HYDROGEOCHEMISTRY

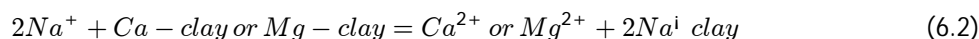
At the GW96128 nested bore site, there is a considerable increase in groundwater conductivity from 6410 $\mu\text{S}/\text{cm}$ at 11 m to 9400 $\mu\text{S}/\text{cm}$ at 1.5 m. This suggests either that evaporative concentration is a major process or there is a shallow source of salt.

A mildly negative redox potential in the shallowest GW96128 bore at the main study site suggests that shallow redox processes may be occurring, and that the system within 2 m of the surface may not be in complete connection with the atmosphere.

On the piper diagram (Figure 5.37), waters in the Snake Gully catchment show a trend from deep Mg-Na-Cl- HCO_3 type groundwater, to shallow Na-Mg-Cl-(HCO_3) type groundwater, and then to Mg-Na-Cl-(HCO_3) surface waters. The piper diagram shows that processes other than just simple mixing are occurring. The trend on the piper diagram indicates that halite dissolution occurs as the groundwater passes from the deep to the shallow system, in the reaction:



This is followed by ion exchange between the shallow sodium rich groundwater and clays in the debris flow units, in the reaction:



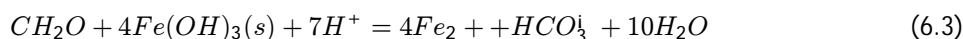
Ionic ratios were examined for evidence of geochemical processes. The ratio of chloride to EC shows a linear relationship (as expected) for all water samples, with the significant exception of Piezo 13c. This bore yielded very little, but extremely turbid water from which it was difficult to obtain an EC reading. It is suggested that this water has a much higher EC than that indicated by the field reading, but which could not be determined due to the muddy consistency of the water. The very high EC is probably the result of extensive evaporative concentration, hence the geochemical results from this hole are not representative of the groundwater system in which that bore is located. This is supported by the unusual position of Piezo 13c on many of the ionic ratio plots.

If evaporative concentration were causing the high ionic concentrations, the Na:Cl ratio would approximate one, even at high concentration. Clearly, this is not the case. The ratios of sodium to chloride and sodium to chloride versus EC show that the majority of waters deviate from simple halite dissolution/precipitation, and that this occurs at all ionic concentrations. This confirms that sodium is being removed from solution by processes such as ion exchange, in the reaction presented in Equation 6.2.

The ratio of sodium to magnesium shows deviation from unity in the majority of water types. This also confirms that sodium is being removed from and magnesium added to solution by processes such as ion exchange, in the reaction presented in Equation 6.2.

The ratio of calcium to sulphate shows deviation from the gypsum dissolution/precipitation line in the majority of water types. This suggests that calcium is being added to solution by processes such as ion exchange, in the reaction presented in 6.2.

The ratio of calcium to bicarbonate shows deviation from the calcite dissolution/precipitation line in the majority of water types. This suggests that bicarbonate is being added to solution at all depths by redox processes such as the reduction of ferric iron, as indicated in the reaction:



The strongly negative redox potential in the deep groundwater system indicates that species must exist in reduced form in that system.

As noted earlier in this section, marginally negative redox potentials also occur in the shallow groundwater systems including shallow basement, unconsolidated sediments and one seep. The presence of black ferrous iron a few centimetres below the surface of saturated sediments in the creek line, supports the suggestion of shallow microbially mediated redox processes. A Nicholson (2001, pers. comm., 11 Nov) confirms that strong reduction can occur in soils due to bacterial activity.

6.7 ENVIRONMENTAL ISOTOPES

The oxygen-18 and deuterium isotope results show that evaporative concentration only affects surface waters, and is not a significant process in shallow or deep groundwaters at the study site.

The distinct isotopic difference between groundwaters at the study site and soda waters at Ballimore, suggests that mixing of Na-HCO₃ groundwater with local groundwater is not a significant process at this site.

6.8 GROUNDWATER LEVELS

Hydraulic head is consistently highest, and EC consistently lowest, in the intermediate depth bore at the nested site. This bore is screened between 11m and 14m in weathered basement. One possible explanation is that recharge may be entering the groundwater system upslope, where weathered basement is close to surface or exposed. This material may have a higher hydraulic conductivity than the sediments which overly it in the valley floor, so groundwater can travel laterally downslope towards the drainage line. As groundwater moves under the low hydraulic conductivity clay-rich sediments in the valley floor it becomes partially confined and pressure builds up in this intermediate depth system. The confining effect of these clay-rich units on basement groundwater flow has been demonstrated at Yass in a number of studies (Acworth et al. 1997; Jankowski & Acworth 1997).

Groundwater level change is related to rainfall, with a response time in the order of two days. If this response was in reaction to gradual saturation of the overlying sediments, a gradual response since commencement of rainfall would be expected, however this is not the case. The mechanism of the response is unknown, but is critical in the understanding of salinity processes at this site. Hourly rainfall measurements would enable clarification of this issue. Water levels are clearly affected by changes in barometric pressure.

If vertical flux was occurring after rainfall, it would be expected that water level response would occur first in the shallowest bore, and then progressively with some period of lag and lower order of magnitude, in the deeper bores. The identical response in water level change for all three bores, indicates that effects are transmitted to each part of the groundwater system at the same time, and the deepest bore responds with a slightly larger magnitude. It is concluded that the simultaneous response is due to hydraulic loading rather than mass transfer of water, however further investigation of this concept is required.

Low groundwater flow rates are supported by the low hydraulic conductivities of 0.002 to 0.3m/d, and CFC age of 36 years, derived by Mahamed (1999a) from slug testing and sampling of bores in the unconsolidated sediments.

6.9 SALT STORAGE AND EXPORT

Emerson Aggregate testing demonstrates that the sedimentary units are moderately to highly dispersive. Aqueous extracts confirm that Units Two, Three, and Four contain appreciable amounts of salt. Using parameters derived in this study, the following estimate is made of salt load exported to the surface water system for a small amount of erosion of these units.

6.9.1 Average Salt Store in Unconsolidated Sedimentary Units

Average TDS over Units One, Two and Three is 193 mg/L. This is corrected for 1:5 dilution by multiplying by 5 to get mg/L (or mg/kg), or by 5,000 to get mg/m³: $193 \text{ mg/kg} \times 5,000 \text{ L} = 965,000 \text{ mg/m}^3 = 0.965 \text{ kg/m}^3$.

6.9.2 Salt Stored In Catchment

The catchment is 10 km (or 10,000 m) long. Assuming the sedimentary units have a width of 200 m and are distributed along the floor of the catchment at a conservatively estimated thickness of 2 m: $10,000 \text{ m} \times 100 \text{ m} \times 2 \text{ m} = 2,000,000 \text{ m}^3$. This represents $2,000,000 \text{ m}^3 \times 0.965 \text{ kg/m}^3 = 1,930,000 \text{ kg}$ or 1,930 tonnes of salt stored.

6.9.3 Salt Exported During Erosion Of Sedimentary Units

Assuming an area of sedimentary unit erosion 20 m by 20 m wide, and 2 m deep: The amount of soluble salt in this volume would be 772 kg.

Chapter 7

CONCEPTUAL MODEL FOR SALINITY

7.1 ALTERNATIVE SALINITY MODELS

The three conceptual models for salinity in the Snake Gully catchment have been assessed based on the findings of this research project.

7.1.1 Salinity Due To Deep Groundwater Discharge Through Faults

Although there is no doubt that faulting does control groundwater discharge in places (Please, Knight, & Corpuz 1989; Morgan & Jankowski 2004), it is difficult to envisage that this model can account for the widespread nature of salinisation. Patchy salinity occurrences related to the distribution of permeable faulting would be expected, however salinity effects are widespread at this study site.

If a permeable faulted zone, capable of permitting upwards groundwater flow existed in the basement, these deep narrow structures should be apparent in electrical imaging across the salinity sites. At the site of this study, the bulk electrical conductivity distribution seen in section (electrical imaging) does not indicate any deep linear conductive zones controlling the salinity.

If this model was appropriate, the deepest bore at the nested monitoring bore site GW96128, would have the highest head, but it does not. Hydrographs between these three different depth nested bores would be expected to show a different magnitude and timing of response to recharge, however they show almost identical responses.

Hydrogeochemistry indicates that groundwaters in the catchment are mainly Na-Cl type, however, Schofield (1998) concluded that deep groundwater in the area was of Na-HCO₃ type. The deep groundwater discharge model does not provide a source of chloride of the levels observed in bores sampled in this study.

If deep groundwater was the source of salts and cause of salinity, then a process of simple mixing with shallow groundwater would be indicated. When surface and groundwaters from the Snake Gully catchment are plotted on a piper diagram, the progression from deep to shallow groundwater follows a path of halite dissolution followed by ion exchange, rather than simple mixing.

It is concluded that evidence derived from this study does not support this model.

7.1.2 Salinity Due To Evaporative Concentration of Shallow Groundwater Through In-situ Soils

Groundwater levels are demonstrated to be very shallow within the Snake Gully catchment, and evaporative concentration will occur at surface if the watertable is within the critical depth (Taylor 1996).

Under normal conditions, the watertable is shallowest in depressions and deepest on hilltops (Freeze & Cherry 1979). If evaporative concentration was the process solely responsible for salinisation in this catchment, the bulk electrical conductivity mapped by EM31 should reflect the deepening of the watertable away from depressions, and conductivity highs should have a direct correlation with low points in the catchment. This is not the case. In fact, the main conductivity high is displaced from the current drainage line.

The results from oxygen-18 and deuterium do not indicate that deep or shallow groundwaters are undergoing evaporative concentration, and that this process only occurs in surface waters in the catchment.

If evaporative concentration were causing the high ionic concentrations in groundwater, the Na:Cl ratio would approximate one, even at high concentration, however, this is not the case, with ratios of about 0.5.

It is concluded that evidence derived from this study does not support this model.

7.1.3 Salinity Due To A Shallow Exotic Salt Source In Partially Confining Clay, Mobilised By A Shallow Pressurised Water Table

These units have an unconformable angular contact with Palaeozoic basement, so could not have been derived from in-situ basement weathering and must be exotic. Stratigraphic relationships, unit distinctive 1:5 extract geochemistry, and internal textural evidence in the sedimentary units, support a hypothesis of cycles of debris-flow type deposition.

The conductivity of 1:5 extract solutions indicate that all sedimentary materials have salt in them. The apparent electrical conductivity distribution produced by the EM31 survey at the study site can not be explained by either the first or second model, however it could be explained by the existence of a palaeochannel which is proposed in this model.

The confirmed age of sedimentary Unit Two in Snake Gully is between 180 and 330 years, indicating recent deposition during a period of minor global cooling and aridity. Particle size analyses show that all units have characteristic frequency peaks at the 2 and 7 micron size, demonstrating that they have a significant aeolian component. In the bores at nested site GW96128, redox potential's become more negative from the deep to the shallow system, suggesting that the shallow system is partially confined from atmosphere.

Hydraulic heads in bores at nested site GW96128 indicate a downwards hydraulic gradient between 15 and 30 metres, however heads indicate an upwards hydraulic gradient between 15 m and 2 m. This confirms partial confinement at the intermediate depth of about 15 m, causing pressure build up.

Hydrogeochemical trends and ionic ratios suggest that the major processes affecting groundwaters in this catchment are shallow halite dissolution and ion exchange, supporting a shallow clay and salt rich aeolian source.

It is concluded that evidence derived from this study constrains and supports this model.

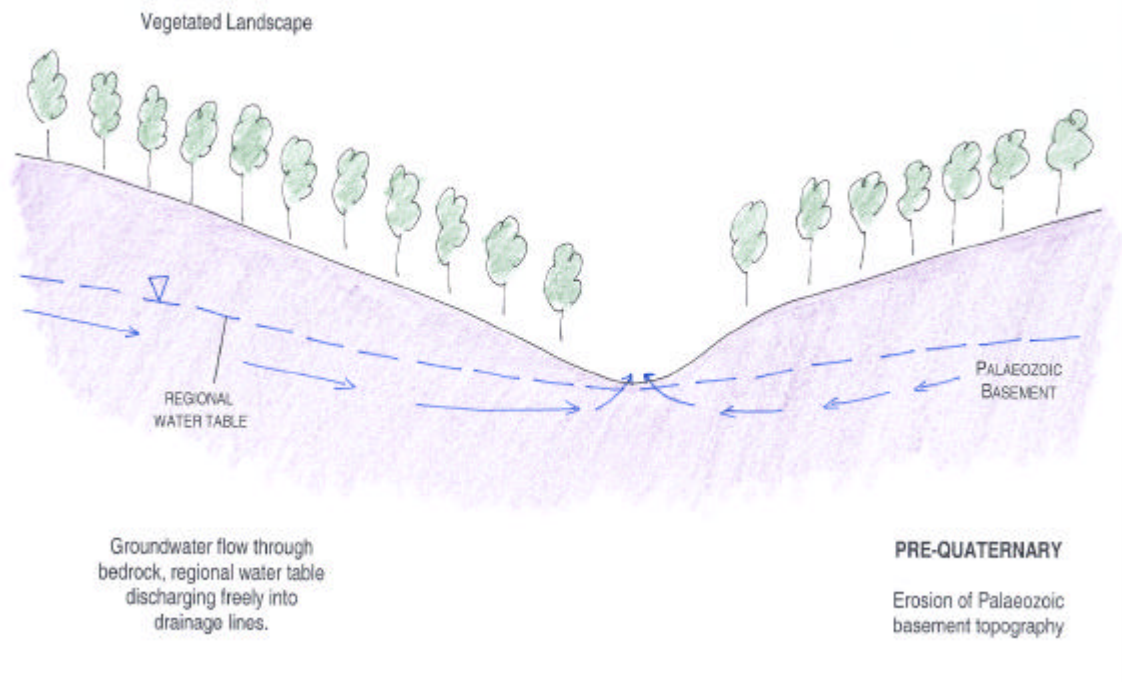


Figure 7.1: Conceptual Model - Pre-Quaternary

7.2 CONCEPTUAL MODEL FOR SALINITY IN SNAKE GULLY

A conceptual model for salinity in Snake Gully is proposed, based on the results and interpretation discussed above, and in previous chapters. This model is presented in Figures 7.1 to 7.4.

Large quantities of aeolian dust and salt were deposited across the landscape during times of glacial aridity throughout the Quaternary. These clayey materials became saturated during warmer, wetter interglacial periods and flowed into valley floors and along drainage lines, entraining clasts of local bedrock.

Multiple phases of debris flow deposition and erosion occurred, and a palaeochannel up to 8 metres thick was formed in the valley floor away from the present location of the drainage line. European settlement in the 1850's initiated massive erosion, as land was cleared for grazing and cropping. This produced the most recent phase of alluvial deposition. The deposition of sheets of clay-rich material across the drainage line has impeded groundwater discharge, causing pressure to build up and watertables to rise. Saturation of the salty clays by rising groundwater dissolves entrained salts and these are mobilised closer to the ground surface.

When the watertable reaches within about 2m of the ground surface the top of the tension saturated zone will be almost at ground surface in low permeability units and salts can be concentrated directly by evaporation. Where the watertable intersects the land surface, for example in severe gullies (Figure 7.5), saline seepages form and drain into the creek. Where the watertable intersects the base of the channel, saline groundwater discharges directly into the creek.

Ion exchange between shallow Na-rich water and clays in the debris flow units causes them to become highly sodic and dispersive. During the 1940's plague rabbits denuded much of the groundcover, leaving the area susceptible to erosion. In the 1950's, several very wet years saw the commencement of land salinisation and severe gully erosion to depths of over 4m in the creek line (Figure 7.6). Erosion of these sedimentary units released salts and clays into the surface water system and has resulted in the features observed in the creek line today.

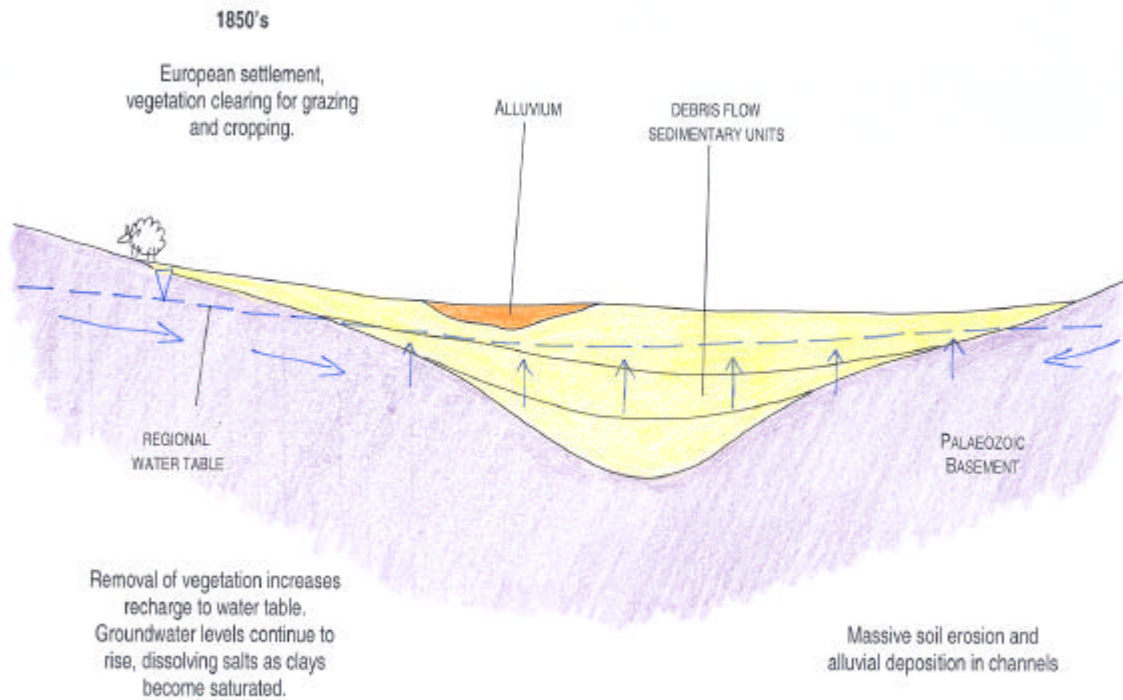


Figure 7.2: Conceptual Model - Quaternary to 200 BP

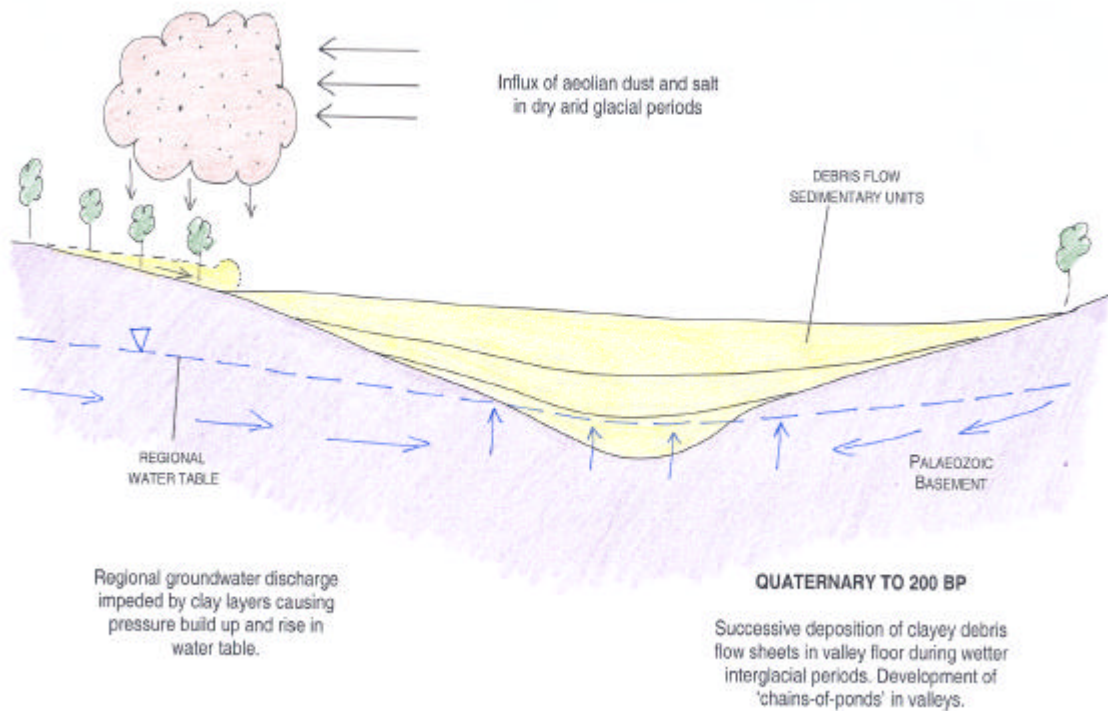


Figure 7.3: Conceptual Model - 1850's to 1940's

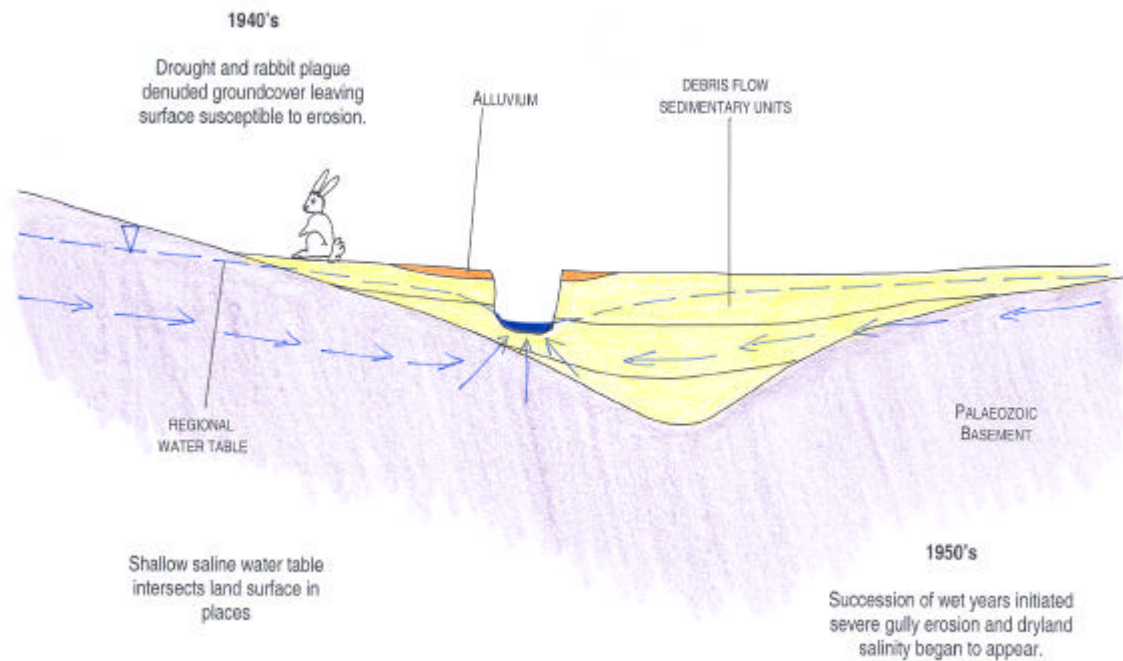


Figure 7.4: Conceptual Model - 1940's to Present



Figure 7.5: Gullying and Groundwater Seepage at Study Site



Figure 7.6: New Gully Head Progressing Back Up Creek Line In Snake Gully Catchment

Clearing of vegetation and changes in land use have allowed additional water to recharge the groundwater system, exacerbating shallow watertables. In spite of this, both rising and falling groundwater trends occur depending on patterns of annual rainfall.

The unconsolidated sedimentary units in Snake Gully control catchment salinity processes by impeding groundwater discharge and assisting watertable rise; providing a source of salt; and generating dispersive erodable soils. Anecdotal evidence, and personal observations by the author, suggest that these type of sodic multi-layered units are widespread across the tablelands and slopes of the central west region. If this is the case they could be a major cause of salinity.

Chapter 8

CONCLUSIONS

A combination of geoscientific techniques has been applied to investigate unconsolidated sedimentary units and their role in the development of salinity in the Snake Gully catchment.

A review of published studies from across south-eastern Australia confirms that Quaternary glacial maxima were periods of substantial aeolian transport and deposition. Detailed studies of unconsolidated sedimentary units at Yass show them to be composed of aeolian clay dust and salt, which were reworked as debris flowed into the valley floor.

A number of possible conceptual models for salinity in the Snake Gully catchment have been proposed and assessed against the findings of this study. The results exclude deep groundwater discharge through faults and evaporative concentration of shallow groundwater through in-situ soils as major salinity processes; and support a shallow exotic source of salt in partially confining sedimentary clays, mobilised by a shallow pressurised watertable.

A conceptual model is presented that provides an explanation for the occurrence of dryland salinity in the Snake Gully catchment. Several phases of erosion and deposition of aeolian derived materials have been identified.

During wetter interglacials, aeolian sediments were reworked as debris flows that deposited sheets of unconsolidated sedimentary units across the valley floor. Since deposition, these units have controlled catchment salinity processes by impeding groundwater discharge, exacerbating watertable rise, providing a source of salt, and generating dispersive erodable soils. Inappropriate land management practices compounded by severe environmental events have resulted in the problems of erosion and dryland salinity now apparent in the catchment.

Although the model is based upon studies in one catchment, the Quaternary dust transport path covered a large area of south-eastern Australia, and consequently the effects of aeolian additions to soils must have been widespread.

The findings of this study clearly demonstrate the major role that aeolian derived unconsolidated sedimentary units play in the development of salinity in the tablelands and slopes. The wider distribution of these types of units across the Macquarie River catchment is suggested, but is unknown, and requires further investigation.

8.1 MAJOR FINDINGS

A summary of major findings is provided in the following list:

1. Mapping of an eroded creek section and logging of drillholes in the Snake Gully catchment, central western NSW, has defined four unconsolidated sedimentary units that unconformably overly Palaeozoic bedrock. Unit One is a gravelly sandy silt, Unit Two is a clayey silt, Unit Three is a dense gravelly silty clay and Unit Four is a dense sandy clayey silt.
2. Aqueous 1:5 extracts indicate that Unit One is non-saline, but that Units Two, Three, and Four are moderately to highly saline, with a mean EC of $359 \mu S/cm$ and a mean TDS of 193 mg/L. Soluble salts are dominated by sodium and chloride.
3. Emerson Aggregate dispersion testing determined that all four sedimentary units are moderately to highly dispersible, with the exception of the top 10 cm of Unit One, which if undisturbed, protects underlying dispersive material.
4. Downhole geophysical logging shows that there is a close relationship between EC1:5 and bulk EC. Results of integrated geophysical surveys and geological analyses suggest that these unconsolidated sedimentary units occupy a palaeochannel at least 8 metres deep that is offset from the current creek line.
5. Pebble imbrication, graded bedding and scour and fill structures in Unit One are consistent with alluvial deposition. Strong bimodality and massive matrix supported textures in Units Two, Three and Four are consistent with deposition as liquefied debris flows.
6. Particle size analysis on the sub-50 micron fraction of all sedimentary units confirms an aeolian component, with frequency peaks at 2 microns (clay) and 7 microns (fine silt).
7. Entrainment of a plough disc into Unit One dates this unit at less than 150 years, having been deposited since European settlement of the area. Radiocarbon dating near the top of Unit Two gives a date of emplacement of between 180 and 330 years before present (ie 1670 to 1820), which is prior to European settlement at the end of the 'Little Ice Age'. From regional dating and palaeoclimatic evidence, ages of deposition are estimated for Units Three and Four, at 13,000 to 25,000 years and greater than 50,000 years, respectively.
8. Hydrogeochemistry indicates that the main processes affecting the ionic composition and concentration of groundwaters are dissolution of halite, ion exchange, and redox reactions. Ionic ratios and stable isotopes verify that evaporation is not a significant process affecting the ionic concentration of the groundwaters at this site.
9. Groundwater levels at the study site are between 2.3 and 1.3 metres below surface. They have fluctuated about 0.5 m in the ten months of observation, with rises two days after major rainfall. Overall groundwater levels have been declining throughout this time, which apart from February 2002, has been a period of drought. Groundwater levels continued to decline between August 2002 and March 2003 with no recharge episodes indicated.
10. Bores at the nested site GW96128 show an upwards hydraulic gradient between the intermediate (12 m) and shallow (1.5 m) depth bores; and a downwards hydraulic gradient between the shallow and intermediate bores, and the deep bore (28 m). This appears to be due to lateral flow at the intermediate level.
11. Identical hydrograph responses in the GW96128 nested bores, demonstrates that hydraulic loading is the significant groundwater process rather than mass transfer of water by flow.
12. It is estimated that 1,930 tonnes of salt is stored in the debris flow sediments in the catchment; and that erosion of an area of these units 20 m x 20 m x 2 m thick, with an average salinity of 193 mg/L, would release 772 kg of salt into the waterway.

8.2 IMPLICATIONS FOR SALINITY MANAGEMENT

If future salinity planning and management is to be effective, a shift in focus is required from groundwater flow driven salinity models to valley floor sedimentary units, in order to reflect the important control these units have on groundwater and salinity processes.

The conceptual model presented here provides a basis for future salinity management planning, enabling appropriate actions to be applied, investment to be targeted and outcomes measured.

Protection of the salt rich sediments from erosion and release of salt should be the priority management strategy; along with on-going actions to minimise local groundwater recharge. In combination, these measures will considerably reduce salt export, so that downstream salinity targets can be realised.

8.3 FURTHER WORK

Further possibilities become evident during the course of research and investigation for this project that cannot be followed up owing to time constraints. The following lines of research and investigation would enable refinement of the conceptual salinity model presented and establish the regional distribution and effects of these units and processes.

8.3.1 Refinement of Conceptual Model

1. Additional dating of the unconsolidated sedimentary units using radiocarbon and thermoluminescence (TL) techniques to constrain the date of emplacement and possible palaeoenvironment of deposition.
2. Conduct detailed EM31 surveys at other locations in the catchment, to determine the spatial location and extent of the high conductivity material.
3. Complete several cored holes to investigate EM31 anomalies in the sedimentary units, and determine physical and chemical characteristics.
4. Construct nested monitoring bores in transects across the catchment, including hilltops to establish water levels and three-dimensional hydraulic gradients. This would allow groundwater flow and discharge rates to be estimated and applied to salinity management planning.
5. Install a continuous rainfall collection station, and continuous water level and EC dataloggers into selected monitoring bores throughout the catchment to examine the rate and magnitude of response to recharge events and allow resolution of groundwater response mechanisms.
6. Analyse groundwaters for radioactive isotope ^{36}Cl to assess age of chloride, and determine whether the source of halite is from young sedimentary units, or a Palaeozoic/Mesozoic source.
7. XRD clay analysis of sedimentary units and weathered bedrock for comparison, in order to identify the level of contribution from local weathered materials.
8. Petrological and mineralogical studies of component grains of each sedimentary unit to expand the understanding of composition and source of these materials.

8.3.2 Assessment of the Regional Distribution and Nature of Debris Flow Type Units

This could be achieved by:

1. A combination of EM31, electrical imaging, and downhole geophysical logging techniques at key upland valley sites throughout the region, to investigate the distribution of highly conductive units.
2. These key sites to be calibrated by a number of cored holes converted into monitoring bores.

Bibliography

- Acworth, R. I. (1998). Electromagnetic induction logs from selected bores in the botany sands aquifer. In G. H. McNally & J. Jankowski (Eds.), *Environmental Geology of the Botany Basin*, pp. 143–159. Environmental, Engineering and Hydrogeology Specialist Group (EEHSG) of the Geological Society of Australia.
- Acworth, R. I. (1999). Investigation of dryland salinity using the electrical image method. *Australian Journal of Soil Research* 37(4), 623–636.
- Acworth, R. I. & Beasley, R. (1998). Investigation of EM-31 Anomalies at Yarramanbah/Pump Station Creek, on the Liverpool Plains of New South Wales. Research Report 195, Water Research Laboratory. ISBN 0 85824 0289.
- Acworth, R. I., Broughton, A., Nicoll, C., & Jankowski, J. (1997). The role of debris-flow deposits in dryland salinity development in the Yass River Catchment, New South Wales, Australia. *Hydrogeology Journal* 5(1), 22–36.
- Acworth, R. I. & Jankowski, J. (1997). The relationship between bulk electrical conductivity and dryland salinity in the Narrabri Formation at Breeza, Liverpool Plains, New South Wales, Australia. *Hydrogeology Journal* 5(3), 109–123.
- Acworth, R. I. & Jankowski, J. (2001). Salt source for dryland salinity - evidence from an upland catchment on the Southern Tablelands of New South Wales. *Australian Journal of Soil Science* 39(1), 39–59.
- American Public Health Association (1992). Standard methods for the examination of water and wastewater. Technical report, American Public Health Association. 18th edition.
- Beck, R. (1998). Chemistry Laboratory Manual - Water Research Laboratory.
- Blatt, H., Middleton, G., & Murray, R. (1980). *Origin of Sedimentary Rocks* (3rd ed.). Englewood Cliffs, New Jersey, USA: Prentice Hall.
- Bowler, J. (1976). Aridity in Australia: Age, Origins and Expression in Aeolian Landforms and Sediments. *Earth-Science Reviews* 12, 279–310.
- Bowler, J. (1982). Aridity in the Late Tertiary and Quaternary of Australia. In W. Barker & P. Greenslade (Eds.), *Evolution of the Flora and Fauna of Arid Australia*. Frewville, South Australia: Peacock Publications.
- Bowler, J. (1983). Lunettes as indices of hydrological change: A review of Australian evidence. *Proceedings Royal Society Victoria* 95(3), 147–168.
- Bowler, J. (1990). The last 500,000 years. In N. Mackay & D. Eastburn (Eds.), *The Murray*, pp. 95–104. The Murray-Darling Basin Commission, Canberra, Australia: The Murray-Darling Basin Commission.
- Broughton, A. (1992). The effect of parna-rich debris flow deposits on upland salinity occurrences in the southern tablelands, New South Wales. Master's thesis, Department of Applied Geology, University of New South Wales.
- Butler, B. (1956). Parna, an aeolian clay. *Australian Journal of Soil Science* 18, 145–151.

- Butler, B. (1959). Periodic phenomena in landscapes as a basis for soil studies. Australian Soil Publication 14, Commonwealth Scientific and Industrial Research Organisation.
- Butler, B. (1974). A contribution towards the better specification of parna and some other aeolian clays in Australia. *Z. Geomorphol., Suppl. Bd. 20*, 106–116.
- Charman, P. (1978). *Soils of New South Wales, Their Characterisation, Classification and Conservation*. Number 1. Soil Conservation Service of New South Wales.
- Charman, P. & Murphy, B. (2000). *Soils; Their Properties and Management*. Melbourne: Oxford University Press.
- Clarke, I. & Fritz, P. (1997). *Environmental Isotopes in Hydrogeology*. Lewis Publishers.
- Coram, J., Dyson, P., & Evans, R. (2001). An Evaluation Framework for Dryland Salinity. Technical report, Bureau of Rural Sciences. A report prepared for the National Land and Water Resources Audit Dryland Salinity Project.
- Crowley, T. (1996). Remembrance of things past: greenhouse lessons from the geological record. *Consequences, the Nature and Implications of Environmental Change* 2(1), 1–11.
- CSIRO (2001). Australia State of the Environment 2001, Independent report to the Commonwealth Minister for the Environment and Heritage. Technical report, CSIRO, CSIRO Publishing, Colingwood, Victoria.
- Dare-Edwards, A. (1984). Aeolian clay deposits of south-eastern Australia: parna or loessic clay? *Transactions Institute British Geographers* 9, 337–344.
- Downes, R. (1954). Cyclic salt as a dominant factor in the genesis of soils in south east Australia. *Australian Journal of Agricultural Research* 5, 448–464.
- Evans, R., Brown, C., & Kellet, J. (1990). Geology and Groundwater. In N. Mackay & D. Eastburn (Eds.), *The Murray*, pp. 77–94. The Murray-Darling Basin Commission, Canberra, Australia: The Murray-Darling Basin Commission.
- Evans, W. R. (1998). What does Boorowa tell us? Salt stores and groundwater dynamics in a dryland salinity environment. In T. R. Weaver & C. Lawrence (Eds.), *Groundwater: Sustainable Solutions, Proceedings of the International Groundwater Conference 1998, Melbourne 11-13 February, 1998*, pp. 267–274. University of Melbourne: Melbourne.
- Fetter, C. (1994). *Applied Hydrogeology* (Third ed.). MacMillans.
- Flannery, T. (1994). *The Future Eaters: An Ecological History of the Australian Lands and People*. Australia: Reed Books.
- Folk, R. (1980). *Petrology of Sedimentary Rocks*. Austin, Texas, USA: Hemphill Publishing Company.
- Frank, R. (1971). The clastic sediments of Wellington Caves, New South Wales. *Helictite* 9(1), 3–26.
- Freeze, R. & Cherry, J. (1979). *Groundwater*. Prentice-Hall, Inc., Englewood Cliffs, NJ.
- Geeves, G., Craze, B., & Hamilton, G. (2000). Soil physical properties. In P. Charman & B. Murphy (Eds.), *Soils: Their Properties and Management*. Oxford University Press.
- Ghassemi, F., Jakeman, A., & Nix, H. (1995). *Salinisation of Land and Water Resources*. Sydney: University of New South Wales Press Ltd.
- G. Rayment & Higginson, F. (1992). *Australian Laboratory Handbook of Soil and Water Chemical Methods*. Inkata Press.
- Griffiths, D. & Barker, R. (1993). Two-dimensional resistivity imaging and modelling in areas of complex geology. *Journal of Applied Geophysics* 29, 211–226.
- Griffiths, D. & King, R. (1981). *Applied Geophysics for Geologists and Engineers* (2nd ed.). Exeter, UK: Pergamon Press.

- Hazelton, P. & Murphy, B. (1992). What do all the numbers mean? a guide for the interpretation of soil test results.
- Hem, J. (1985). Study and interpretation of the chemical characteristics of natural water. Water Supply Paper 2254, US Geological Survey.
- Herczeg, A., Dogramaci, S., & Leaney, F. (2001). Origin of dissolved salt in a large, semi-arid groundwater system: Murray Basin, Australia. *Marine and Freshwater Research* 52, 41–52.
- Hesse, P. (1994). The record of continental dust from Australia in Tasman Sea sediments. *Quaternary Science Reviews* 13, 257–272.
- Hogg, A. (2002a). Liquid scintillation counting by quantulus. University of Waikato Radiocarbon Dating Laboratory.
- Hogg, A. (2002b). Liquid scintillation counting (lsc). University of Waikato Radiocarbon Dating Laboratory.
- Jankowski, J. & Acworth, R. I. (1997). Impact of debris-flow deposits on hydrogeochemical processes and dryland salinity development in the Yass River Catchment, New South Wales, Australia. *Hydrogeology Journal* 5(2), 71–88.
- Junor, P. C. R. (1989). Saline seepage and land degradation - a New South Wales perspective. *BMR Journal of Australian Geology & Geophysics* 11, 195–203.
- Kearey, P. & Brooks, M. (1991). *An introduction to Geophysical Exploration* (2nd ed.). Cambridge, UK: Blackwell Science.
- Keys, W. S. (1989). *Borehole Geophysics Applied to Ground-Water Investigations*. 6375 Riverside Drive, DUBLIN, OH 43017: National Water Well Association.
- Kiefert, L. (1995). *Characteristics of Wind Transported Dust in Eastern Australia*. Ph. D. thesis, Faculty of Environmental Sciences, Griffith University.
- King, C. (1957). An Outline of Closer Settlement in NSW - Part One: The Sequence on the Land Laws 1788 - 1956. Technical report, NSW Department of Agriculture, Sydney.
- Knight, A., McTainsh, G., & Simpson, R. (1995). Sediment loads in an Australian dust storm: implications for present and past dust processes. *Catena* 24, 195–213.
- Ladanay-Bell, J. & Acworth, R. (2002). Salinisation processes in the irrigation environment, Riverine Plain, Murray-Darling Basin. In *IAH International Conference - Balancing the Groundwater Budget, Darwin, 12 - 17 May, 2002*.
- Leaney, F. (2001). Isotope analysis service.
- Lines, W. (1991). *Taming the Great South Land: A History of the Conquest of Nature in Australia*. Athens and London: The University of Georgia Press.
- Logan, J. (1958). Erosion problems on salt-affected soils. *Journal of Soil Conservation Service, New South Wales* 14, 220–242.
- Loke, M. & Barker, R. (1995). Least squares deconvolution of apparent resistivity pseudosections. *Geophysics* 60(6), 1682–1690.
- Loke, M. & Barker, R. (1996). Rapid least squares inversion of apparent resistivity pseudosections by a quasi-newton method. *Geophysical Prospecting* 44, 131–152.
- Loke, M. H. (1999). Electrical imaging surveys for environmental and engineering studies - A practical guide to 2D and 3D surveys. 5, Cangkat Minden Lorong 6, Minden Heights, 11700 Penang, Malaysia (mhoke@pc.jaring.my). Downloaded from <http://www.abem.se>.
- Mahamed, M. (1999a). Hydrogeology and Dryland Salinity, Spicers Creek Catchment Area: Final Report of Investigations. Insearch Report C97/44/010, National Centre for Groundwater Management. Prepared for the Spicers Creek / Talbragar Catchment Management Landcare Group.

- Mahamed, M. (1999b). Hydrogeology and Dryland Salinity, Spicers Creek Catchment Area: Preliminary Report of Investigations. Insearch Report C97/44/010, National Centre for Groundwater Management. Prepared for the Spicers Creek / Talbragar Catchment Management Landcare Group.
- McCave, I. & Syvitsky, J. (1991). Principles and methods of geological particle size analysis. In J. Syvitski (Ed.), *Principles, Methods and Applications of Particle Size Analysis*, pp. 3–21. Cambridge, USA: Cambridge University Press.
- McElroy, S. (2000). Hydrogeological Study of Spicers Creek, Talbragar Catchment. Technical report, Jewell and Associates Pty Ltd, Wentworth Falls, NSW. Prepared for the Spicers Creek / Talbragar Catchment Management Landcare Group.
- McKenzie, F. (2002). A historical perspective of land use change in the Mid Talbragar Catchment.
- McNeil, J. (1980). Electromagnetic Terrain Conductivity Measurement at Low Induction Numbers - Technical Note TN-6. Technical report, Geonics Limited.
- McNeil, J. (1986). Geonics EM39 Borehole Conductivity Meter - Theory of Operation. Technical report, Geonics Limited. TN-20.
- McTainsh, G. (1989). Quaternary aeolian dust processes and sediments in the Australian region. *Quaternary Science Reviews* 8, 235–253.
- McTainsh, G. & Lynch, A. (1996). Quantitative estimates of the effect of climate change on dust storm activity in Australia during the Last Glacial Maximum. *Geomorphology* 17, 263–271.
- MDBMC (1999). The Salinity Audit of the Murray-Darling Basin - A 100-year perspective. Technical report, The Murray Darling Basin Ministerial Council, Canberra.
- Meakin, N., Colquhoun, G., Pogson, D., & Barron, L. (1997). Cobbora 1:100 000 Geological Sheet 8733. Technical report, Geological Survey of New South Wales, Canberra.
- Melis, M. (1998). Provenance of Cainozoic deposits and related dryland salinity, Upper Dicks Creek catchment, New South Wales. Master's thesis, Civil and Environmental Engineering, University of New South Wales. 139 Pages.
- Melis, M. I. & Acworth, R. I. (2001). A possible aeolian component in Pleistocene and Holocene valley aggradation, Dicks Creek Catchment, New South Wales. *Australian Journal of Soil Science* 39(1), 13–38.
- Milnes, A. & Hutton, J. (1983). Calcretes in Australia. In *Soils: An Australian Viewpoint*, pp. 119–162. CSIRO.
- Morgan, K. & Jankowski, J. (2002). Determination of the source of salinity within the dryland salinity affected Spicers Creek catchment, Central West, NSW, Australia. In *The Water Challenge: Balancing the Risks*. I. E. Australia. Hydrology and Water Resources Symposium, Melbourne, 20 - 23 May 2002.
- Morgan, K. & Jankowski, J. (2004). Saline groundwater seepage zones and their impact on soil and water resources in the Spicers Creek catchment, central west, New South Wales, Australia. *Environmental Geology* 46(2), 273–285.
- Murphy, B. & Lawrie, J. (1998a). Soil landscapes of the Dubbo 1:250 000 sheet. Technical report, NSW Department of Land and Water Conservation, Sydney.
- Murphy, B. & Lawrie, J. (1998b). Soil landscapes of the Dubbo 1:250 000 sheet si 55-4. Technical report, NSW Department of Land and Water Conservation, Sydney.
- Nicoll, C. & Scowan, J. (1993). Dryland Salinity in the Yass Valley: Processes and Management. Department Land and Water Conservation, Sydney. Final Technical Report to the Natural Resources Management Strategy.
- NLWRA (2001). Australian Dryland Salinity Assessment 2000: Extent, Impacts, Processes, Monitoring and Management Options. Technical report, National Land and Water Resources Audit, ACT.

- Olley, J. & Wasson, R. (2003). Changes in the flux of sediment in the Upper Murrumbidgee catchment, SE Australia, since European settlement. *Hydrological Processes* *In press*.
- Osborne, R. (2001). Karst geology of Wellington Caves: a review. *Helictite* 37, 3–12.
- Please, P., Knight, M., & Corpuz, A. (1989). Role of large scale geological structures in groundwater driven dryland salinity. In *Management of Soil Salinity in South Eastern Australia*. Australian Society of Soil Science.
- R.D.Barker (1989). Depth of investigation of a generalised colinear 4-electrode array. *Geophysics* 54, 1031–1037.
- Salas, G. & Smithson, A. (2002). Rainfall controls on standing water levels in a fractured rock area of central NSW, Australia. In *IAH International Groundwater Conference - Balancing the Groundwater Budget*. Darwin, 12 - 17 May, 2002.
- Schofield, S. (1998). *The Geology, Hydrogeology and Hydrogeochemistry of the Ballimore Region, Central New South Wales*. Ph. D. thesis, School of Applied Geology, The University of New South Wales.
- Scott, A. (2001). Water erosion in the Murray-Darling Basin: Learning from the past. Technical Report 43/01, CSIRO Land and Water.
- Shaver, R. (1997). The determination of glacial till specific storage in north dakota. *Ground Water* 36, 552–557.
- Smithson, A. (2002). *An Investigation of unconsolidated sedimentary units and their role in the development of salinity in the Snake Gully Catchment, Central New South Wales*. M.Eng.Sci. Coursework Report, School of Civil and Environmental Engineering, University of New South Wales.
- Sprigg, R. (1982). Alternating wind cycles of the Quaternary era and their influences on aeolian sedimentation in and around the dune deserts of south eastern Australia. In R. Wasson (Ed.), *Quaternary Dust Mantles of China, New Zealand and Australia*, INQUA Loess Commission Workshop, Canberra, 1982, Canberra, pp. 211–240. Australian National University.
- Taylor, K., Hess, J., & Mazzela, A. (1989). Field evaluation of a slim-line borehole induction tool. *Ground Water Monitoring Review* 9(4), 100–104.
- Taylor, S. (1996). Dryland Salinity Introductory Extension Notes. DLWC, Bathurst. 64 pages.
- Timms, W., Acworth, R. I., & Young, R. (2002). Natural leakage pathways through smectite clay: A hydrogeological synthesis of data from the Hudson Agricultural Trial Site on the Liverpool Plains. Research Report 209, Water Research Laboratory, 110 King Street, MANLY VALE 2093, NSW Australia. Available for download as a pdf file at www.wrl.unsw.edu.au/research.
- Townsend, F. (1997). *Aeolian additions to the soils of the south east Australian Highlands*. B.Sc. (Hons) Thesis, School of Earth Sciences, Macquarie University.
- van Dijk., D. (1959). Soil features in relation to erosional history in the vicinity of Canberra. Soil Publication 13, Commonwealth Scientific and Industrial Research Organization, Australia.
- van Dijk, D. (1969). Relict salt, a major cause of recent land damage in the Yass Valley, Southern Tablelands, NSW. *The Australian Geographer* 11, 13–21.
- Vogelsang, D. (1995). *Environmental Geophysics: A Practicle Guide*. Berlin: Springer-Verlag.
- Walker, P. & Costin, A. (1971). Atmospheric dust accession in south-eastern Australia. *Australian Journal Soil Research* 9, 1–5.
- Wasson, R. (1986). Geomorphology and quaternary history of the Australian continental dunefields. *Geographical Review of Japan* 59, 55–67.
- Wasson, R. & Donnelly, T. (1991). Palaeoclimatic reconstructions for the last 30 000 years in australia - a contribution to prediction of future climate. Technical Report 91/3, CSIRO Division of Water Resources. Technical Memorandum.

White, M. (1994). *After the Greening*. East Roseville, NSW: Kangaroo Press.

Williams, M., Decker, P. D., Adamson, D., & Talbot, M. (1991). Episodic fluvial, lacustrine and aeolian sedimentation in a late Quaternary desert margin system, central western New South Wales. In M. Williams, P. D. Decker, & A. Kershaw (Eds.), *The Cainozoic in Australia: A Re-appraisal of the Evidence*, Number 18 in Special Publication. Geological Survey of Australia.

Williams, M., Dunkerley, D., Decker, P. D., Kershaw, A., & Stokes, T. (1993). *Quaternary Environments*. Edward Arnold.

Williamson, D. (1998). Land degradation processes and water quality effects: waterlogging and salinisation. In J. Williamson (Ed.), *Farming Action Catchment Reaction*. Collingwood, Victoria: CSIRO Publishing.

Young, R., Young, A., Price, D., & Wray, R. (2002). Geomorphology of the Namoi alluvial plain, northwestern New South Wales. *Australian Journal of Earth Sciences* 49, 509–523.